Calculation of Scattering from Stretched Copolymers Using the Tube Model: Incorporation of the Effect of Elastic Inhomogeneities

D. J. Read*

Department of Applied Mathematics, University of Leeds, Leeds LS2 9JT, United Kingdom

Received August 21, 2003; Revised Manuscript Received January 9, 2004

ABSTRACT: This paper presents a theory, based upon the tube model and the random phase approximation, for calculating the scattering from a stretched melt of partially labeled polymers and copolymers. The new feature of this theory is that it includes the effect of elastic fluctuations and inhomogeneities in the entanglement network of the melt. It is already known that such inhomogeneities give rise to the "butterfly" patterns seen in deformed networks and strongly bimodal melts. Here we show that they can also have a strong effect on the anisotropy of the correlation hole peak of a deformed branched block copolymer by coupling to the motion of the relaxed chain ends. By comparison with recent scattering data from melts of H-shaped polymers, we show that previous difficulties in fitting these data can be largely (but not wholly) overcome by the inclusion of this additional mechansism. We discuss the remaining discrepancies with data, indicating where theoretical developments and further experiments are required.

1. Introduction

In recent years, neutron scattering has been emerging as an experimental tool, complementary to rheology, for probing the deformation of polymer chains in melts under flow. This is possible because many theories (particularly the tube model[1]) which predict the rheological response of the polymer melt do so by predicting the distribution of chain conformations in the flowing or deformed state. In principle, such theories can be used to predict the scattering from partially labeled melts, and these predictions can be tested against experiment.

In fact, such scattering experiments on deformed melts go back as far as the early progress made by Boué and co-workers,[2−6] who studied relaxation after a step uniaxial deformation polystyrene melts. In their initial experiments, the labeled and unlabeled linear chains had similar molecular weights, which meant that they were measuring, as directly as possible, the single-chain scattering function.[2,3] They were hoping to detect a signature in the scattering of the predicted chain retraction along the tube contour,[1] though they were unable to detect such a signature. Subsequent experiments by the same group studied the relaxation after step deformation of both asymmetric melts (with long labeled chains and short unlabeled ones) and networks swollen by a labeled solvent.[4−6] In each case, interchain correlations between labeled and unlabeled species become highly important, and "butterfly" patterns were seen on time scales greater than the relaxation time of the short chains or solvent. The generally accepted explanation for these "butterfly" patterns is that elastic fluctuations and inhomogeneities in the entanglement network of the long polymers, or in the chemically bonded network, couple to the motion of the short chains or solvent. The result is enhanced scattering in directions parallel to the stretch.[7] A number of theories containing this essential physics have been suggested,[8−13] and although there are quantitative differences in their predictions,[5] they all predict butterfly patterns via essentially the same mechanism. One feature of the predicted butterfly patterns is that the scattering parallel to the stretch is enhanced down to the zero wavevector limit because the elastic inhomogeneities are present even on large length scales, and the mobile short chains or solvent can move large distances in response to these.

Another recent set of scattering experiments are concerned with the deformation behavior of branched polymer melts. These experiments have focused on H-shaped polymers, the simplest architecture containing the minimum two branch points required to exhibit nonlinear deformation behavior substantially different from that of linear polymer chains.[14−18] These experiments take advantage of advances in controlled polymer synthesis, using "block copolymer" chains that are partially labeled with deuterium. Previously published work[16,17] has used H-shaped polyisoprene in which the tips of the polymer arms were deuterium-labeled; the accompanying experimental paper[18] presents new results for a polybutadiene H-polymer in which the crossbar is labeled but the arms are unlabeled. In common with the early experiments of Boué and coworkers, all these experiments examine the relaxation of the polymer melt following a uniaxial step strain. The particular labeling on these polymers was designed with a view toward detecting a relaxation mechanism specific to branched polymers: retraction of the branchpoints into the central polymer tube.[14] It was conjectured[15] that the localization of labeled material produced when the arms were pulled into the same tube segment should produce an increased scattering.

It is worth emphasizing that the interpretation of the scattering data for these stretched copolymers is much less straightforward than for melts with wholly labeled chains. Even in the unstretched melt, one needs to use the random phase approximation (RPA) to describe the "correlation hole" peak observed in pure copolymers.[19,20] A first attempt to describe theoretically the scattering from the stretched copolymer melt[21] made use of the fact that there is a wide distribution of relaxation times in branched polymer melts. It made a distinction between variables that relax quickly on the experimental time scale which could be treated as "annealed" variables (and which could be averaged over) and

* E-mail: d.j.read@leeds.ac.uk.

10.1021/ma030438u CCC: $27.50
Published on Web 05/26/2004

variables (such as the tube conformation) that relaxed more slowly than the experimental time scale and which should be treated as "quenched". A consequence of this was that a component of the composition fluctuations from the melt prior to the stretch is "frozen in" on the experimental time scale, so that two applications of the RPA become necessary: one in the melt prior to the stretch, to obtain the frozen-in composition variations, and a second for the melt after the stretch, to obtain the new composition fluctuations about this frozen-in mean. One feature of this theory was that, through careful consideration of the distribution of quenched variables in the system, it reproduced the known RPA result for the unstretched melt (as, clearly, it should do).

However, despite this careful treatment of the quenched variables, and despite using, as closely as possible, the tube model description of the chain deformation, this theory did not accurately describe the experimental H-polyisoprene data.[17] While there were indications that including effects such as a partial branchpoint withdrawal[22] improved the fit, the fact remained that there were aspects of the experimental data which were not correctly described. These discrepancies were most evident at the longest relaxation times probed in the experiments, when one would expect most of the H-polymer arms to have escaped their original tube and relaxed their orientation. In this limit, the intensity of the apparent "correlation hole" peak parallel to the stretch direction was significantly greater than at shorter relaxation times, while the perpendicular peak remained at approximately the same magnitude. This increase in anisotropy occurred despite the fact that the stress was relaxing. Although the theory could to some extent reproduce this effect qualitatively, the magnitude of the anisotropy defied explanation by the theory. Moreover, a "four-point" pattern appeared in the scattering data, and this was not at all predicted by the theory.

A number of possible mechanisms, which qualitatively accounted for this discrepancy between theory and experiment, were suggested.[17,21] Each of these required additional theoretical work to elucidate the effect on the scattering. The purpose of this paper is to investigate one of these mechanisms. The suggestion was that the same elastic fluctuations and inhomogeneities that gave rise to the butterfly patterns in the experiments of Boué et al. were having an effect on the scattering in these H-polymer experiments. In contrast to the "classical" butterfly experiments, however, there are no free chains or solvent in the H-polymer melt. Nevertheless, it did seem plausible that the arms of the H-polymer could act as an effective "solvent", and though they could not move sufficiently large distances to produce an enhancement of the scattering down to the zero wavevector limit, they could move far enough (a distance on the order of their radius of gyration) to produce enhanced scattering at finite wavevectors.

To investigate this effect, this paper will describe a detailed theory which is effectively a combination of the network theories of Panyukov and Rabin[11] and Panyukov and Potemkin[12] (which are "RPA" theories for butterfly patterns), with the previous "double RPA" theory[21] for stretched copolymer melts. This new theory is able to describe, within the same general formalism, both the butterfly patterns in asymmetric melts and swollen networks and an enhancement of scattering at finite wavevector in systems where there is no fully mobile "solvent". It will show that the elastic inhomogeneities have a significant effect on the scattering from stretched H-polymer melts, giving a greatly improved qualitative description of the data. In the case of the polybutadiene data in the accompanying experimental paper and most of the polyisoprene data, it is possible to obtain an accurate quantitative description of the data using this theory.

As with the previous work,[21] the theory to be presented in this paper is specifically designed to treat relaxation, at fixed strain, following a step deformation. In the experiments, the "step deformation" is effected by deforming the melt close to its glass transition temperature. Scattering patterns are then taken after different waiting times at low temperatures; during the actual scattering the melt is quenched to a temperature well below the glass transition in order to prevent any molecular motion. The low-temperature "waiting times" can be converted to room temperature "relaxation times" using WLF time−temperature shift factors.[17] The theory to be presented makes a distinction between variables that have time to relax on the time scale of the experiment (i.e., during the waiting time) and other variables (such as the configuration of the polymer "tube") that do not have time to relax on the experimental time scale. The former are treated as "annealed" variables, and these are averaged over in the derivation of the free energy functional for composition fluctuations. The latter are formally treated as "quenched" variables, and these are not averaged over until the end of the scattering calculation. In doing this, the theory is relying on the wide distribution of relaxation time scales that are present in branched polymer melts, so that this distinction between "fast" and "slow" variables can, at least approximately, be made.

This theory, however, remains approximate, and there are aspects (notably the *other* proposed mechanisms for increasing the parallel scattering in refs 17 and 21) which could, and should, be improved upon. This paper will attempt to give an honest assessment of the remaining approximations, of how this current theory relates to the available experimental data, and the likely avenues for further research (both experimental and theoretical). Before embarking on a description of the full theory, however, we consider a phenomenological model which is illustrative of the main physics to be included.

2. Phenomenological Model

The central goal of this paper is the calculation of a neutron scattering function, following a step strain, for a melt of polymers partially labeled with deuterium. Specifically, we wish to include two important pieces of physics, namely (i) the effect of confining tube variables, which do not relax on the time scale of the experiment (these we shall treat as "quenched variables"), and (ii) elastic fluctuations of the entanglement network. The main physics included in the full theory to be presented below can be illustrated quite simply using a phenomenological model for composition and elastic fluctuations in an entangled or cross-linked blend, stretched from an initial isotropic state. We write the free energy of the system as a sum of three free energy terms, representing the blend free energy for composition variations, a "polarization" energy for local relative motion of the blend components, and an elastic energy for displacements of the network. The first two of these

terms were used in an earlier model[23] for phase separation in cross-linked blends.

For an incompressible blend, we express local fluctuations in composition in terms of a density variable $\rho(\mathbf{r})$, with Fourier transform $\rho_{\mathbf{q}}$. In the absence of any cross-link or entanglement constraints, the free energy for composition fluctuations in the blend can be written as

$$F_{\text{blend}} = \frac{1}{2}\sum_{\mathbf{q}}\left(1 + \frac{Q^2}{2} + \frac{B}{Q^2}\right)|\rho_{\mathbf{q}}|^2 \tag{1}$$

where Q is the magnitude of the wavevector, normalized by the typical molecular dimensions, and B is a parameter that can be set to zero if we wish to describe a blend of homopolymers and is finite if we wish to describe a block copolymer system. We are explicitly considering the limit where the Flory interaction parameter, χ, is zero.

The presence of cross-links or entanglement constraints which are long-lived on the experimental time scale prevents the blend from exploring all its degrees of freedom. As detailed in ref 23, if these constraints are held at fixed positions, then the monomers can only explore a finite volume (e.g., the tube diameter in entangled systems). As a result, the composition is constrained to fluctuate about a "frozen-in" composition $\rho_{0\mathbf{q}}$ related to the state of the melt at the beginning of the experiment. This constraint was expressed as a "polarization" free energy:[23]

$$F_{\text{pol}} = \frac{1}{2}\sum_{\mathbf{q}}\frac{c}{Q^2}|\rho_{\mathbf{q}} - \rho_{0\mathbf{q}}|^2 \tag{2}$$

Suitable statistics for the quenched variable $\rho_{0\mathbf{q}}$ are obtained below. The parameter c is related to the network mesh size as compared to the overall molecular size.

Reference 23 did not allow for the possibility that the entanglement or cross-link network could itself undergo significant displacements. Such displacements give rise to the "butterfly" patterns seen in scattering from stretched gels, as local network displacements couple to the composition fluctuations. We therefore modify the simple model of ref 23 to include displacements of the network.

We represent a local displacement of the network via vectors $\mathbf{w}(\mathbf{r})$, with Fourier transform $\mathbf{w}_{\mathbf{q}}$. Only the "compressive" components of $\mathbf{w}_{\mathbf{q}}$ cause changes in local network density, so we define a field $\Gamma_{\mathbf{q}} \sim i\mathbf{q}\cdot\mathbf{w}_{\mathbf{q}}$ and aim to write a free energy in terms of $\rho_{\mathbf{q}}$ and $\Gamma_{\mathbf{q}}$, representing composition fluctuations and elastic fluctuations of the network, respectively. The network displacements cause changes in the "frozen-in" composition $\rho_{0\mathbf{q}}$ in the manner suggested in ref 11:

$$\rho_{0\mathbf{q}} = \rho_{\mathbf{q}\text{ref}} + \beta_{\mathbf{q}}\Gamma_{\mathbf{q}} \tag{3}$$

where $\rho_{\mathbf{q}\text{ref}}$ is the frozen-in composition in the "reference state" of zero network displacement. Here, the function $\beta_{\mathbf{q}}$ is chosen to reflect the physics of the blend being described. In the case where one component is unconstrained by cross-links or entanglements (e.g., the solvent in a gel or the short chains in a bimodal blend), then the composition fluctuations can be affected by network motion at large length scales and there is no upper length scale cutoff to $\beta_{\mathbf{q}}$. The small length scale cutoff is on the order of the network mesh size, and so we use

$$\beta_{\mathbf{q}} = \exp\left(-\frac{Q^2}{c}\right) \tag{4}$$

On the other hand, if both components are tied to the network, then network motion at large length scales carries both components equally and can produce no composition variations (and, moreover, incompressibility will prevent such motion). Nevertheless, we anticipate that displacements at intermediate length scales will predominantly couple to density variations of the more constrained component, giving a contribution to $\rho_{\mathbf{q}}$. A suitable choice of $\beta_{\mathbf{q}}$ is

$$\beta_{\mathbf{q}} = \exp\left(-\frac{Q^2}{c}\right) - \exp\left(-\frac{Q^2}{c_1}\right) \tag{5}$$

where c_1 is related to the dimensions over which the least constrained component is localized.

Finally, we include the elastic free energy for the network deformation, and (inspired by the full model detailed in the next section) this is of form

$$F_{\text{el}} = \frac{1}{2}\sum_{\mathbf{q}}(A_{\mathbf{q}}\Gamma_{\mathbf{q}}\Gamma_{-\mathbf{q}} - 2F_{-\mathbf{q}}\Gamma_{\mathbf{q}}) \tag{6}$$

$A_{\mathbf{q}}$ is related to the elastic modulus for network displacements, while the $F_{-\mathbf{q}}$ represent quenched random stresses in the network and reflect the fact that the reference state of the network is highly unlikely to be at the energy minimum with respect to the displacements $\mathbf{w}(\mathbf{r})$. In this phenomenological theory, we use a simple model along the lines of that detailed in Appendix C, in which the network elasticity is assumed to come from polymer strands distributed uniformly through the system, each with an end-to-end vector that deforms affinely with the local strain of the network. For a network deformed macroscopically by deformation tensor $\mathbf{E}$, this gives a form

$$A_{\mathbf{q}} = n_{\text{r}}\left(\frac{Q_{\text{s}}^{\,2}}{Q^2} + 1\right) \tag{7}$$

and, denoting an average over a quenched variable by an overbar, the second moment of the quenched field $F_{\mathbf{q}}$ is

$$\overline{F_{\mathbf{q}}F_{-\mathbf{q}}} = 2n_{\text{r}}\frac{Q_{\text{s}}^{\,4}}{Q^4} \tag{8}$$

where $Q_{\text{s}}^2 = \mathbf{Q}\cdot\mathbf{E}\cdot\mathbf{E}^{\text{T}}\cdot\mathbf{Q}$ and n_{r} is (approximately) the ratio of the typical molecular weight of the blend components to the molecular weight of the network strands. In this simple model, the source of the quenched random stresses is the variation in orientation between the network strands.

There remains to specify suitable statistics for $\rho_{\mathbf{q}\text{ref}}$. To do this, we consider the free energies F_{blend} and F_{pol}. We consider fluctuations in an isotropic initial melt state, treating both $\rho_{\mathbf{q}}$ and $\rho_{0\mathbf{q}}$ as annealed variables, in which case we obtain

$$\langle|\rho_{\mathbf{q}}|^2\rangle = \left(1 + \frac{Q^2}{2} + \frac{B}{Q^2}\right)^{-1}$$

$$\langle|\rho_{\mathbf{q}} - \rho_{0\mathbf{q}}|^2\rangle = \frac{Q^2}{c}$$

The sum of these provides a suitable second moment average for $\rho_{\mathbf{q}\mathrm{ref}}$ in the isotropic state. For the case when the blend is stretched, we allow an affine deformation of the initial density fluctuations $\langle|\rho_{\mathbf{q}}|^2\rangle$, giving

$$\overline{\rho_{\mathbf{q}\mathrm{ref}}\rho_{-\mathbf{q}\mathrm{ref}}} = \left(1 + \frac{Q_s^2}{2} + \frac{B}{Q_s^2}\right)^{-1} + \frac{Q^2}{c} \tag{9}$$

The full free energy functional is obtained as the sum of eqs 1, 2, and 6.

$$F\{\rho_{\mathbf{q}},\Gamma_{\mathbf{q}}\} = F_{\mathrm{blend}} + F_{\mathrm{pol}} + F_{\mathrm{el}}$$

To obtain the scattering function, we integrate out the network fluctuations, $\Gamma_{\mathbf{q}}$, and note that the resulting free energy functional represents fluctuations $\Delta\rho_{\mathbf{q}}$ about a nonzero mean $\langle\rho_{\mathbf{q}}\rangle$ such that

$$\langle\Delta\rho_{\mathbf{q}}\Delta\rho_{-\mathbf{q}}\rangle = \left(1 + \frac{Q^2}{2} + \frac{B}{Q^2} + \frac{cA_{\mathbf{q}}}{Q^2A_{\mathbf{q}} + c\beta_{\mathbf{q}}^2}\right)^{-1} \tag{10}$$

$$\langle\rho_{\mathbf{q}}\rangle = \frac{\left(\rho_{\mathbf{q}\mathrm{ref}} + \frac{\beta_{\mathbf{q}}}{A_{\mathbf{q}}}F_{\mathbf{q}}\right)\frac{cA_{\mathbf{q}}}{Q^2A_{\mathbf{q}} + c\beta_{\mathbf{q}}^2}}{\left(1 + \frac{Q^2}{2} + \frac{B}{Q^2} + \frac{cA_{\mathbf{q}}}{Q^2A_{\mathbf{q}} + c\beta_{\mathbf{q}}^2}\right)} \tag{11}$$

The scattering function is then

$$\begin{aligned} S(\mathbf{q}) &= \overline{\langle\rho_{\mathbf{q}}\rho_{-\mathbf{q}}\rangle} \\ &= \overline{\langle\rho_{\mathbf{q}}\rangle\langle\rho_{-\mathbf{q}}\rangle} + \langle\Delta\rho_{\mathbf{q}}\Delta\rho_{-\mathbf{q}}\rangle \\ &= \frac{\left(\overline{\rho_{\mathbf{q}\mathrm{ref}}\rho_{-\mathbf{q}\mathrm{ref}}} + \frac{\beta_{\mathbf{q}}^2}{A_{\mathbf{q}}^2}\overline{F_{\mathbf{q}}F_{-\mathbf{q}}}\right)\left(\frac{cA_{\mathbf{q}}}{Q^2A_{\mathbf{q}} + c\beta_{\mathbf{q}}^2}\right)^2}{\left(1 + \frac{Q^2}{2} + \frac{B}{Q^2} + \frac{cA_{\mathbf{q}}}{Q^2A_{\mathbf{q}} + c\beta_{\mathbf{q}}^2}\right)^2} + \\ &\qquad \langle\Delta\rho_{\mathbf{q}}\Delta\rho_{-\mathbf{q}}\rangle \end{aligned} \tag{12}$$

In the limit of no stretching, $Q_s^2 = Q^2$ and the scattering function reduces to

$$S(\mathbf{q}) = \left(1 + \frac{Q^2}{2} + \frac{B}{Q^2}\right)^{-1} \tag{13}$$

which is the expected scattering based simply on the blend free energy of eq 1. This important property is shared by the full theory to be presented below, as discussed in section 3.5.

We can use this phenomenological model to illustrate the central physics in this paper by considering the predicted scattering from three networks prepared in slightly different ways, as illustrated schematically in Figure 1: (a) a blend of homopolymers in which one component is instantaneously cross-linked but the other is not, (b) a blend of homopolymers in which one component is cross-linked but the other becomes a "dangling chain", attached to the network by a single end, and (c) a blend of copolymers in which one component is cross-linked. The predicted scattering for the three systems, stretched uniaxially by a factor 2, is shown in Figure 2.

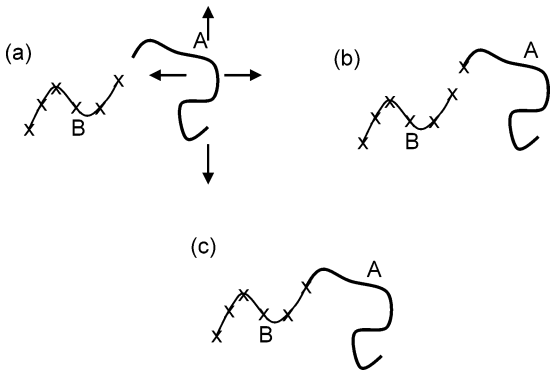

Figure 1. Schematic representation of three different networks: (a) the A chains are un-cross-linked, but the B chains are cross-linked; (b) the A chains are attached at one end to the network while the B chains are cross-linked; (c) the network is formed from an AB block copolymer, in which the B blocks are cross-linked.

To model case a, we set $B = 0$ for a homopolymer blend and use eq 4 for $\beta_{\mathbf{q}}$ since one component is unconstrained by the cross-links. The resulting scattering pattern exhibits the "butterfly" contours expected for such a system. The scattering parallel to the stretch is strongly enhanced by the presence of elastic inhomogeneities, and because the unconstrained component is free to move large distances, this enhancement is present down to the limit of zero scattering angle (such that the value of the scattering in the limit $q \rightarrow 0$ depends on the direction from which this limit is taken). This is a feature of the butterfly pattern observed in stretched gels and gives rise to the (now) well-known "8" shape in the contours.

To model case b, we set $B = 0$ for a homopolymer blend but use eq 5 for $\beta_{\mathbf{q}}$ since both components are now attached to the network. However, there is a strong difference in the degree of confinement of the two components, which we model by setting $c_1 = 0.03$. For all but the smallest scattering angles, parts a and b of Figure 2 are practically identical, indicating that the small scale structure of the two networks is the same. However, because all chains are now anchored, they are not free to move large distances in response to inhomogeneities on large length scales. For this reason, the scattering in the limit of $q \rightarrow 0$ must remain at the same magnitude as in the initial melt state; it is determined by the composition fluctuations that were present in the initial melt and which were frozen in by the cross-linking process. There is no mechanism available to relax, or enhance, these large scale fluctuations. Hence, the "butterfly" effect does not persist down to zero scattering angle in this network, and the scattering in the limit $q \rightarrow 0$ is independent of the direction in which it is approached. Nevertheless, the "dangling chains" are able to move smaller distances, of the order of their radius of gyration, in response to the elastic inhomogeneities, giving rise to the enhanced scattering parallel to the stretch at finite wavevectors. For this particular set of parameters, this results in a small peak parallel to the stretch.

To model case c, we set $B = 0.5$ for a diblock blend and use eq 5 for $\beta_{\mathbf{q}}$. In this case, the scattering at zero wavevector, in both the initial melt and the network, is zero. This is due to the "correlation hole" effect[19,20]—there can be no large length scale composition fluctua-

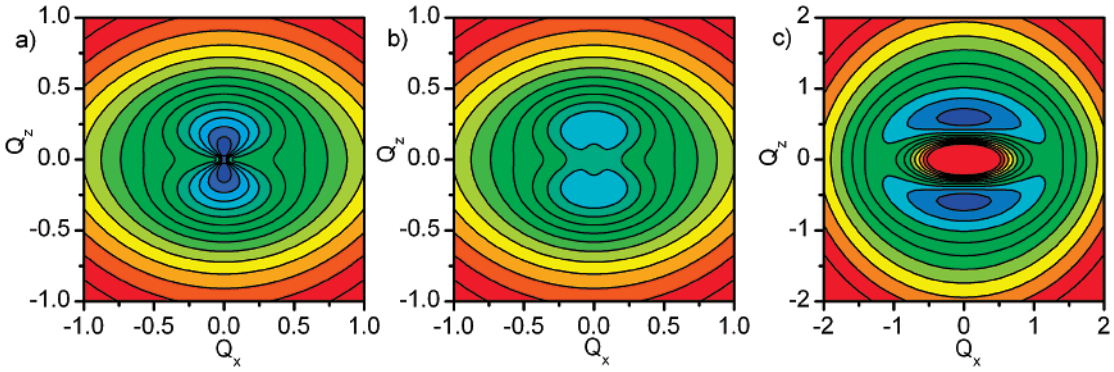

Figure 2. Scattering patterns as predicted by the phenomenological model of section 2 for the three different networks of Figure 1 when stretched in the z direction by a factor 2. All plots use parameters are $n_r = 5$, $c = 5$. (a) $B = 0$, with eq 4 used for $\beta_{\mathbf{q}}$ and contours at evenly spaced intensities of 0.5, 0.55, 0.6, ..., 1.15. (b) $B = 0$, with eq 5 and $c_1 = 0.03$ used for $\beta_{\mathbf{q}}$ and contours at evenly spaced intensities of 0.5, 0.55, 0.6, ..., 1.0. (c) $B = 0.5$, with eq 5 and $c_1 = 0.03$ used for $\beta_{\mathbf{q}}$ and contours at evenly spaced intensities of 0.25, 0.283, 0.316, ..., 0.547.

tions because each diblock molecule contains the same fraction of A and B monomers, and the near "incompressibility" of the melt prevents fluctuations in the density of these molecules. Instead, there is a "correlation hole" peak at finite wavevector, and the major issue is how this peak is affected when the network is stretched. Although the effect is relatively subtle, some enhancement of the peak parallel to the stretch is evident. The physical mechanism at work is the same as in the second network: the elastic inhomogeneities couple to the motion of the free chain ends, allowing the scattering to be affected at finite wavevectors, but not at zero wavevectors where the scattering remains at zero.

The H-polymer experiments[17,18] are physically closest to case c above. However, a detailed comparison with these experiments is not possible with this simple phenomenological theory. Instead, we require a more detailed theory that is able to capture the microscopic details of these complex experimental systems, such as the precise chain architecture and labeling (including impurities and polydispersity effects) obtained from the reaction chemistry or the molecular motions suggested by the physics of the tube model (for example, chain retraction along the tube). The full RPA-based theory to be presented below contains essentially the same contributions to the free energy as in the phenomenological model above but is formulated in a manner that allows such microscopic details to be included and hence a careful comparison with experiments to be made.

3. Outline of the Full Theory

The full calculation of this scattering function is very lengthy and so is presented in detail in Appendices A−E. The Appendices are organized as follows: Appendix A gives a derivation of the basic form of the free energy functional; Appendix B deals with variations in composition due to small network fluctuations; Appendix C details the approximate tube model used to obtain, and gives a derivation of, the elastic contributions to the free energy; Appendix D obtains a general expression for the scattering; and Appendix E details the calculation of individual correlation functions for a melt of H-shaped polymers. We also include, in Appendix F, a comparison of the results derived here with earlier results obtained by Panyukov and Potemkin[12] for a simpler single-component network system.

Here we shall outline the physics involved in the calculation and direct the reader to the main results. We also state, from the outset, that this calculation necessarily makes approximations, specifically in the treatment of the entanglements and polymer tubes (for which a detailed microscopic treatment via statistical mechanics remains lacking). It is difficult to convey the nature of these approximations without reference to the detailed calculation; the interested reader is referred particularly to the discussions after eq 50 in Appendix A, at the start of Appendix C, and in the calculation of correlation functions in Appendix E.

3.1. Definitions of Fields for Composition and Elastic Fluctuations. Denoting the labeled polymers by "A" and the unlabeled ones by "B", we define Fourier transformed density fields $\rho_{\mathbf{q}}^{\mathrm{A}}$ and $\rho_{\mathbf{q}}^{\mathrm{B}}$ for the two species. Assuming the system to be effectively incompressible (i.e., $\rho_{\mathbf{q}}^{\mathrm{A}} = -\rho_{\mathbf{q}}^{\mathrm{B}} = \rho_{\mathbf{q}}$), the scattering function is

$$S(\mathbf{q}) = \overline{\langle \rho_{\mathbf{q}} \rho_{-\mathbf{q}} \rangle_{\mathrm{an}}} \tag{14}$$

where the overbar $\overline{(...)}$ is used to denote an average over quenched variables and $\langle ... \rangle_{\mathrm{an}}$ will be used to denote an average over *all* annealed variables. (We shall retain the angle brackets without the "an" subscript for a specific average over a subset of the annealed variables, to be defined below.)

We first consider the confining tube variables. If one were able to fix the tubes at a given position (i.e., suppressing the local position fluctuations of the entanglement network), then each monomer would be constrained to fluctuate in a small volume, given by the tube constraint, about a mean position. The effect of this on the density fields $\rho_{\mathbf{q}}^{\mathrm{A}}$ and $\rho_{\mathbf{q}}^{\mathrm{B}}$ is that they are also constrained to fluctuate about a nonzero mean.[11,21] We define new fields, $d_{\mathbf{q}}^{\mathrm{A}}$ and $d_{\mathbf{q}}^{\mathrm{B}}$, which represent average values of $\rho_{\mathbf{q}}^{\mathrm{A}}$ and $\rho_{\mathbf{q}}^{\mathrm{B}}$:

$$d_{\mathbf{q}}^{\mathrm{I}} = \langle \rho_{\mathbf{q}}^{\mathrm{I}} \rangle_0 \tag{15}$$

The average denoted by the angle brackets is taken over the positions of the monomers confined by tubes *at fixed tube position*, but in the absence of excluded-volume interactions (denoted by a subscript "0"). Excluded-volume interactions will be included later, using the RPA formalism.

In general, it is not the case that $d_{\mathbf{q}}^{A} = -d_{\mathbf{q}}^{B}$ in a two-component incompressible system. Although the overall density is subject to incompressibility, the tube variables might impose a different degree of constraint on each of the two components, so that the average in eq 15 is very different for each component. In the extreme case where one component is unconstrained by the tubes, we have, for that component only, $d_{\mathbf{q}}^{I} = 0$.

We now consider elastic fluctuations in local network position. We suppose that, under these fluctuations, the mean position $\hat{\mathbf{r}}_s$ of monomer s is displaced as

$$\hat{\mathbf{r}}_s = \hat{\mathbf{r}}_{\mathrm{ref},s} + \mathbf{w}(\hat{\mathbf{r}}_{\mathrm{ref},s}) \tag{16}$$

from a reference position $\hat{\mathbf{r}}_{\mathrm{ref},s}$. We take the reference configuration $\hat{\mathbf{r}}_{\mathrm{ref},s}$ to be the one that is affinely deformed from the initial melt state before the step deformation and treat the $\hat{\mathbf{r}}_{\mathrm{ref},s}$ as quenched variables. The vector field $\mathbf{w}(\mathbf{r})$ (with Fourier transform $\mathbf{w}_{\mathbf{q}}$) represents the local displacement of the entanglement network about the reference configuration. It is shown in Appendix B that, for small $\mathbf{w}$, the mean monomer density $d_{\mathbf{q}}^{I}$ varies as

$$d_{\mathbf{q}}^{I} = d_{\mathbf{q},\mathrm{ref}}^{I} + \beta_{\mathbf{q}}^{I}\Gamma_{\mathbf{q}} \tag{17}$$

where $\Gamma_{\mathbf{q}} \sim i\mathbf{q}\cdot\mathbf{w}_{\mathbf{q}}$ is related to the dilational component of $\mathbf{w}_{\mathbf{q}}$. $\beta_{\mathbf{q}}^{I}$ is a cutoff function that can be derived from the microscopic model used for the polymer tubes. $d_{\mathbf{q},\mathrm{ref}}^{I}$ is the value of $d_{\mathbf{q}}^{I}$ in the reference configuration, and this is treated as a "quenched" field variable.

We use the field $\Gamma_{\mathbf{q}}$ because the density of the polymers is affected only by the dilational component of the Fourier transformed displacement (i.e., the component of $\mathbf{w}_{\mathbf{q}}$ parallel to $\mathbf{q}$) but not the shear components of $\mathbf{w}_{\mathbf{q}}$. For the particular model used here to obtain a second-order expansion of the free energy in the field variables, $\Gamma_{\mathbf{q}}$ does not couple to the shear components of $\mathbf{w}_{\mathbf{q}}$. Note that this is not true in general, and for other models it can be necessary to include all components of $\mathbf{w}_{\mathbf{q}}$ as in ref 12 (see Appendix F for more details).

3.2. Expression for the Free Energy. In the Appendix, we obtain the "free energy" functional of the incompressible system in terms of the fields $\rho_{\mathbf{q}}$ and $\Gamma_{\mathbf{q}}$ (representing concentration fluctuations and fluctuations in network displacement, respectively):

$$F\{\rho_{\mathbf{q}},\Gamma_{\mathbf{q}}\} = F_0\{\rho_{\mathbf{q}}|d_{\mathbf{q}}^{I}\} + F_1\{d_{\mathbf{q}}^{I}\} - \frac{N}{N_e}\sum_{\mathbf{q}} f_{-\mathbf{q}}\Gamma_{\mathbf{q}} + \frac{1}{2}\sum_{\mathbf{q}} A_{\mathbf{q}}\Gamma_{\mathbf{q}}\Gamma_{-\mathbf{q}} \tag{18}$$

where

$$F_0\{\rho_{\mathbf{q}}|d_{\mathbf{q}}^{I}\} = \frac{1}{2}\sum_{\mathbf{q}} [T_{\mathbf{q}}^{BB}|\rho_{\mathbf{q}} - d_{\mathbf{q}}^{A}|^2 + T_{\mathbf{q}}^{AA}|\rho_{\mathbf{q}} + d_{\mathbf{q}}^{B}|^2 + 2T_{\mathbf{q}}^{AB}(\rho_{\mathbf{q}} - d_{\mathbf{q}}^{A})(\rho_{-\mathbf{q}} + d_{-\mathbf{q}}^{B})]/[T_{\mathbf{q}}^{AA}T_{\mathbf{q}}^{BB} - (T_{\mathbf{q}}^{AB})^2] \tag{19}$$

and

$$F_1\{d_{\mathbf{q}}^{I}\} = \frac{1}{2}\sum_{\mathbf{q}} \frac{\Delta_{0\mathbf{q}}^{BB}|d_{\mathbf{q}}^{A}|^2 + \Delta_{0\mathbf{q}}^{AA}|d_{\mathbf{q}}^{B}|^2 - 2\Delta_{0\mathbf{q}}^{AB}d_{\mathbf{q}}^{A}d_{-\mathbf{q}}^{B}}{\Delta_{0\mathbf{q}}^{AA}\Delta_{0\mathbf{q}}^{BB} - (\Delta_{0\mathbf{q}}^{AB})^2} \tag{20}$$

The correlation functions $T_{\mathbf{q}}^{IJ}$ and $\Delta_{0\mathbf{q}}^{IJ}$ are defined in eqs 43 and 54, respectively.

F_0 and F_1 together are equivalent to the blend and polarization free energies in the phenomenological model of section 2. F_0 is the free energy for concentration fluctuations $\rho_{\mathbf{q}}$ about a nonzero mean (this mean is related to $d_{\mathbf{q}}^{A}$ and $d_{\mathbf{q}}^{B}$). F_0 is of precisely the same form as the *whole* free energy obtained in ref 21, where fluctuations in network position were not included and $d_{\mathbf{q}}^{A}$ and $d_{\mathbf{q}}^{B}$ were fixed. In the present theory, $d_{\mathbf{q}}^{A}$ and $d_{\mathbf{q}}^{B}$ are not fixed but are constrained to vary with the network fluctuations $\Gamma_{\mathbf{q}}$ as given in eq 17. Such local changes in composition result in further changes of the free energy, as expressed by F_1. As discussed at the end of Appendix A, integrating over the mean densities $d_{\mathbf{q}}^{A}$ and $d_{\mathbf{q}}^{B}$ in these two terms (which is equivalent to an average over the tube positions) reproduces the standard RPA expression $F_{\mathrm{RPA}}\{\rho_{\mathbf{q}}\}$ for the free energy of composition fluctuations, in the absence of quenched tube variables, i.e.

$$\int D\{d_{\mathbf{q}}^{A},d_{\mathbf{q}}^{B}\}\exp(-F_0\{\rho_{\mathbf{q}}|d_{\mathbf{q}}^{I}\} - F_1\{d_{\mathbf{q}}^{I}\}) = \exp(-F_{\mathrm{RPA}}\{\rho_{\mathbf{q}}\}) \tag{21}$$

where

$$F_{\mathrm{RPA}}\{\rho_{\mathbf{q}}\} = \frac{1}{2}\sum_{\mathbf{q}} \frac{S_{0\mathbf{q}}^{BB} + S_{0\mathbf{q}}^{AA} + 2S_{0\mathbf{q}}^{AB}}{S_{0\mathbf{q}}^{AA}S_{0\mathbf{q}}^{BB} - (S_{0\mathbf{q}}^{AB})^2}|\rho_{\mathbf{q}}|^2 \tag{22}$$

and $S_{0\mathbf{q}}^{IJ} = T_{\mathbf{q}}^{IJ} + \Delta_{0\mathbf{q}}^{IJ}$.

The last two terms in eq 18 give the contributions to the free energy from the *elastic* stretching of the entanglement network that results from local network displacements. As discussed by Panyukov and Rabin,[11] the network in the reference configuration is highly unlikely to be in the minimum-energy state with respect to these fluctuations, and so in addition to the second-order term in $\Gamma_{\mathbf{q}}\Gamma_{-\mathbf{q}}$ (where $A_{\mathbf{q}}$ is related to the elastic modulus for network deformations) there is a first-order term in $\Gamma_{\mathbf{q}}$, in which the $f_{-\mathbf{q}}$ are related to quenched random stresses. For the particular model of the tube used in this paper, expressions for $A_{\mathbf{q}}$ and $f_{-\mathbf{q}}$ are given by eqs 80, 82, and 83, obtained in Appendix C.

3.3. Sources of Elastic Inhomogeneities in the Microscopic Model. For the particular microscopic model used in this paper, there are two physical sources of "elastic inhomogeneities" or (more precisely) "frozen-in stresses". The "incoherent" component to these stresses arises from the differences in orientation between different tube segments. This component does not depend on the spatial distribution of tube segments but depends on the random deviations of individual tube segments from their mean orientation. Some regions of space will contain tube segments oriented more in one direction, and other regions will contain segments oriented more in another direction, giving variations in local polymeric stress.

The "coherent" component to the frozen-in stresses occurs only when the network is deformed. The chains become stretched, and the oriented tube segments all "pull" in a similar direction. In this case, the fact that tube segments are spatially correlated by being on the same chain means that there are now correlations between the frozen-in stresses and monomer densities. Note, in particular, that after a given experimental relaxation time the remaining oriented tube segments surround only part of each chain, suggesting that there

should be fluctuations in "tube segment density", analogous to the fluctuations in monomer density on a partially labeled chain. These fluctuations are the source of the "coherent" component to the frozen in stresses in the microscopic model.

Both these sources of stress inhomogeneities are long-lived in the melt; since they are related to tube orientation, they relax on the same time scale as the macroscopic stress. Hence, they should be treated as "quenched" variables for any scattering experiment with time scale shorter than the longest stress relaxation time. Elastic inhomogeneities are known to be present in the melt state, since butterfly patterns have been observed in strongly stretched bimodal melts.[4,6] We demonstrate below that they are also present, and significant, in scattering experiments on stretched H-polymers.[17,18]

We have not included in this theory a further possible source of elastic inhomogeneities: fluctuations in entanglement density in the melt. Certainly, fluctuations in cross-link density would appear to be a significant source in polymer networks,[13] giving an additional contribution to the incoherent component of the frozen-in stresses. The physics is less clear in the case of entanglements.

3.4. Expression for the Scattering Intensity. Having obtained the free energy in eq 18, the scattering function $S(\mathbf{q}) = \overline{\langle \rho_{\mathbf{q}} \rho_{-\mathbf{q}} \rangle_{an}}$ is obtained by integrating out the network fluctuations $\Gamma_{\mathbf{q}}$ (i.e., minimizing the free energy with respect to $\Gamma_{\mathbf{q}}$) and then identifying that the resulting free energy functional represents composition fluctuations $\Delta\rho_{\mathbf{q}}$ about a nonzero mean $\langle \rho_{\mathbf{q}} \rangle_{an}$, the latter of which depends explicitly on the quenched variables. The scattering function contains contributions from both the mean $\langle \rho_{\mathbf{q}} \rangle_{an}$ and the fluctuations $\Delta\rho_{\mathbf{q}}$ and is of form

$$S(\mathbf{q}) = \langle \Delta\rho_{\mathbf{q}} \Delta\rho_{-\mathbf{q}} \rangle_{an} + \overline{\langle \rho_{\mathbf{q}} \rangle_{an} \langle \rho_{-\mathbf{q}} \rangle_{an}}$$
$$= \langle \Delta\rho_{\mathbf{q}} \Delta\rho_{-\mathbf{q}} \rangle_{an} + r_A^2 \overline{C_{\mathbf{q}}^A C_{-\mathbf{q}}^A} + r_B^2 \overline{C_{\mathbf{q}}^B C_{-\mathbf{q}}^B} - 2 r_A r_B \overline{C_{\mathbf{q}}^A C_{-\mathbf{q}}^B} \quad (23)$$

where

$$C_{\mathbf{q}}^I = d_{\mathbf{q},ref}^I + \frac{N}{N_e A_{\mathbf{q}}} \beta_{\mathbf{q}}^I f_{\mathbf{q}} \quad (24)$$

are linear combinations of the quenched fields $d_{\mathbf{q},ref}^I$ and $f_{\mathbf{q}}$.

The full expression for the scattering function resulting from this procedure is algebraically quite lengthy and is given by eqs 94−110 and 115−117 in the Appendix. To evaluate the scattering for a particular system, there are a number of correlation functions to calculate: $T_{\mathbf{q}}^{IJ}$, $\Delta_{0\mathbf{q}}^{IJ}$, $\Delta_{0\mathbf{q}}^{If}$, $\Delta_{0\mathbf{q}}^{ff}$, $D_{\mathbf{q}}^I$, $D_{\mathbf{q}}^f$, $S_{\mathbf{q}}^{tot}$, $\beta_{\mathbf{q}}^I$, $A_{1\mathbf{q}}$, and $A_{2\mathbf{q}}$, as detailed in the Appendix. For a two-component system (I, J = A or B) this represents 17 functions, and each of these is dependent on both the polymer chain architecture and the specific model used to describe the chains and tubes. The particular model used in this paper, and the resulting expressions, are described in Appendix E. As in previous calculations for the H-shaped polymer architecture,[16,17,21] these are based on the Warner−Edwards[24] model for the tube, in which monomers are localized in space by quadratic confining potentials. The calculation of some of these correlation functions ($T_{\mathbf{q}}^{IJ}$, $\Delta_{0\mathbf{q}}^{IJ}$, $D_{\mathbf{q}}^I$, $S_{\mathbf{q}}^{tot}$) has been described elsewhere[21]—this is reiterated in Appendix E, along with details of the calculation for the other correlation functions.

3.5. Scattering in the Unstretched State. Remarkably, in the limit where the melt is not stretched, the predicted scattering is exactly the same as the standard RPA prediction:

$$S(\mathbf{q}) = \frac{S_{0\mathbf{q}}^{AA} S_{0\mathbf{q}}^{BB} - (S_{0\mathbf{q}}^{AB})^2}{S_{0\mathbf{q}}^{AA} + S_{0\mathbf{q}}^{BB} + 2S_{0\mathbf{q}}^{AB}} \quad (25)$$

where $S_{0\mathbf{q}}^{IJ} = T_{\mathbf{q}}^{IJ} + \Delta_{0\mathbf{q}}^{IJ}$, evaluated in the limit of no stretching. This is reproduced despite the obvious complexity of the above procedure and the resulting scattering expression, but only under specific conditions (which are fulfilled in the present model). These conditions relate to the distribution of the quenched variables in the system and their associated fields. They can be summarized by the statement that these quenched variables must have a distribution commensurate with values they would take under normal fluctuations of the polymer melt. The standard RPA treats all variables as annealed, averaging over all the possible configurations of the polymer melt. In this calculation, we quench some of the variables, but nevertheless their quenched values must be consistent with the averaging in the standard RPA. Hence, the reproduction of eq 25 in the unstretched limit represents a test that the quenched variables have been treated consistently in the model.

Two particular aspects of this constraint on the quenched variables must be emphasized. First, there are correlations between the quenched positions of the tubes from different chains. Such correlations exist because of excluded-volume interactions between chains in the melt before the stretch. These interactions give rise to correlations between the chains in the melt and hence correlations between the tube positions. These correlations must be accounted for in the averaging over the quenched fields $d_{\mathbf{q},ref}^I$ and $f_{\mathbf{q}}$, and this is done using a method developed in ref 21 and described briefly in Appendix D.1. This method involves a second application of the RPA to enforce incompressibility in the melt before the stretch.

Second, there are restrictions on the distribution of the frozen in stresses represented by $f_{\mathbf{q}}$. Specifically, in the unstretched state, these should be of a distribution and magnitude commensurate with thermal fluctuations of an elastic network with modulus related to $A_{\mathbf{q}}$ and (furthermore) uncorrelated with frozen-in density fluctuations. In terms of the correlation functions calculated in the Appendix, this means that, in the unstretched state, we require

$$\Delta_{\mathbf{q}}^{ff} = \overline{f_{\mathbf{q}} f_{-\mathbf{q}}} = \left(\frac{N_e}{N}\right)^2 A_{\mathbf{q}} \quad (26)$$

which satisfies the constraint on the magnitude of $f_{\mathbf{q}}$. We also require

$$\Delta_{\mathbf{q}}^{If} = \overline{d_{\mathbf{q},ref}^I f_{-\mathbf{q}}} = 0 \quad (27)$$

We can interpret this last equation as a statement that, in the unstretched state, the random stresses are spatially uncorrelated and, in particular, there is no correlation between the random stress contributions of distant tube segments on the same chain. In the

unstretched state, then, the random stresses are no different from those that would be obtained from a "random gas" of tube segments; the spatial correlations that exist between tube segments on the same chain are irrelevant. Hence, only the "incoherent" part of the frozen in stresses are present in the unstretched state.

One needs to be very careful with any microscopic model used to calculate the elastic contributions to the free energy given by $A_{\mathbf{q}}$ and $f_{\mathbf{q}}$; the above constraints on these variables are by no means "automatic". In the model described in Appendix C, we use a "quasi-network" approach based on tube segments being represented by vectors **h** which are distributed in a Gaussian manner. In this model, we are making use of the fact that we know what the distribution of the vectors **h** should be in order for the "tube" to be consistent with the known Gaussian statistics of the chains. If one were to pursue a more detailed and complicated model for the tube, it should nevertheless reproduce this basic fact that the chains are, on average, Gaussian.

3.6. Parameters in the Model. As with the previous scattering calculations,[16,17,21] there are a number of variables required in the tube model calculation of the correlation functions. Since this paper is primarily concerned with calculations for an H-shaped polymer architecture (for which experimental data exists), we list here the full set of parameters required in such a calculation. These are based largely on the predicted relaxation mechanisms for an H-shaped polymer following a large step strain, as listed in some detail in ref 17. The variable set used in that case was:

1. The fraction of each chain which is contained in the crossbar and the fraction of arms which are labeled. These two variables are fixed by the reaction chemistry.

2. The monomer step length for Gaussian chain statistics. This can be measured in terms of a radius of gyration parameter by fitting the standard RPA result to a scattering experiment on an unstretched sample.

3. The tube diameter, used in the Warner−Edwards tube model,[24] can in principle be obtained by fitting to the linear rheological response of the polymers. However, the precise correlation between the Warner−Edwards model (in which the monomers are localized by quadratic potentials) and the melt tube (in which monomers can fluctuate along the tube length) is unclear. It is doubtful whether the Warner−Edwards "tube diameter" and the melt tube diameter inferred from rheology are the same. Nevertheless, one would anticipate that they be of the same order of magnitude. Furthermore, the tube diameter should be scaled to account for tube dilation by constraint release as

$$d_0 = d_{00}\phi^{-\alpha/2} \tag{28}$$

where d_{00} is the "undiluted" tube diameter and ϕ is the fraction of unrelaxed chain material at a given relaxation time. The exponent α is taken to be[16,25] $4/3$.

4. The fraction, x, of the arms that have relaxed at a given relaxation time. An estimate of this can be obtained from the fitting the linear rheology spectrum using the theory of ref 16, though we should note that this relaxation spectrum is not necessarily appropriate for relaxations in the nonlinear regime.

5. The degree of retraction of the arms. Following a nonlinear stretch, it is conjectured[14] that the H-polymer arms (which are stretched to above their equilibrium length in the tube by the Doi−Edwards factor[1] $\alpha(\mathbf{E})$) should retract back to their equilibrium length in the tube. There is no impediment to this motion, and the theoretically predicted time scale for this is the Rouse relaxation time of the arms (which is typically shorter than the experimental time scale, so the arms should have retracted to their equilibrium tube length). In the fits to data below, these retractions are reported as a "degree of retraction", z_r, defined so that the chains are retracted within the tube by a factor

$$\gamma = z_r(\alpha(\mathbf{E}) - 1) + 1 \tag{29}$$

where $\alpha(\mathbf{E})$ is the Doi−Edwards tube elongation factor. Hence, a value of $z_r = 0$ represents an unretracted chain, whereas a value of $z_r = 1$ represents a chain that is "fully" retracted by the Doi−Edwards factor, $\alpha(\mathbf{E})$.

6. The degree of branchpoint withdrawal. The H-polymer crossbar is, like the arms, stretched to above its equilibrium length in the tube. However, its retraction is impeded by the entropic penalty of pulling the branchpoints into the central tube. Ideally, there would be no branchpoint withdrawal at stretches less than $\lambda \approx 4$, for which[14] $\alpha(\mathbf{E}) = 2$, but there may be some branchpoint withdrawal due to local displacement of the branchpoint within the smooth elastic potential minimum of the tube branchpoint site.[22] Such branchpoint withdrawal must be on the order of magnitude of a tube diameter (note that the tube diameter can increase with time due to tube dilation). The theoretically predicted time scale for branchpoint withdrawal is roughly the Rouse time of the whole polymer. In the fits below, the amount of branchpoint withdrawal is reported in terms of the degree of retraction of the crossbar, defined analogously to the arm degree of retraction.

Additionally, in this present calculation, we use the following parameters. The first two of these could (and should) have been included in previous calculations for the H-polymer melt.[16,17,21] The third is the only extra parameter required in this new theory.

7. In some of the experiments (notably in the H-shaped polybutadiene sample in the accompanying experimental paper[18]) there is evidence of a significant quantity of two major impurities: an "H" polymer with an arm missing (i.e., a star polymer with on long arm) and an "H" polymer with a double-backbone unit. These are present in sufficiently large quantities to affect the scattering and so must be included in the calculation. This involves calculating correlation functions for these impurities and adding these to the correlation function of the "pure" H-polymer in an appropriately weighted manner (see Appendix E.10). There is also evidence of enough polydispersity in the blocks to have a significant effect on the low wavevector scattering. Methods for dealing with this are described in some detail in the accompanying paper[18] and are also utilized below.

8. It has been predicted, in the case of polymer networks, that the magnitude of the localizing potentials in the Warner−Edwards model should deform affinely with the strain,[26−29] such that the Warner−Edwards "tube diameter" in the Cartesian direction μ varies as

$$d_\mu = d_0\lambda_\mu^{\nu} \tag{30}$$

where λ_μ is the macroscopic stretch ratio in this Cartesian direction and the exponent ν is predicted to take a value of $1/2$ in the case of networks. It should be noted that the Warner−Edwards model is a somewhat arti-

ficial construct, especially in the case of melts as indicated above. Bearing this in mind, we have allowed ourselves a choice of the exponent ν; typically, we have tried both $\nu = 0$ and $\nu = {}^1/_2$.

9. The new theory requires just one additional parameter, N/N_e, which is the ratio of a reference degree of polymerization, N, to the entanglement molecular weight, N_e. The typical degree of polymerization of the polymers (N) determines the magnitude of composition fluctuations in the system. Hence, the ratio N/N_e sets the ratio between composition and elastic fluctuations in the system. Although N_e is related to the tube diameter, we noted above that the Warner−Edwards tube diameter is a poorly understood quantity, so we keep the variables N_e and d_0 as separate variables. (Nevertheless, we expect $d_0^2 \approx N_e b^2$ at least in order of magnitude.) Just as the tube diameter is dilated by constraint release via eq 28, so N_e must vary as

$$N_e = N_{e0}\phi^{-\alpha} \tag{31}$$

It is clear from the above that, while there are many variables in the model, all of them either are fixed or remain strongly constrained by physical considerations respecting the tube model.

4. Comparison of Theory with Available H-Polymer Data

4.1. Polybutadiene Data. The accompanying experimental paper[18] presents neutron scattering data from a melt of H-shaped polybutadiene polymers, in which the crossbar is wholly labeled with deuterium. The melt also contained quite significant impurities: a "three-arm" polymer (25 vol %) and a "double-crossbar" H-polymer (about 5 vol %). The melt was uniaxially stretched by a factor of $\lambda = 2$ and then allowed to relax at constant strain, with scattering data obtained at various times of relaxation. That paper also shows a detailed comparison with the present theory. It is found that those scattering data are well represented by this theory, using parameters consistent with tube model fits to linear rheological data. In particular, the fraction of the arms that has relaxed orientationally at each of the measured times corresponds very well with the values obtained from linear rheology. At relaxation times where one would expect a large fraction of each arm to have relaxed the scattering data exhibit a strong increase in the peak scattering parallel to the stretch, together with a small decrease perpendicular to the stretch, and this feature is very well predicted by the theory. The apparent mechanism for this is the same as described above for the "block copolymer" network above: the elastic inhomogeneities couple to the motion of the relaxed H-polymer arms, giving an increased scattering parallel to the stretch. Since the arms can only move a finite distance, the order of their radius of gyration, the scattering is enhanced only at wavevectors commensurate with this length scale and not at smaller wavevectors. Moreover, the enhancement of the scattering is not possible until the arms have relaxed sufficiently, so that the scattering anisotropy increases with increasing arm relaxation.

One further aspect of the theoretical fit in this experiment is that these data are best represented by the theory when the Warner−Edwards tube diameter is allowed to vary with strain with an exponent $\nu = {}^1/_2$ (the same as predicted for polymer networks). Because of the numerous approximations in the present model (these will be discussed further in the conclusions), this result is thought indicative at best, as it is likely to be model-dependent. It is possible to obtain a reasonable fit to the data using other choices of the tube deformation parameter. The more robust conclusion from these data is that the elastic inhomogeneities are the prime cause of the large scattering anisotropy at late times, as this feature is qualitatively predicted by the model for a wide range of parameter choices.

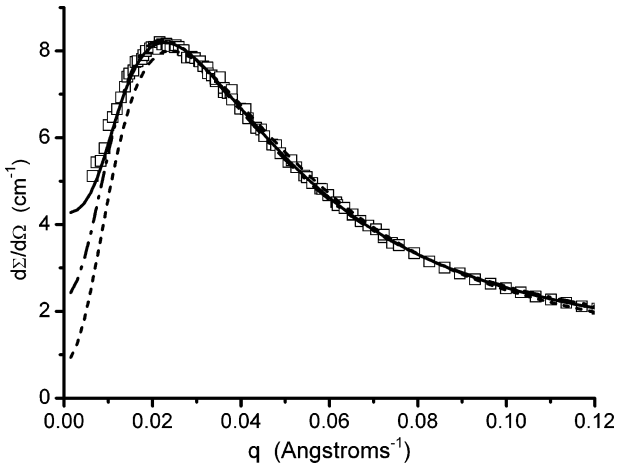

Figure 3. Scattering from isotropic H-polyisoprene sample, together with theoretical fits to the data: without polydispersity corrections (dashes); with each tip independently polydisperse using parameter $\epsilon = 0.4$ (dot−dash); with approximate polydispersity correction, using $a = 0.7$ (solid line).

4.2. Polyisoprene Data. Previously published work[17] presented scattering data from a melt of H-shaped polyisoprene polymers, with a backbone molecular weight of 111K and arm molecular weight 52.5K. The outermost 10K of each arm was labeled with deuterium. The size of this H-polymer, relative to its tube diameter, is similar to that of the polybutadiene sample above ($M_e \approx$ 4K−5K for PI, $M_e \approx$ 2K for PB). Hence, as far as the tube model theory is concerned, experiments on the two samples monitor the relaxation of essentially the "same" polymer but with different labeling. It is thought, however, that the impurities in this polyisoprene melt are present at lower volume fractions: 3 vol % of the "double-crossbar" polymer and roughly 10% of the "three-arm" polymer. (It is difficult to put a precise value on this, since the three-arm polymer has an almost identical hydrodynamic radius to the H-shaped polymer, and so the two are not resolved by SEC.)

Scattering data from this melt are available at two different values for the uniaxial stretch, at both $\lambda = 2$ and $\lambda = 3$. We will discuss each case separately below. However, in the previous publication of these polyisoprene data,[17] neither the impurities nor polydispersities of the blocks were taken into account in the theoretical fits. In the accompanying paper on the polybutadiene sample, it is shown that both the impurities and the polydispersity were important in achieving a good description of the data, especially for the peak perpendicular to the stretch. For this reason, we begin with a consideration of the isotropic data to obtain a reasonable estimate of the magnitude of the polydispersity.

4.2.1. Isotropic Data. Figure 3 shows the isotropic scattering data for the sample, together with theoretical

fits both without and with two different polydispersity corrections. The corrections made for polydispersity proceed along similar lines to the accompanying polybutadiene paper.[18] However, in this sample, the effects are dominated by the polydispersity of the labeled arm tips. (This is due to the fact that the tips constitute a small fraction of the overall polymer size, so variations in the tip length result in larger changes in the fractional deuterium content of a molecule than equivalent variations in, say, the backbone length.) Additionally, smaller blocks formed by anionic polymerization tend to have larger polydispersities; hence, the small labeled tips would be expected to have the largest polydispersity out of the constituent blocks of these molecules. For this reason, we include only polydispersity of the labeled arm tips in fitting the data, assuming the backbone and unlabeled sections of arm to be monodisperse.

In the first (and more realistic) polydispersity-corrected fit shown in Figure 3, we assume that each of the labeled tips has a degree of polymerization distributed uniformly between $N_{b0}(1-\epsilon)$ and $N_{b0}(1+\epsilon)$. The length of each tip is assumed to vary independently of the others. Under this assumption, all tips have polydispersity

$$\left.\frac{M_w}{M_n}\right|_{tip} = 1 + \frac{\epsilon^2}{3} \tag{32}$$

The polydispersity of the whole H-polymer under this assumption is

$$\left.\frac{M_w}{M_n}\right|_{H-polymer} = 1 + \frac{4\epsilon^2 f_{tip}^{\ 2}}{3} \tag{33}$$

where f_{tip} is the fraction of the H-polymer contained in a single tip of average length. The fit shown uses a value of $\epsilon = 0.7$, which corresponds to a tip polydispersity of 1.16 (this is realistic for such a short chain) and an H-polymer polydispersity of 1.0006. In practice, the H-polymer polydispersity will be larger than this because the other blocks are also polydisperse (but without such a strong effect on the scattering).

Again, following the method described in ref 18, we show a fit to the data using a more "artificial" polydispersity correction, as follows. We model the melt as a blend of three separate populations of chains; (i) in which all the chains have the degree of polymerization and architecture defined by the mean parameters of the melt; (ii) in which all the labeled tips are increased in length by a factor $(1 + a)$, and (iii) in which all the labeled tips are decreased in length by a factor $(1 - a)$. These three populations are included with equal weight in the calculation of correlation functions for the sample. Note that, in contrast to the polybutadiene case[18] in which the whole arms had the same labeling, we only adjust the length of the labeled tips and not the unlabeled blocks. Each population contains both the H-polymer and impurities at the levels given above. The fit shown uses a parameter $a = 0.4$ and gives a similar result to the more realistic polydispersity correction in the range of the experimental data. To avoid further complication to the theory, we use this approximate method (with the same value of $a = 0.4$) to model the polydispersity in all the stretched sample data presented below.

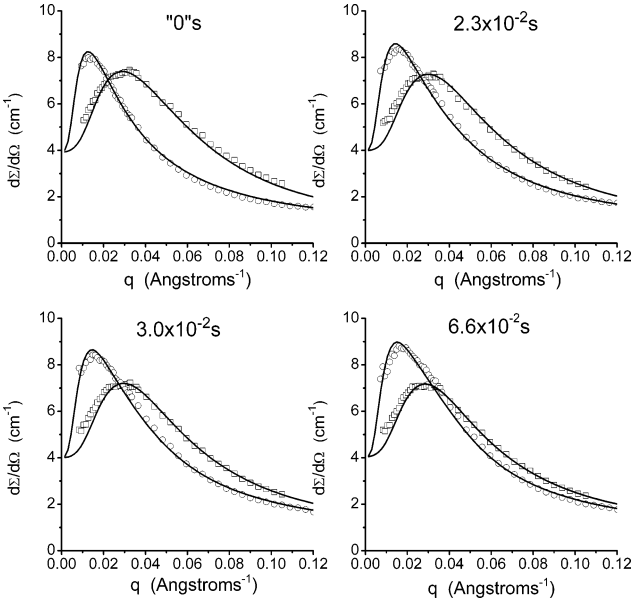

Figure 4. Scattering parallel (circles) and perpendicular (squares) to a stretch of $\lambda = 2$ for the H-polyisoprene sample after various relaxation times, together with theoretical fits to the data. Fitting parameters given in Table 1.

All the fits shown use the same value of the radius of gyration of the polymer. As detailed in the correlation function calculations of Appendix E, this is parametrized in terms of the radius of gyration of a linear polymer of the same degree of polymerization as the H-polymer, for which we use a value of $R_g = 175$ Å. This suggests that for linear polyisoprene polymers

$$R_g = 0.309\sqrt{M} \tag{34}$$

This is in good agreement with the scaling law given in the literature[30] but is very slightly smaller than that used in previous fits on the same sample[17] which did not account for the polydispersity or impurities.

4.2.2. $\lambda = 2$ Data. The available data for stretches of $\lambda = 2$ are straightforward to fit by the theory. Figures 4 and 5 show fits to the data using equivalent parameters to those used above in matching the polybutadiene data (i.e., using the deformed tube diameter with exponent $\nu = {}^1/_2$, although fits of similar quality could be obtained using an undeformed tube diameter). The parameters used to obtain the fits shown are given in Table 1. As was found previously in fitting the same data with an earlier theory, the polymers appear to be much less relaxed than is predicted from the experimental relaxation time. In particular, to fit the data, one needs to use much lower values of the parameter x (the fraction of the arms that has relaxed) than is obtained from the linear rheology. The main feature of the scattering data that causes this discrepancy is the persistently high anisotropy at large wavevectors—larger values of x do not give such a high anisotropy within this present theory. (Indeed, it seems unlikely that *any* RPA-based theory would give such large anisotropies in the high-q region at larger values of x.) A second feature is that the data do not show the increase of anisotropy at low wavevectors that would be expected of a more relaxed sample. The most reasonable interpretation is that the chains, for some unknown reason (either instrumental or due to specific problems

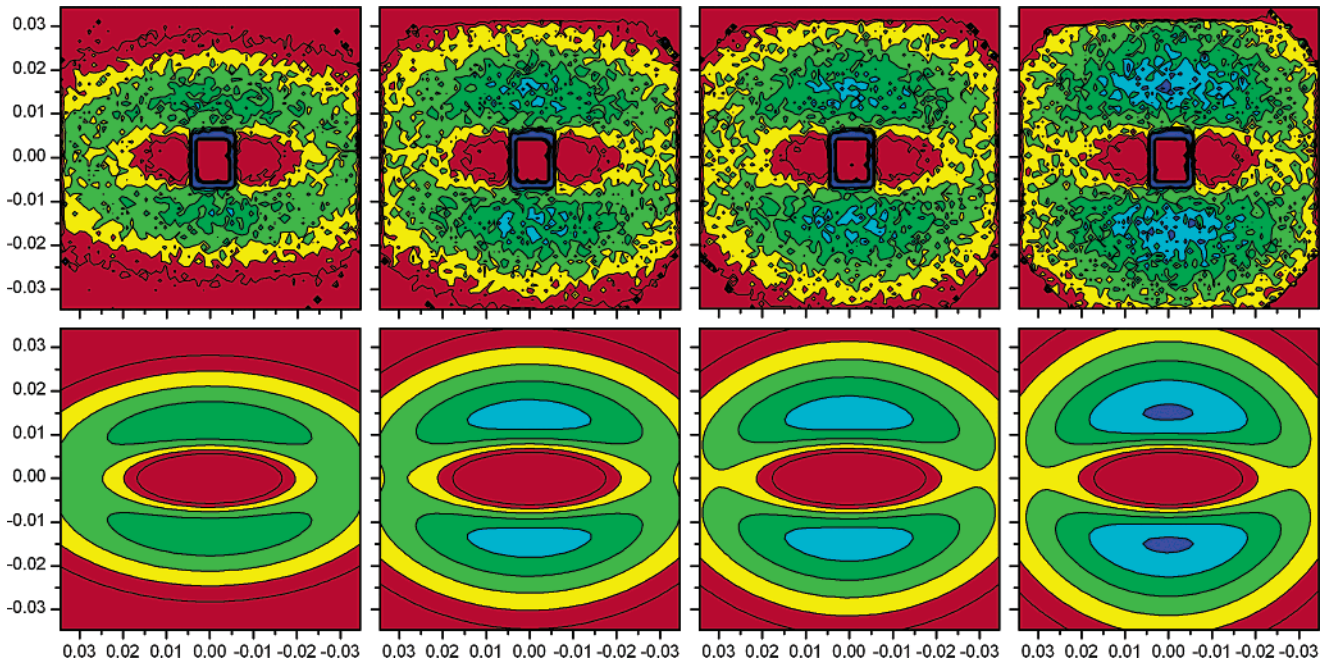

Figure 5. Top: 2D scattering for the H-polyisoprene sample after a stretch of $\lambda = 2$ with increasing relaxation time from left to right. Bottom: theoretically predicted 2D scattering, using the same parameters as gave the fits of Figure 6 (in Table 1). Contours are evenly spaced at intensities of 6, 6.583, 7.167, ..., 8.917 cm^{-1}.

Table 1. Fitting Parameters for the Tip Labeled HPI Data, at a Sample Deformation of $\lambda = 2$

relaxation time[a]	"0" s[b]	2.3×10^{-2} s	3.0×10^{-2} s	6.6×10^{-2} s
polydispersity parameter, a	0.4	0.4	0.4	0.4
d_{00}	32 Å	32 Å	32 Å	32 Å
N/N_{e0}	64	64	64	64
H-arm relaxation, x (rheology value[c])	0.06 (0.12)	0.095 (0.38)	0.11 (0.41)	0.15 (0.48)
long-star-arm relaxation, x_L	0.02	0.035	0.04	0.055
H-arm degree of retraction, z_{rarm}	0	1	1	1
long-star-arm retraction, z_{rL}	0	0	0	0
double-H-crossbar retraction, z_{rcr2}	0	0	0	0
tube deformation exponent, ν	0.5	0.5	0.5	0.5

[a] Relaxation time at room temperature based on WLF shifting of time and temperature data. [b] Estimated relaxation time is 10^{-3} s. [c] Rheology values based on fits to oscillatory linear rheology data.

with the sample), are not in fact as relaxed as they "should" be. For example, although great care was taken with the temperature measurement for the sample, one could speculate that there might have been some problems with the WLF time−temperature shifting of the relaxation times. With this one caveat regarding the degree of relaxation of the polyisoprene sample, then, we can say that the polybutadiene and polyisoprene data are consistent at stretches of $\lambda = 2$ and that both can be fit by the theory.

4.2.3. $\lambda = 3$ Data. Figures 6 and 7 show respectively the along axes and 2D scattering data for the sample uniaxially stretched by a factor of 3 at various times of relaxation. The parameters used to obtain the data fits shown are given in Table 2. As with previous theories,[17] the first two relaxation times are well described by this present theory, although (in common with the above data at $\lambda = 2$) one needs to assume that the polymers are less relaxed than would be expected from the experimental relaxation time. Again, one needs to use much lower values of x (the fraction of the arms that has relaxed) than is obtained from the linear rheology. The main reason for this remains the larger than expected anisotropy at high wavevectors.

In contrast, the data at the longest two times of relaxation do show the expected decrease in anisotropy at high wavevectors and a strongly increasing anisotropy at low wavevectors, with increasing relaxation time of the sample. It was this strong increase in anisotropy in the low wavevector region at late times that prevented these data being satisfactorily fit with the previous theory.[17] One would expect, then, that this present theory, which includes effects due to elastic inhomogeneities, would give an improved description of these data, as in fact it does. At the third relaxation time (nominally 8.7×10^{-2} s), it is now possible, with this present theory, to obtain a very good description of the along-axis data (Figure 6). The 2D data are reasonably well described, although the parallel peak in the experimental data is clearly broader in the off-axis direction than is suggested by the theory; this breadth of the parallel peak appears to be a precursor to the four-point pattern in the longest relaxation time described in more detail below.

The value of x used to fit the third relaxation time at $\lambda = 3$ is, in fact, consistent with the linear rheology value. In this context, it is remarkable that the anisotropy in the high wavevector region disappears almost completely between the second and third relaxation times, even though the experimental data suggest they are of similar order of magnitude (2.3×10^{-2} and 8.7×10^{-2} s). There appears to have been a great deal of "relaxation" between the two sets of data. It is reasonable to infer that whatever caused the lack of relaxation

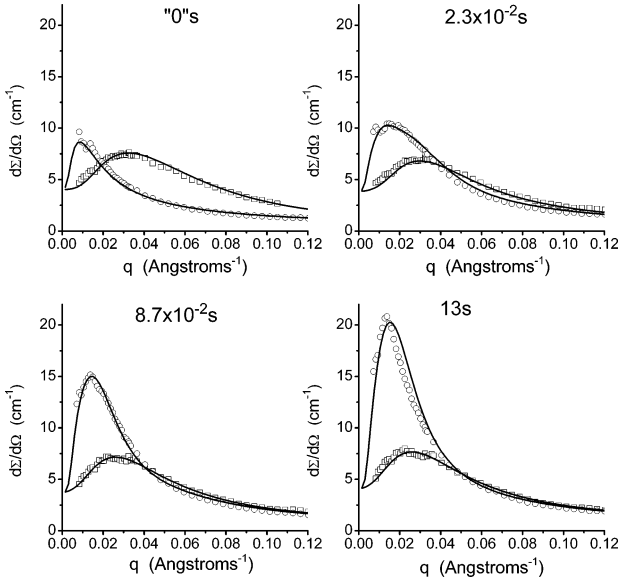

Figure 6. Scattering parallel (circles) and perpendicular (squares) to a stretch of $\lambda = 3$ for the H-polyisoprene sample after various relaxation times, together with theoretical fits to the data. Fitting parameters given in Table 2.

in the $\lambda = 2$ data could be present to some extent in the first two relaxation times at $\lambda = 3$ but is present to a much lesser extent in the last two relaxation times of the $\lambda = 3$ data—this is reflected in the fitting parameters, especially in the values of the relaxed arm fraction, x. These data for the first three relaxation times are also best fit using a deformed tube diameter, using an exponent $\nu \approx 0.4$ that is slightly smaller than the value used to fit the $\lambda = 2$ data. Nevertheless, this still represents a tube that is more deformed than at $\lambda = 2$. There is no a priori reason the tube deformation should follow a precise power law as a function of stretch in the melt (or even remain the same at different relaxation times).

The last relaxation time in these data still presents significant problems as regards fitting by the theory. At this relaxation time, one would expect (from linear rheology) a fraction $x = 0.8$ of the arm to have relaxed. For the tip-labeled polyisoprene sample, the theory in fact predicts an increasing peak anisotropy up to $x \approx 0.5$ but then decreasing peak anisotropy after that. (In contrast, the previous theory[17,21] without elastic inhomogeneities gave increasing peak anisotropy only up to $x \approx 0.3$.) In the experimental data, however, the last relaxation time shows an extremely strong peak anisotropy and, moreover, displays a four-point pattern. It is possible, by choosing appropriate parameters in the theory, to match the degree of peak anisotropy, though not the peak shape, as shown in Figure 6 (to do this typically requires choosing a smaller value of the exponent ν). However, the parameters required to achieve this are inconsistent with those used to fit the rest of the H-polymer data and with the linear rheology. Moreover, they do not give a four-point pattern and so, as demonstrated in Figure 7, do not give a good representation of the full 2D scattering data. It is possible, with other choices of parameter, to produce a "four-point" pattern with the theory, but this does not give the correct magnitude of the scattering. The indication is that either (i) some of the approximations used for calculation of the correlation functions and the magnitude of the elastic inhomogeneities begin to break down at this magnitude of stretch and relaxation time or (ii) there are important aspects of the physics, not yet included in the theory, which manifest themselves most strongly at this late relaxation time and for larger stretches. These possibilities will be discussed further in the concluding section.

5. Discussion and Conclusions

This paper has presented a new theory for the prediction of scattering from partially labeled polymer melts, following relaxation after a step strain. The theory is based upon the random phase approximation (RPA) but includes (in the manner of Panyukov and Rabin[11]) the effect of elastic fluctuations and inhomogeneities in the entanglement mesh that are thought to give rise to the anomalous "butterfly patterns" in scattering from stretched polymer networks and gels. One feature of this present theory is that it reproduces the standard RPA prediction for scattering from an unstretched melt. For it to do this, there are constraints on the quenched variables used to describe the elastic inhomogeneities and frozen in composition variations caused by the polymer tubes; these must be "quenched" at values commensurate with normal fluctuations in the unstretched melt. In particular, this requires an application of the RPA to deal with excluded-volume interactions in the melt prior to the stretch, as with a previous theory.[21]

The elastic inhomogeneities couple to the motion of free, unentangled "species" in the melt. In polymer networks or melts containing short (quickly relaxing) chains or solvent, these species are free to move large distances, giving the "butterfly" patterns. We have demonstrated in this paper that the elastic inhomogeneities can also couple to the motion of chains attached at one end to the chemical or entanglement network. Because such chains cannot move large distances, the result is an enhancement of the scattering parallel to the stretch, but only at finite wavevectors commensurate with the radius of gyration of the partially free species. The theory developed in this paper is able to describe both these effects, provided appropriate correlation functions are chosen to describe each of the constituent species.

We have demonstrated that this latter mechanism has a significant effect on the predicted scattering for stretched melts of H-shaped polymers. The relaxing H-polymer arms act as partially free species, which couple to the elastic inhomogeneities. Inclusion of this effect results in the theory being able to fit quantitatively most of the available scattering data from the stretched H-polymer melts. This is despite the numerous approximations that evidently remain in the calculation. It would appear that elastic inhomogeneities are indeed present in polymer melts. (In fact, this was demonstrated much earlier in refs 4 and 6 where butterfly patterns were seen in bimodal melts of linear polymers.) We have now shown that they also have an effect when there is no completely free component.

However, scattering data at the longest relaxation time for the "tip-labeled" polyisoprene sample, stretched by a factor of 3, remain impossible to fit by the theory with the current set of approximations. This fact leads one to examine, critically, the remaining approximations, which are made for the sake of simplifying what is already a very long calculation. One can certainly criticize the use of the Warner−Edwards model for the

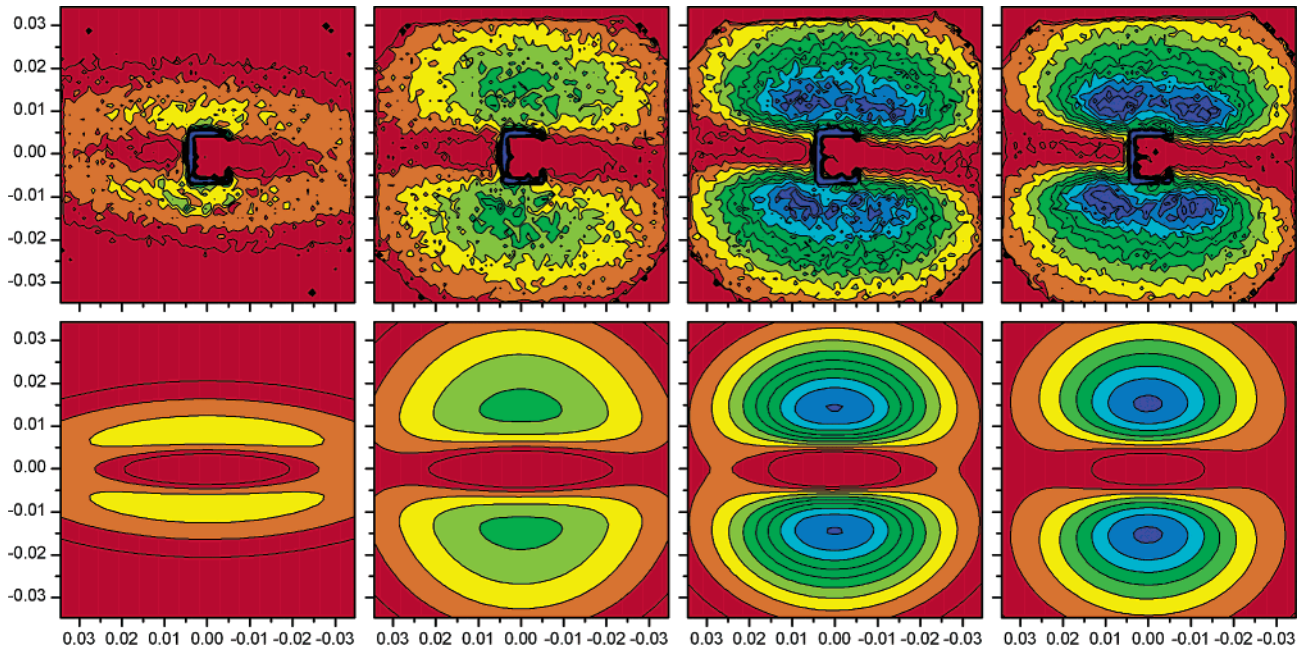

Figure 7. Top: 2D scattering for the H-polyisoprene sample after a stretch of $\lambda = 3$ with increasing relaxation time from left to right. Bottom: theoretically predicted 2D scattering, using the same parameters as gave the fits of Figure 8 (in Table 2). Contours are evenly spaced at intensities of 6, 7, 8, ..., 15 cm^{-1}, except for the rightmost plots which use 6, 8, 10, ..., 20 cm^{-1}.

Table 2. Fitting Parameters for the Tip Labeled HPI Data, at a Sample Deformation of $\lambda = 3$

relaxation time[a]	"0" s[b]	2.3×10^{-2} s	8.7×10^{-2} s	13 s
polydispersity parameter, a	0.4	0.4	0.4	0.4
d_{00}	32 Å	32 Å	32 Å	32 Å
N/N_{e0}	64	64	64	64
H-arm relaxation, x (rheology value[c])	0.04 (0.12)	0.18 (0.38)	0.58 (0.50)	0.58 (0.86)
long-star-arm relaxation, x_L	0.015	0.07	0.23	0.23
H-arm degree of retraction, z_{rarm}	0	1	1	1
long-star-arm retraction, z_{rL}	0	1	1	1
H-crossbar retraction, z_{rcross}	0	0.2	0.25	0.3
double-H-crossbar retraction, z_{rcr2}	0	0.1	0.125	0.15
tube deformation exponent, ν	0.4	0.4	0.4	0.2

[a] Relaxation time at room temperature based on WLF shifting of time and temperature data. [b] Estimated relaxation time is 10^{-3} s. [c] Rheology values based on fits to oscillatory linear rheology data.

polymer tube in the calculation of the correlation functions. In a melt, one expects there to be significant fluctuation of the chain along the tube contour since there is no impediment to this motion. Such fluctuations are not included in the Warner−Edwards model, in which monomers are constrained in all three dimensions by quadratic localizing potentials. In this context, it is worth noting that these along-tube fluctuations have a magnitude which varies with position along the chain in a branched polymer and which is dependent on the architecture of the chain. However, in an unstretched melt, one expects the chain conformation to be Gaussian *after averaging over these fluctuations along the tube.* It is clear that the statistical shape of the tube contour must depend on the size of these fluctuations and hence must vary with position along a branched chain! This fact appears to be absent from all tube model theories to date. The correct mathematical description of along-tube fluctuations in a scattering calculation for branched polymers is a challenging task.

A second, somewhat related, approximation in this work is the use of a single variable, x, to represent the fraction of each polymer arm that has relaxed (and escaped the oriented tube) in a given time. In fact, this relaxation is a stochastic process, and it is not the case that all the polymer arms will have relaxed to exactly the same degree. It would be better to have used a distribution of the variable x, independently distributed for each arm.

Similarly, the "quasi-network" approach used in this work to calculate the magnitude of the elastic contributions to the free energy (and the elastic inhomogeneities) is very much open to criticism, although it is consistent with the usual tube model calculation of the time-dependent modulus. One reason for choosing this approach, however, was that an exact solution was known, so that the model gave a self-consistent distribution for the quenched random stresses and hence a correct expression for the scattering in the unstretched limit.

Finally, as has been pointed out before,[17,21] this calculation assumes that all the chains retract by the same amount within the tube after a large stretch. This assumes that all the polymer tubes are extended by the same factor, the Doi−Edwards elongation ratio, $\alpha(\mathbf{E})$. This factor is, indeed, the average elongation of a very long tube containing *many* tube segments. However, the chains used in the H-polymer experiments are relatively short, containing (roughly) 20 undiluted tube segments along the H-polymer backbone. Furthermore, it is more appropriate to consider the tube after the "dynamic dilution" that occurs as the arms relax. At the end of full arm relaxation, the H-polymer backbones contain

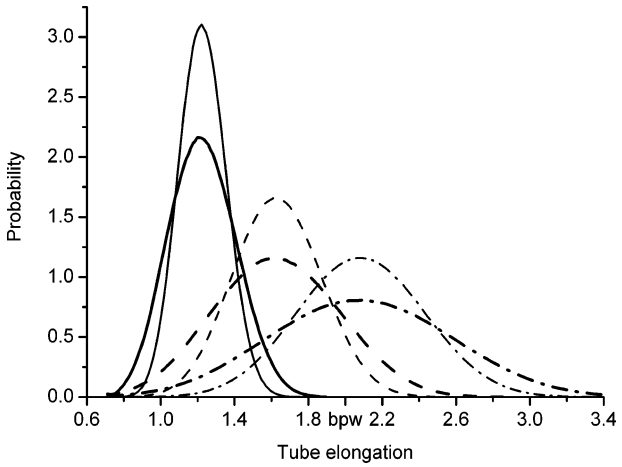

Figure 8. Tube elongation distribution for tubes containing 5 (thick lines) and 10 (thin lines) tube segments, after stretches of $\lambda = 2$ (solid lines), $\lambda = 3$ (dashed lines), and $\lambda = 4$ (dot−dashed lines). Distributions are numerically generated from affine deformation of tube paths containing randomly oriented tube segments. The ideal critical backbone tube elongation for branchpoint withdrawal[14] is marked as "bpw" on the *x*-axis.

only about five diluted tube segments. Some of these tube segments will be oriented more parallel to the stretch, and some more perpendicular, so one would expect there to be quite a strong variation in the actual elongation of individual tubes, affecting both the degree of retraction of chains and the amount of branchpoint withdrawal. Figure 8 shows the expected distribution of elongation factors of tubes containing 5 and 10 tube segments at uniaxial stretches of $\lambda = 2$, 3, and 4. (These curves are numerically generated by obtaining the elongation ratio after an affine deformation of "tubes" made from randomly oriented tube segments.) It is clear that each curve is, to reasonable approximation, a Gaussian distribution about the Doi−Edwards average $\alpha(\mathbf{E})$. However, the standard deviation increases with both increasing stretch and increasing tube dilation (i.e., decreasing number of tube segments). In particular, for tubes comprising five segments at $\lambda = 3$, more than 10% of the tubes are above the critical elongation ratio of 2, which corresponds to the ideal maximum stretch condition of an H-polymer backbone.[14] On this basis, it is perhaps not such a surprise that the present theory fails at the longest relaxation time for $\lambda = 3$ while providing a reasonable description of the available $\lambda = 2$ data.

Future work, then, should aim to remove some of these remaining approximations from the calculation. It should also examine the effect of other proposed refinements to the tube model, expected to have an effect particularly at large nonlinear stretches, such as convective constraint release[31−34] and nonaffine entanglement deformation from local chain force balance.[35] It would clearly be very useful to have a greater range of available experimental data—for example, data on the polybutadiene sample at stretches of $\lambda = 3$ would confirm whether it is, as speculated above, the larger stretch in the polyisoprene data that causes problems for the theory. This paper has investigated just one of the possible refinements to the theory suggested in an earlier publication.[17] It has shown that elastic inhomogeneities do indeed have a significant effect of the scattering from partially labeled H-shaped polymers and that their inclusion in the theory resolves some of the discrepancies between theory and experiment. While some strong discrepancies remain, it is possible to speculate on the reasons for this and to suggest further routes for investigation.

Acknowledgment. I am very grateful for the financial support of an EPSRC Advanced Research Fellowship. I also acknowledge very helpful discussions with T. C. B. McLeish, M. Heinrich, and W. Pyckhout-Hintzen.

Appendix A. Derivation of Free Energy Functional

In this Appendix, we derive a free energy for concentration fluctuations of the different monomer species in the partially labeled polymers, including elastic fluctuations in the entanglement network. The result is similar in form to that derived by Panyukov and Rabin[11] for swollen gels and is effectively a combination of their result with one derived earlier[21] for concentration fluctuations in the present of *fixed* tube constraints (i.e., in the absence of elastic fluctuations).

We consider the statistical mechanics of fluctuations in the melt following a step deformation from an equilibrated, isotropic state. As argued in the Introduction and in ref 21, we suppose that the experimental time scale is such that some of the tube variables are effectively "quenched"—relaxing on time scales much slower than the experimental time. We shall make a formal separation between such "quenched" variables and annealed variables which can relax on the experimental time scale, calculating a free energy functional subject to these "quenched" variables remaining fixed.

We define Fourier transformed densities of the different monomer species, I, as

$$P^{\mathrm{I}}_{\mathbf{q}}\{\mathbf{r}_{\alpha,s}\} = \frac{1}{(\Omega\rho N)^{1/2}} \sum_{\alpha,s} y^{\mathrm{I}}_{\alpha,s} \exp(i\mathbf{q}\cdot\mathbf{r}_{\alpha,s}) \qquad (35)$$

where $\mathbf{r}_{\alpha,s}$ is the position of monomer s on chain α and $y^{\mathrm{I}}_{\alpha,s} = 1$ if this monomer is of species I and is zero otherwise (I = A or B for the majority of this paper). Ω is the total volume of the system, and ρ is the total momomer density (we shall assume all "monomers" occupy the same volume) so that $\Omega\rho$ is the total number of monomers. N is a reference degree of polymerization, included in this definition for later convenience. (In a pure copolymer system, for example, it is most convenient to set N to be the degree of polymerization of the copolymer.)

Note that, in eq 35, we have used the "dummy" variable $P^{\mathrm{I}}_{\mathbf{q}}$ to represent a quantity which is an explicit function of the monomer positions $\mathbf{r}_{\alpha,s}$, retaining the variable $\rho^{\mathrm{I}}_{\mathbf{q}}$ for the associated field (introduced below). This explicit distinction is useful when performing the detailed calculation. In the main text of the paper, for the sake of brevity and clarity, we do not make such a distinction and use only the variable $\rho^{\mathrm{I}}_{\mathbf{q}}$.

We shall assume that the tube constraints are such that, in the absence of elastic fluctuations of the network (i.e., at *fixed* tube positions), each monomer (α, s) is restricted to fluctuate about some mean position, denoted as $\hat{\mathbf{r}}_{\alpha,s}$. However, the effect of network fluctuations is that the tubes (and hence the mean monomer positions) are able to move. We suppose that, under these fluctuations, the mean monomer position is displaced as

$$\hat{\mathbf{r}}_{\alpha,s} = \hat{\mathbf{r}}_{\mathrm{ref},\alpha,s} + \mathbf{w}_{\alpha,s} \tag{36}$$

where $\mathbf{w}_{\alpha,s}$ is the displacement from a reference position $\hat{\mathbf{r}}_{\mathrm{ref},\alpha,s}$. We shall take this reference configuration $\hat{\mathbf{r}}_{\mathrm{ref},\alpha,s}$ to be the one that is *affinely* deformed from the initial melt state before the step deformation, and we shall treat the $\hat{\mathbf{r}}_{\mathrm{ref},\alpha,s}$ as quenched variables.

With these definitions, we can write the partition function of the system as

$$Z = \int D\{\mathbf{w}_{\alpha,s}\} \sum_{C} \exp(-U\{P^{\mathrm{I}}_{\mathbf{q}}\}) \tag{37}$$

where the sum is over all internal configurations C available to the system at fixed $\hat{\mathbf{r}}_{\mathrm{ref},\alpha,s}$ and $\mathbf{w}_{\alpha,s}$. The integral represents a sum over all possible network displacements. The energy $U\{P^{\mathrm{I}}_{\mathbf{q}}\}$ accounts for monomer−monomer interactions, such as the excluded-volume interactions which give rise to near "incompressibility" of the system. All energies will be written in units of $k_{\mathrm{B}}T$.

We can replace the sum over internal configurations by an *average* over these configurations multiplied by the number of configurations, $n_{\mathrm{C}}(\{\mathbf{w}_{\alpha,s}\})$. This gives

$$Z = \int D\{\mathbf{w}_{\alpha,s}\}\, n_{\mathrm{C}}(\{\mathbf{w}_{\alpha,s}\}) \langle \exp(-U\{P^{\mathrm{I}}_{\mathbf{q}}\}) \rangle_0 \tag{38}$$

where we have denoted by $\langle ... \rangle_0$ an annealed average over internal configurations available to the system at fixed $\hat{\mathbf{r}}_{\mathrm{ref},\alpha,\,s}$ and $\mathbf{w}_{\alpha,s}$, in the absence of excluded-volume interactions. Note that this is not a full annealed average (as is usually denoted by the angled brackets), since the variables $\mathbf{w}_{\alpha,s}$ are also, technically, annealed variables. To deal with this average, we introduce the density fields $\rho^{\mathrm{I}}_{\mathbf{q}} \equiv P^{\mathrm{I}}_{\mathbf{q}}$ via delta functions in the standard way (see refs 21 and 36)

$$Z = \int D\{\rho^{\mathrm{I}}_{\mathbf{q}}\} \exp(-U\{\rho^{\mathrm{I}}_{\mathbf{q}}\}) \int D\{\mathbf{w}_{\alpha,s}\}\, n_{\mathrm{C}}(\{\mathbf{w}_{\alpha,s}\}) \times R_1\{\rho^{\mathrm{I}}_{\mathbf{q}}, \mathbf{w}_{\alpha,s}, \hat{\mathbf{r}}_{\mathrm{ref},\alpha,s}\} \tag{39}$$

where

$$R_1\{\rho^{\mathrm{I}}_{\mathbf{q}}, \mathbf{w}_{\alpha,s}, \hat{\mathbf{r}}_{\mathrm{ref},\alpha,s}\} = \Big\langle \prod_{\mathbf{q},\mathrm{I}} \delta(\rho^{\mathrm{I}}_{\mathbf{q}} - P^{\mathrm{I}}_{\mathbf{q}}) \Big\rangle_0 \tag{40}$$

It was shown, in ref 21, that this could be evaluated to second order in the $\rho^{\mathrm{I}}_{\mathbf{q}}$ field variables and in particular that a preaverage over the second-order correlation functions was justified, giving

$$R_1\{\rho^{\mathrm{I}}_{\mathbf{q}}, \mathbf{w}_{\alpha,s}, \hat{\mathbf{r}}_{\mathrm{ref},\alpha,s}\} = \exp(-F_0\{\rho^{\mathrm{I}}_{\mathbf{q}} | \langle P^{\mathrm{I}}_{\mathbf{q}} \rangle_0\}) \tag{41}$$

where for the two-component system

$$F_0\{\rho^{\mathrm{I}}_{\mathbf{q}} | \langle P^{\mathrm{I}}_{\mathbf{q}} \rangle_0\} = \frac{1}{2}\sum_{\mathbf{q}} \frac{T^{\mathrm{BB}}_{\mathbf{q}} |\Delta\rho^{\mathrm{A}}_{\mathbf{q}}|^2 + T^{\mathrm{AA}}_{\mathbf{q}} |\Delta\rho^{\mathrm{B}}_{\mathbf{q}}|^2 - 2T^{\mathrm{AB}}_{\mathbf{q}} \Delta\rho^{\mathrm{A}}_{\mathbf{q}} \Delta\rho^{\mathrm{B}}_{-\mathbf{q}}}{T^{\mathrm{AA}}_{\mathbf{q}} T^{\mathrm{BB}}_{\mathbf{q}} - (T^{\mathrm{AB}}_{\mathbf{q}})^2} \tag{42}$$

and the second-order correlation functions are

$$T^{\mathrm{IJ}}_{\mathbf{q}} = \overline{\langle P^{\mathrm{I}}_{\mathbf{q}} P^{\mathrm{J}}_{-\mathbf{q}} \rangle_0 - \langle P^{\mathrm{I}}_{\mathbf{q}} \rangle_0 \langle P^{\mathrm{J}}_{-\mathbf{q}} \rangle_0}^{\,0} \tag{43}$$

The "0" superscript denotes that the quenched average includes no correlations between the quenched tube variables $\hat{\mathbf{r}}_{\mathrm{ref},\alpha,s}$ of separate chains (as would be caused by excluded-volume interactions in the melt before the stretch). This is discused in more detail in ref 21. The variable $\Delta\rho^{\mathrm{I}}_{\mathbf{q}} = \rho^{\mathrm{I}}_{\mathbf{q}} - \langle P^{\mathrm{I}}_{\mathbf{q}} \rangle_0$ represents a concentration variation about the mean, which is nonzero in the presence of quenched variables. In ref 21, network fluctuations were ignored, and so $\langle P^{\mathrm{I}}_{\mathbf{q}} \rangle_0$ was, itself, fixed by the quenched variables. However, with network fluctuations, this quantity is not fixed, so we introduce a second set of field variables $d^{\mathrm{I}}_{\mathbf{q}} \equiv \langle P^{\mathrm{I}}_{\mathbf{q}} \rangle_0$, again using delta functions to give

$$Z = \int D\{\rho^{\mathrm{I}}_{\mathbf{q}}, d^{\mathrm{I}}_{\mathbf{q}}\} \exp(-U\{\rho^{\mathrm{I}}_{\mathbf{q}}\}) \exp(-F_0\{\rho^{\mathrm{I}}_{\mathbf{q}} | d^{\mathrm{I}}_{\mathbf{q}}\}) \times \int D\{\mathbf{w}_{\alpha,s}\}\, n_{\mathrm{C}}(\{\mathbf{w}_{\alpha,s}\}) \prod_{\mathbf{q},\mathrm{I}} \delta(d^{\mathrm{I}}_{\mathbf{q}} - \langle P^{\mathrm{I}}_{\mathbf{q}} \rangle_0) \tag{44}$$

The next task is to incorporate field variables to represent the network fluctuations and the effect that these have on the density variables, $d^{\mathrm{I}}_{\mathbf{q}}$. We are primarily interested in small fluctuations of the network (since large deformations will be penalized by both excluded-volume interactions and large elastic free energies), and so we use a formulation that is appropriate to this limit. We begin by defining a displacement field $\mathbf{w}^{\mathrm{I}}(\mathbf{r})$ for each species I so that for all monomers of that species

$$\mathbf{w}_{\alpha,s} = \mathbf{w}^{\mathrm{I}}(\hat{\mathbf{r}}_{\mathrm{ref},\alpha,s}) = \frac{1}{\Omega}\sum_{\mathbf{q}} \mathbf{w}^{\mathrm{I}}_{\mathbf{q}} \exp(-i\mathbf{q}\cdot\hat{\mathbf{r}}_{\mathrm{ref},\alpha,s}) \tag{45}$$

where $\mathbf{w}^{\mathrm{I}}_{\mathbf{q}}$ is the Fourier transform of $\mathbf{w}^{\mathrm{I}}(\mathbf{r})$. We decompose this into components parallel and perpendicular to the wavevector so that

$$\mathbf{w}^{\mathrm{I}}_{\mathbf{q}} = \mathbf{w}^{\mathrm{I}}_{\mathbf{q}\perp} - i\frac{\mathbf{q}}{q^2}\left(\frac{N\Omega}{\rho}\right)^{1/2} \gamma^{\mathrm{I}}_{\mathbf{q}} \tag{46}$$

where

$$\gamma^{\mathrm{I}}_{\mathbf{q}} = i\left(\frac{\rho}{N\Omega}\right)^{1/2} \mathbf{q}\cdot\mathbf{w}^{\mathrm{I}}_{\mathbf{q}} \tag{47}$$

This equation should be read as a definition of a quantity, $\gamma^{\mathrm{I}}_{\mathbf{q}}$, related to the "parallel-to-wavevector" component of the Fourier transformed displacement field. The perpendicular component of this field represents "shear" waves, and the parallel component represents a compressive wave. We shall show in Appendix B that, for small entanglement network displacements, the change in mean polymer density depends only on this parallel component and can be written as

$$d^{\mathrm{I}}_{\mathbf{q}} = d^{\mathrm{I}}_{\mathbf{q},\,\mathrm{ref}} + \beta^{\mathrm{I}}_{\mathbf{q}} \gamma^{\mathrm{I}}_{\mathbf{q}} \tag{48}$$

where $\beta^{\mathrm{I}}_{\mathbf{q}}$ is a cutoff function to be defined below and $d^{\mathrm{I}}_{\mathbf{q},\mathrm{ref}} = \langle P^{\mathrm{I}}_{\mathbf{q}} \rangle_0$ evaluated in the reference state (with $\mathbf{w}_{\alpha,s} = 0$).

Note that, as introduced above, the fields $\mathbf{w}^{\mathrm{I}}(\mathbf{r})$ and $\gamma^{\mathrm{I}}_{\mathbf{q}}$ are dependent upon the displacements $\mathbf{w}_{\alpha,s}$. We can introduce fields $\Gamma^{\mathrm{I}}_{\mathbf{q}} \equiv \gamma^{\mathrm{I}}_{\mathbf{q}}\{\mathbf{w}_{\alpha,s}\}$ in the partition function via delta functions, as before, giving

$$Z = \int D\{\rho_{\mathbf{q}}^{\mathrm{I}}, d_{\mathbf{q}}^{\mathrm{I}}, \Gamma_{\mathbf{q}}^{\mathrm{I}}\} \exp(-U\{\rho_{\mathbf{q}}^{\mathrm{I}}\}) \exp(-F_0\{\rho_{\mathbf{q}}^{\mathrm{I}}|d_{\mathbf{q}}^{\mathrm{I}}\}) \times \int D\{\mathbf{w}_{\alpha,s}\} n_{\mathrm{C}}(\{\mathbf{w}_{\alpha,s}\}) \prod_{\mathbf{q},\mathrm{I}} \delta(\Gamma_{\mathbf{q}}^{\mathrm{I}} - \gamma_{\mathbf{q}}^{\mathrm{I}}) \delta(d_{\mathbf{q}}^{\mathrm{I}} - \langle P_{\mathbf{q}}^{\mathrm{I}} \rangle_0) \quad (49)$$

For small $\Gamma_{\mathbf{q}}^{\mathrm{I}}$ we can use eq 48, which is a linear relation between $\gamma_{\mathbf{q}}^{\mathrm{I}}$ and $d_{\mathbf{q}}^{\mathrm{I}}$. Using this, we can write $\gamma_{\mathbf{q}}^{\mathrm{I}}$ implicitly in terms of the fields $d_{\mathbf{q}}^{\mathrm{I}}$ (rather than in terms of the $\mathbf{w}_{\alpha,s}$), giving

$$Z = \int D\{\rho_{\mathbf{q}}^{\mathrm{I}}, d_{\mathbf{q}}^{\mathrm{I}}, \Gamma_{\mathbf{q}}^{\mathrm{I}}\} \exp(-U\{\rho_{\mathbf{q}}^{\mathrm{I}}\}) \exp(-F_0\{\rho_{\mathbf{q}}^{\mathrm{I}}|d_{\mathbf{q}}^{\mathrm{I}}\}) \times \prod_{\mathbf{q},\mathrm{I}} \delta\left(\Gamma_{\mathbf{q}}^{\mathrm{I}} - \frac{d_{\mathbf{q}}^{\mathrm{I}} - d_{\mathbf{q},\,\mathrm{ref}}^{\mathrm{I}}}{\beta_{\mathbf{q}}^{\mathrm{I}}}\right) \int D\{\mathbf{w}_{\alpha,s}\} n_{\mathrm{C}}(\{\mathbf{w}_{\alpha,s}\}) \times \prod_{\mathbf{q},\mathrm{I}} \delta(d_{\mathbf{q}}^{\mathrm{I}} - \langle P_{\mathbf{q}}^{\mathrm{I}} \rangle_0) \quad (50)$$

The integrand in this expression is strictly only valid for small $\Gamma_{\mathbf{q}}^{\mathrm{I}}$, but this is the limit that we are primarily interested in.

Finally, we need to consider the number of configurations $n_{\mathrm{C}}(\{\mathbf{w}_{\alpha,s}\})$, which deals with the number of internal configurations of the system for a given mesh deformation $\mathbf{w}_{\alpha,s}$. Unfortunately, to do this correctly requires a full microscopic model of the tube and topological entanglement constraints, which we do not possess at present. We must, therefore, resort to approximate means for evaluating the important contributions to this term. We make the following statements:

1. The entanglement constraints mean that the mesh moves as a whole. In particlar, this implies that there are not separate deformation fields, $\mathbf{w}^{\mathrm{I}}(\mathbf{r})$, for each of the components of the system. We can express this constraint in terms of delta functions, constraining all the $\Gamma_{\mathbf{q}}^{\mathrm{I}}$ to be the same.

$$\int D(\Gamma_{\mathbf{q}}) \prod_{\mathbf{q},\mathrm{I}} \delta(\Gamma_{\mathbf{q}}^{\mathrm{I}} - \Gamma_{\mathbf{q}})$$

2. There are changes in $n_{\mathrm{C}}(\{\mathbf{w}_{\alpha,s}\})$ due to local stretching of the tube segments, and these will give rise to rubber-elastic terms in the free energy functional. As detailed below, we shall evaluate these contributions by introducing vectors $\mathbf{H}_{\alpha,m}$ representing the local orientation of the mth tube segment on chain α. Assuming these vectors to be deformed from quenched initial values, we evaluate the effect of the deformation field $\Gamma_{\mathbf{q}}$ on these vectors and hence on the number of configurations of the chain within the tube. This will give rise to a factor $n_{\mathrm{el}}\{\Gamma_{\mathbf{q}}\}$ in n_{C}.

3. The tube is a mean field construction representing the topological effect that surrounding chains have on the conformation of a test chain, and in particular, the chain is constrained by the tube to be in a stretched configuration after the step strain. In dealing with the mean density $\langle P_{\mathbf{q}}^{\mathrm{I}} \rangle_0$ terms in eq 50, we treat the integral over the $\mathbf{w}_{\alpha,s}$ as an effective averaging over positions of the tube. We note that this includes an average over the chain center of mass that provides translational symmetry in the average. For each individual chain contribution to $\langle P_{\mathbf{q}}^{\mathrm{I}} \rangle_0$, we should also include the effect on the tube *conformation* of variations in $\mathbf{w}_{\alpha,s}$ along the tube contour. However, these must be penalized by the elastic energy from the deformation of the surrounding network required to effect such a change in conformation of our test chain. There should be a coupling between averages involving $\langle P_{\mathbf{q}}^{\mathrm{I}} \rangle_0$ and the elastic energy term $n_{\mathrm{el}}\{\Gamma_{\mathbf{q}}\}$. Nevertheless, we note that the effect of such elastic energy penalties is to keep the tube close to its affinely stretched configuration. For the present calculation, as regards dealing with the terms in mean density $\langle P_{\mathbf{q}}^{\mathrm{I}} \rangle_0$, we ignore the details of this coupling, and treat the internal tube conformation as being effectively frozen in its stretched configuration. We retain only an average over tube centers of mass displacements $\mathbf{w}_{\alpha,\mathrm{CM}}$. In doing this, we note that (i) these center-of-mass displacements are, in fact, still implicitly penalized via the $n_{\mathrm{el}}\{\Gamma_{\mathbf{q}}\}$ elastic energy term and (ii) the effect of network fluctuations on the tube configuration must, to first order, already be included in many models used to describe the tube, since their effect is to allow the tube (and hence, chain) to fluctuate about a mean configuration.

Combining these contributions to $n_{\mathrm{C}}(\{\mathbf{w}_{\alpha,s}\})$ allows us to rewrite eq 50 as

$$Z = \int D\{\rho_{\mathbf{q}}^{\mathrm{I}}, d_{\mathbf{q}}^{\mathrm{I}}, \Gamma_{\mathbf{q}}^{\mathrm{I}}, \Gamma_{\mathbf{q}}\} \exp(-U\{\rho_{\mathbf{q}}^{\mathrm{I}}\}) \times \exp(-F_0\{\rho_{\mathbf{q}}^{\mathrm{I}}|d_{\mathbf{q}}^{\mathrm{I}}\}) n_{\mathrm{el}}\{\Gamma_{\mathbf{q}}\} \prod_{\mathbf{q},\mathrm{I}} \delta(\Gamma_{\mathbf{q}}^{\mathrm{I}} - \Gamma_{\mathbf{q}}) \times \delta\left(\Gamma_{\mathbf{q}}^{\mathrm{I}} - \frac{d_{\mathbf{q}}^{\mathrm{I}} - d_{\mathbf{q},\mathrm{ref}}^{\mathrm{I}}}{\beta_{\mathbf{q}}^{\mathrm{I}}}\right) \int D\{\mathbf{w}_{\alpha,\mathrm{CM}}\} \prod_{\mathbf{q},\mathrm{I}} \delta(d_{\mathbf{q}}^{\mathrm{I}} - \langle P_{\mathbf{q}}^{\mathrm{I}} \rangle_0) \quad (51)$$

Now, recognizing that the integral over the $\mathbf{w}_{\alpha,\mathrm{CM}}$ is equivalent to an average over the equivalent quenched tube center-of-mass variables in the reference state, we can (following the same method as in refs 21 and 36) expand to second order in $d_{\mathbf{q}}^{\mathrm{I}}$, writing

$$\int D\{\mathbf{w}_{\alpha,\mathrm{CM}}\} \prod_{\mathbf{q},\mathrm{I}} \delta(d_{\mathbf{q}}^{\mathrm{I}} - \langle P_{\mathbf{q}}^{\mathrm{I}} \rangle_0) \propto \exp(-F_1\{d_{\mathbf{q}}^{\mathrm{I}}\}) \quad (52)$$

where

$$F_1\{d_{\mathbf{q}}^{\mathrm{I}}\} = \frac{1}{2} \sum_{\mathbf{q}} \frac{\Delta_{0\mathbf{q}}^{\mathrm{BB}} |d_{\mathbf{q}}^{\mathrm{A}}|^2 + \Delta_{0\mathbf{q}}^{\mathrm{AA}} |d_{\mathbf{q}}^{\mathrm{B}}|^2 - 2\Delta_{0\mathbf{q}}^{\mathrm{AB}} d_{\mathbf{q}}^{\mathrm{A}} d_{-\mathbf{q}}^{\mathrm{B}}}{\Delta_{0\mathbf{q}}^{\mathrm{AA}} \Delta_{0\mathbf{q}}^{\mathrm{BB}} - (\Delta_{0\mathbf{q}}^{\mathrm{AB}})^2} \quad (53)$$

and the second-order correlation functions are

$$\Delta_{0\mathbf{q}}^{\mathrm{IJ}} = \overline{\langle P_{\mathbf{q}}^{\mathrm{I}} \rangle_0 \langle P_{-\mathbf{q}}^{\mathrm{J}} \rangle_0}^{0} \quad (54)$$

Again, the superscript "0", denoting no correlations between tubes of different chains, is appropriate because this average is a direct result of the integral over the $\mathbf{w}_{\alpha,\mathrm{CM}}$.

Substituting back into eq 51 and integrating over $d_{\mathbf{q}}^{\mathrm{I}}$ and $\Gamma_{\mathbf{q}}^{\mathrm{I}}$ gives

$$Z = \int D\{\rho_{\mathbf{q}}^{\mathrm{I}}, \Gamma_{\mathbf{q}}\} n_{\mathrm{el}}\{\Gamma_{\mathbf{q}}\} \exp(-U\{\rho_{\mathbf{q}}^{\mathrm{I}}\}) \times \exp(-F_0\{\rho_{\mathbf{q}}^{\mathrm{I}}|d_{\mathbf{q}}^{\mathrm{I}}\} - F_1\{d_{\mathbf{q}}^{\mathrm{I}}\}) \quad (55)$$

where the mean densities at fixed tube configuration, $d_{\mathbf{q}}^{\mathrm{I}}$, are now slaved to the entanglement network fluctuations $\Gamma_{\mathbf{q}}$ via

$$d_{\mathbf{q}}^{\mathrm{I}} = d_{\mathbf{q},\,\mathrm{ref}}^{\mathrm{I}} + \beta_{\mathbf{q}}^{\mathrm{I}} \Gamma_{\mathbf{q}} \quad (56)$$

The free energy contribution $F_0\{\rho_{\mathbf{q}}^{\mathrm{I}}|d_{\mathbf{q}}^{\mathrm{I}}\}$ is as given in eq

42, with $\Delta\rho^{\mathrm{I}}_{\mathbf{q}} = \rho^{\mathrm{I}}_{\mathbf{q}} - d^{\mathrm{I}}_{\mathbf{q}}$ representing a concentration variation about this mean.

The partition function (eq 55) is equivalent to a free energy functional of form

$$F\{\rho^{\mathrm{I}}_{\mathbf{q}},\Gamma_{\mathbf{q}}\} = F_0\{\rho^{\mathrm{I}}_{\mathbf{q}}|d^{\mathrm{I}}_{\mathbf{q}}\} + F_1\{d^{\mathrm{I}}_{\mathbf{q}}\} - \ln n_{\mathrm{el}}\{\Gamma_{\mathbf{q}}\} + U\{\rho^{\mathrm{I}}_{\mathbf{q}}\} \tag{57}$$

Typically, the melt is considered to be "incompressible" (i.e., fluctuations in composition are considered to be much larger than fluctuations in total density), and in a two-component system, this is modeled by setting

$$\exp(-U\{\rho^{\mathrm{I}}_{\mathbf{q}}\}) \sim \prod_{\mathbf{q}} \delta(\rho^{\mathrm{A}}_{\mathbf{q}} + \rho^{\mathrm{B}}_{\mathbf{q}}) \tag{58}$$

and integrating out over (say) $\rho^{\mathrm{B}}_{\mathbf{q}}$ in the partition function (eq 55). $U\{\rho^{\mathrm{I}}_{\mathbf{q}}\}$ may also include contributions from the Flory interaction parameter, but we shall assume that the A and B species are sufficiently similar for this to be set to zero.

The first two terms in the free energy (eq 57) are due to composition fluctuations in the system and contain contributions from fluctuations of the polymers within the tube (F_0) and displacements of the tubes themselves (F_1). In the absence of the elastic contributions to the free energy (i.e., if composition variations $d^{\mathrm{I}}_{\mathbf{q}}$ do not couple to network displacements $\Gamma_{\mathbf{q}}$), one can integrate out the $d^{\mathrm{I}}_{\mathbf{q}}$ variables to give an effective free energy function in terms of just the $\rho^{\mathrm{I}}_{\mathbf{q}}$

$$\int D\{d^{\mathrm{A}}_{\mathbf{q}},d^{\mathrm{B}}_{\mathbf{q}}\} \exp(-F_0\{\rho^{\mathrm{I}}_{\mathbf{q}}|d^{\mathrm{I}}_{\mathbf{q}}\} - F_1\{d^{\mathrm{I}}_{\mathbf{q}}\} - U\{\rho^{\mathrm{I}}_{\mathbf{q}}\}) = \exp(-F_{\mathrm{RPA}}\{\rho^{\mathrm{I}}_{\mathbf{q}}\} - U\{\rho^{\mathrm{I}}_{\mathbf{q}}\}) \tag{59}$$

where F_{RPA} is of the familiar form

$$F_{\mathrm{RPA}}\{\rho^{\mathrm{I}}_{\mathbf{q}}\} = \frac{1}{2}\sum_{\mathbf{q}} \frac{S^{\mathrm{BB}}_{0\mathbf{q}}|\rho^{\mathrm{A}}_{\mathbf{q}}|^2 + S^{\mathrm{AA}}_{0\mathbf{q}}|\rho^{\mathrm{B}}_{\mathbf{q}}|^2 - 2S^{\mathrm{AB}}_{0\mathbf{q}}\rho^{\mathrm{A}}_{\mathbf{q}}\rho^{\mathrm{B}}_{-\mathbf{q}}}{S^{\mathrm{AA}}_{0\mathbf{q}}S^{\mathrm{BB}}_{0\mathbf{q}} - (S^{\mathrm{AB}}_{0\mathbf{q}})^2} \tag{60}$$

and $S^{\mathrm{IJ}}_{0\mathbf{q}} = T^{\mathrm{IJ}}_{\mathbf{q}} + \Delta^{\mathrm{IJ}}_{0\mathbf{q}}$. This is the form of the free energy obtained in the conventional application of the random phase approximation in the absence of quenched translational degrees of freedom. Hence, the free energy in eq 57 can be interpreted as a combination of the free energy due to composition fluctuations in the system (with the mean densities $d^{\mathrm{I}}_{\mathbf{q}}$ coupled to the network fluctuations $\Gamma_{\mathbf{q}}$) together with an elastic energy penalizing the network fluctuations. We derive an appropriate form for the elastic energy contributions in Appendix C.

Appendix B. Variation of Mean Density for Small Network Fluctuations

The position, $\mathbf{r}_{\alpha,s}$, of a monomer can be expressed as

$$\mathbf{r}_{\alpha,s} = \hat{\mathbf{r}}_{\mathrm{ref},\alpha,s} + \mathbf{w}_{\alpha,s} + \delta\mathbf{r}_{\alpha,s} \tag{61}$$

where $\delta\mathbf{r}_{\alpha,s}$ is a fluctuation about the mean position $\hat{\mathbf{r}}_{\alpha,\ s} = \hat{\mathbf{r}}_{\mathrm{ref},\alpha,s} + \mathbf{w}_{\alpha,s}$. Hence, using eq 35, the mean density for monomers of species I at fixed $\mathbf{w}_{\alpha,s}$ is

$$\langle P^{\mathrm{I}}_{\mathbf{q}}\rangle_0 = \frac{1}{(\Omega\rho N)^{1/2}}\sum_{\alpha,s} y^{\mathrm{I}}_{\alpha,s}\langle\exp(i\mathbf{q}\cdot(\hat{\mathbf{r}}_{\mathrm{ref},\alpha,s} + \mathbf{w}_{\alpha,s} + \delta\mathbf{r}_{\alpha,s}))\rangle_0 \tag{62}$$

Expanding this, for small $\mathbf{w}_{\alpha,s}$ gives

$$\langle P^{\mathrm{I}}_{\mathbf{q}}\rangle_0 = d^{\mathrm{I}}_{\mathbf{q},\mathrm{ref}} + \frac{i}{(\Omega\rho N)^{1/2}}\sum_{\alpha,s}\mathbf{q}\cdot\mathbf{w}_{\alpha,s}y^{\mathrm{I}}_{\alpha,s} \times \exp(i\mathbf{q}\cdot\hat{\mathbf{r}}_{\mathrm{ref},\alpha,\ s})\langle\exp(i\mathbf{q}\cdot\delta\mathbf{r}_{\alpha,s})\rangle_0 \tag{63}$$

where

$$d^{\mathrm{I}}_{\mathbf{q},\mathrm{ref}} = \frac{1}{(\Omega\rho N)^{1/2}}\sum_{\alpha,s} y^{\mathrm{I}}_{\alpha,s}\langle\exp(i\mathbf{q}\cdot(\hat{\mathbf{r}}_{\mathrm{ref},\alpha,s} + \delta\mathbf{r}_{\alpha,s}))\rangle_0 \tag{64}$$

Substituting from eq 45 into eq 63 gives

$$\langle P^{\mathrm{I}}_{\mathbf{q}}\rangle_0 = d^{\mathrm{I}}_{\mathbf{q},\mathrm{ref}} + \frac{i}{\Omega^{3/2}(\rho N)^{1/2}}\sum_{\mathbf{q}'}\mathbf{q}\cdot\mathbf{w}^{\mathrm{I}}_{\mathbf{q}'}\sum_{\alpha,s} y^{\mathrm{I}}_{\alpha,s} \times \exp(i(\mathbf{q}-\mathbf{q}')\cdot\hat{\mathbf{r}}_{\mathrm{ref},\alpha,s})\langle\exp(i\mathbf{q}\cdot\delta\mathbf{r}_{\alpha,s})\rangle_0 \tag{65}$$

Suppose now that the number of chains in the system is n. The sum over the chains produces a dominant (order n) contribution at $\mathbf{q} = \mathbf{q}'$ together with small (order $n^{1/2}$) quenched fluctuations about this (for all $\mathbf{q}'$). In the large n limit, we keep only the dominant term (effectively preaveraging the quenched fluctuations, as is done in ref 21) to give

$$\langle P^{\mathrm{I}}_{\mathbf{q}}\rangle_0 = d^{\mathrm{I}}_{\mathbf{q},\mathrm{ref}} + \frac{i\mathbf{q}\cdot\mathbf{w}^{\mathrm{I}}_{\mathbf{q}}}{\Omega^{3/2}(\rho N)^{1/2}}\sum_{\alpha,s} y^{\mathrm{I}}_{\alpha,s}\langle\exp(i\mathbf{q}\cdot\delta\mathbf{r}_{\alpha,s})\rangle_0 = d^{\mathrm{I}}_{\mathbf{q},\mathrm{ref}} + \beta^{\mathrm{I}}_{\mathbf{q}}\gamma^{\mathrm{I}}_{\mathbf{q}} \tag{66}$$

where

$$\gamma^{\mathrm{I}}_{\mathbf{q}} = i\left(\frac{\rho}{N\Omega}\right)^{1/2}\mathbf{q}\cdot\mathbf{w}^{\mathrm{I}}_{\mathbf{q}} \tag{67}$$

and

$$\beta^{\mathrm{I}}_{\mathbf{q}} = \frac{1}{\Omega\rho}\sum_{\alpha,s} y^{\mathrm{I}}_{\alpha,s}\langle\exp(i\mathbf{q}\cdot\delta\mathbf{r}_{\alpha,s})\rangle_0 \tag{68}$$

Appendix C. Elastic Contribution to the Free Energy

For the free energy calculated in Appendix A, we are required to calculate the elastic contribution to the free energy, $-\ln n_{\mathrm{el}}\{\Gamma_{\mathbf{q}}\}$, from a network fluctuation represented by the field $\Gamma_{\mathbf{q}}$. To do this, we take a very simple model for the tube. We suppose that, prior to the step deformation, the tube consists of a number of segments, each containing N_{e} monomers. The end-to-end vector for the mth segment on chain α is $\mathbf{h}^{\alpha,m}$, which is a quenched variable distributed in the usual Gaussian manner:

$$P(\mathbf{h}^{\alpha,m}) \sim \exp\left(-\frac{3\mathbf{h}^{\alpha,m}\cdot\mathbf{h}^{\alpha,m}}{2N_{\mathrm{e}}b^2}\right) \tag{69}$$

Following the step deformation, represented by the deformation gradient $\mathbf{E}$, the new (affinely deformed) end-to-end vector of this segment is $\mathbf{H}^{\alpha,m} = \mathbf{E}\cdot\mathbf{h}^{\alpha,m}$. We wish to include the possibility of chain retraction within the tube and so allow the chain within the tube segment to retract by a factor $\gamma^{\alpha,m}$. Furthermore, although the tube increases in length on average by the Doi–Edwards factor[1] $\alpha(\mathbf{E})$, it is clear that individual tube

segments increase in length by a factor $(\mathbf{H}^{\alpha,m}\cdot\mathbf{H}^{\alpha,m})^{1/2}/(\mathbf{h}^{\alpha,m}\cdot\mathbf{h}^{\alpha,m})^{1/2}$, depending on the specific quenched orientation of each tube segment. Thus, we would expect some redistribution of the chain between tube segments, with those segments with a larger fractional increase in length obtaining more monomers, at the expense of other segments. Accounting for these effects, to first order, suggests that the number of monomers per chain in tube segment m on chain α is now

$$N_e \frac{\gamma^{\alpha,m}(\mathbf{H}^{\alpha,m}\cdot\mathbf{H}^{\alpha,m})^{1/2}}{\alpha(\mathbf{E})(\mathbf{h}^{\alpha,m}\cdot\mathbf{h}^{\alpha,m})^{1/2}}$$

although this does not account for correlations in chain redistribution between tube segments on a finite chain. Furthermore, due to branchpoint withdrawal,[14,16] it is possible for some tube segments to contain two chains rather than one, so we introduce an additional variable, $n_C^{\alpha,m}$, representing the number of chains contained within a given tube segment.

In addition to the affine deformation of the network, there is the additional nonaffine deformation represented by the network fluctuations $\Gamma_{\mathbf{q}}$. This results in each tube segment being additionally deformed by a small, local deformation gradient $\mathbf{E}_{loc}^{\alpha,m}$, giving a new end-to-end vector $\tilde{\mathbf{H}}^{\alpha,m} = \mathbf{E}_{loc}^{\alpha,m}\cdot\mathbf{H}^{\alpha,m}$. The relationship between $\Gamma_{\mathbf{q}}$ and $\mathbf{E}_{loc}^{\alpha,m}$ will be obtained below. In calculating the number of configurations available to the chains within these tube segments, we shall make the approximation that these small network fluctuations result in no further redistribution of monomers between tube segments, i.e., the number of monomers in a tube segment remains fixed at the value obtained above from the affine deformation.

The model for the tube, as described above, is not wholly satisfactory in the sense that it does omit certain physical aspects that one feels *ought* to be present in a description of a melt tube. For example, one would like the "tube segments" each to be of the same length prior to the deformation (whereas eq 69 implies a distribution of lengths). One would also like to describe mathematically the process by which the chain can redistribute its monomers during the network fluctuations (and, indeed, to allow fluctuations in the number of monomers between tube segments) as is suggested by the physical notion of unimpeded chain motion along the tube contour. However, it is necessary to be very careful while including such effects, in particular with the choice of (quenched) variables representing the tube contour. It must be the case that, in the undeformed state, the probability distribution of the polymer *chains* is of the standard Guassian form; Such a distribution for the chains must be obtained when one combines both the annealed fluctuations of the chain within the tube and the quenched distribution of possible tube contours. For any given model of the tube, the distribution of quenched tube contours is defined by this constraint on the chain distribution. Experience suggests that, while one can, for example, obtain quite plausible *rheological* models without strictly obeying this constraint, such freedom is not available in dealing with scattering models; if such constraints are not obeyed, then one does not reproduce known scattering results (i.e., the standard random phase approximation) in the limit of no stretching because the chain distribution is not correctly modeled in this limit. So, while the model described above does not contain all the physics we would wish to apply, it is at least the case that we know the appropriate distribution of tube contour variables, as in eq 69. Such distributions are not, in fact, known for more complicated models, and their derivation is beyond the scope of this work, constituting a significant theoretical task in themselves.

From the network displacement $\mathbf{w}(\mathbf{r})$ we can define a local deformation gradient

$$E_{loc,ij}(\mathbf{r}) = \delta_{ij} + \frac{\partial w_i}{\partial r_j} \tag{70}$$

We obtain the local deformation gradient appropriate for a particular tube segment, $\mathbf{E}_{loc}^{\alpha,m}$, by averaging $\mathbf{E}_{loc}(\mathbf{r})$ over the volume of the tube segment in the reference state (defined by the spatial mean density of the monomers from that particular tube segment), giving

$$E_{loc,ij}^{\alpha,m} = \delta_{ij} + \int d^3\mathbf{r}\, \frac{\partial w_i}{\partial r_j} d^{\alpha,m}(\mathbf{r}) \tag{71}$$

where

$$d^{\alpha,m}(\mathbf{r}) = \frac{1}{N_{\alpha,m}}\sum_{s\in m}\langle\delta(\mathbf{r} - \mathbf{r}_{\alpha,s})\rangle_0 \tag{72}$$

and $N_{\alpha,m}$ is the number of monomers in the tube segment m. $d^{\alpha,m}(\mathbf{r})$ gives an appropriate lower length scale cutoff to the entanglement network elasticity. Expressing both $\mathbf{w}(\mathbf{r})$ and $d_{\alpha,m}(\mathbf{r})$ in Fourier modes and retaining only the component of $\mathbf{w}_{\mathbf{q}}$ parallel to the wavevector (as defined in eq 46) gives

$$E_{loc,ij}^{\alpha,m} = \delta_{ij} - s_1\sum_{\mathbf{q}}\frac{q_i q_j}{q^2}\Gamma_{\mathbf{q}} d_{\mathbf{q}}^{\alpha,m} \tag{73}$$

where $s_1 = (N/\Omega\rho)^{1/2}$ and

$$d_{\mathbf{q}}^{\alpha,m} = \frac{1}{N_{\alpha,m}}\sum_{s\in m}\langle\exp(i\mathbf{q}\cdot\mathbf{r}_{\alpha,s})\rangle_0 \tag{74}$$

We now express the number of configurations of the chains in the deformed network as

$$n_{el}\{\Gamma_{\mathbf{q}}\} = n_0\int D\{\tilde{\mathbf{H}}^{\alpha,m}\}\times \exp\left(-\frac{3}{2N_e b^2}\sum_{\alpha,m}\theta^{\alpha,m}\tilde{\mathbf{H}}^{\alpha,m}\cdot\tilde{\mathbf{H}}^{\alpha,m}\right)\prod_{\alpha,m}\delta(\mathbf{H}^{\alpha,m} - \mathbf{E}\cdot\mathbf{h}^{\alpha,m}) \tag{75}$$

where

$$\theta^{\alpha,m} = n_C^{\alpha,m}\frac{\alpha(\mathbf{E})(\mathbf{h}^{\alpha,m}\cdot\mathbf{h}^{\alpha,m})^{1/2}}{\gamma^{\alpha,m}(\mathbf{H}^{\alpha,m}\cdot\mathbf{H}^{\alpha,m})^{1/2}} \tag{76}$$

represents the combined effect of the change in the number of monomers within a tube segment and the (possible) change in number of chains within a tube segment due to branchpoint withdrawal. The δ-function constraint representing the quenched tube configuration is expressed as a constraint on the segment end-to-end vector $\mathbf{H}^{\alpha,m}$ before the deformation due to network fluctuations. This is because we wish to evaluate the change in number of chain configurations as a function

of $\Gamma_{\mathbf{q}}$, and hence it is appropriate to retain the *same* constraint as $\Gamma_{\mathbf{q}}$ is varied. Since (as is discussed below) there is a Jacobian involved in the transformation from $\mathbf{H}^{\alpha,m}$ to $\tilde{\mathbf{H}}^{\alpha,m}$, any constraint expressed as a δ-function on $\tilde{\mathbf{H}}^{\alpha,m}$ will represent a different constraint for different values of $\Gamma_{\mathbf{q}}$.

It is convenient to change the integration variable in eq 75 to $\mathbf{H}^{\alpha,m}$ from $\tilde{\mathbf{H}}^{\alpha,m}$ (using $\tilde{\mathbf{H}}^{\alpha,m} = \mathbf{E}_{\mathrm{loc}}^{\alpha,m}\cdot\mathbf{H}^{\alpha,m}$). This change of variable involves a Jacobian, given by

$$J = \prod_{\alpha,m} \det \mathbf{E}_{\mathrm{loc}}^{\alpha,m} \tag{77}$$

$$= \exp\left(\sum_{\alpha,m} \ln \det \mathbf{E}_{\mathrm{loc}}^{\alpha,m}\right) \tag{78}$$

Using eq 73, the term in the exponential can be expanded to second order in the $\Gamma_{\mathbf{q}}$, giving

$$J = \exp\left(-s_1\sum_{\mathbf{q}}\Gamma_{\mathbf{q}}\sum_{\alpha,m} d_{-\mathbf{q}}^{\alpha,m} - \frac{1}{2}\sum_{\mathbf{q}} A_{1\mathbf{q}}\Gamma_{\mathbf{q}}\Gamma_{-\mathbf{q}}\right) \tag{79}$$

where

$$A_{1\mathbf{q}} = {s_1}^2\sum_{\alpha,m}\overline{d_{\mathbf{q}}^{\alpha,m} d_{-\mathbf{q}}^{\alpha,m}} \tag{80}$$

In doing this calculation, the first-order term is exact but there has been a preaverage of the second-order terms. This is justified by the same reasoning as is used to preaverage the other second-order terms in the free energy in Appendix A, as discussed in detail in ref 21. Specifically, the second-order terms are all of form $A_{\mathbf{q},\mathbf{q}'}\Gamma_{\mathbf{q}}\Gamma_{\mathbf{q}'}$. If the number of chains in the system is n, then one finds a dominant (order n) contribution occurring along the "diagonal" at $\mathbf{q}' = -\mathbf{q}$, with order $n^{1/2}$ quenched fluctuations about this for all $\mathbf{q}$ and $\mathbf{q}'$. A preaverage of the second-order terms retains only the diagonal contribution.

The effective contributions to $n_{\mathrm{el}}\{\Gamma_{\mathbf{q}}\}$ from the Jacobian can physically be thought of as coming from "entanglement pressure". This arises because local changes in the network volume restrict the degrees of freedom of the "gas" of entanglement positions.

We also apply the change of variable $\tilde{\mathbf{H}}^{\alpha,m} = \mathbf{E}_{\mathrm{loc}}^{\alpha,m}\cdot\mathbf{H}^{\alpha,m}$ to the integrand of eq 75, again expanding to second order in the $\Gamma_{\mathbf{q}}$, and this gives

$$\exp\left(-\frac{3}{2N_e b^2}\sum_{\alpha,m}\theta^{\alpha,m}\tilde{\mathbf{H}}^{\alpha,m}\cdot\tilde{\mathbf{H}}^{\alpha,m}\right) \tag{81}$$

$$= \exp\left(s_1\sum_{\mathbf{q}}\Gamma_{\mathbf{q}}\sum_{\alpha,m} d_{-\mathbf{q}}^{\alpha,m} + \frac{N}{N_e}\sum_{\mathbf{q}} f_{-\mathbf{q}}\Gamma_{\mathbf{q}} - \frac{1}{2}\sum_{\mathbf{q}} A_{2\mathbf{q}}\Gamma_{\mathbf{q}}\Gamma_{-\mathbf{q}}\right)$$

where

$$A_{2\mathbf{q}} = {s_1}^2\sum_{\alpha,m}\overline{\phi^{\alpha,m}}\;\overline{d_{\mathbf{q}}^{\alpha,m} d_{-\mathbf{q}}^{\alpha,m}} \tag{82}$$

and

$$f_{-\mathbf{q}} = s_1\frac{N_e}{N}\sum_{\alpha,m}(\phi^{\alpha,m} - 1)d_{-\mathbf{q}}^{\alpha,m} \tag{83}$$

$$\phi^{\alpha,m} = \frac{q_i q_j}{q^2}\frac{3}{N_e b^2} H_i^{\alpha,m} H_j^{\alpha,m}\theta^{\alpha,m} \tag{84}$$

Once again, a preaverage has been performed on the second-order terms. The factor N_e/N has been included in $f_{-\mathbf{q}}$ for later convenience.

Combining eqs 79 and 81 into eq 75 gives

$$n_{\mathrm{el}}\{\Gamma_{\mathbf{q}}\} = n_0\exp\left(\frac{N}{N_e}\sum_{\mathbf{q}} f_{-\mathbf{q}}\Gamma_{\mathbf{q}} - \frac{1}{2}\sum_{\mathbf{q}}(A_{1\mathbf{q}} + A_{2\mathbf{q}})\Gamma_{\mathbf{q}}\Gamma_{-\mathbf{q}}\right) \tag{85}$$

and substituting this into eq 57 gives a total free energy of form

$$F\{\rho_{\mathbf{q}}^{\mathrm{I}},\Gamma_{\mathbf{q}}\} = F_0\{\rho_{\mathbf{q}}^{\mathrm{I}}|d_{\mathbf{q}}^{\mathrm{I}}\} + F_1\{d_{\mathbf{q}}^{\mathrm{I}}\} - \frac{N}{N_e}\sum_{\mathbf{q}} f_{-\mathbf{q}}\Gamma_{\mathbf{q}} + \frac{1}{2}\sum_{\mathbf{q}}(A_{1\mathbf{q}} + A_{2\mathbf{q}})\Gamma_{\mathbf{q}}\Gamma_{-\mathbf{q}} + U\{\rho_{\mathbf{q}}^{\mathrm{I}}\} \tag{86}$$

Appendix D. Calculation of Scattering Function

We now obtain an expression for the scattering function $S(\mathbf{q}) = \overline{\langle\rho_{\mathbf{q}}^{\mathrm{A}}\rho_{-\mathbf{q}}^{\mathrm{A}}\rangle_{\mathrm{an}}}$ using the derived free energy (eq 86). The first step is to use the incompressibility constraint (eq 58) to integrate out one of the density variables, $\rho_{\mathbf{q}}^{\mathrm{B}}$ say. This is equivalent to setting $\rho_{\mathbf{q}}^{\mathrm{A}} = -\rho_{\mathbf{q}}^{\mathrm{B}} = \rho_{\mathbf{q}}$ in all but the last term of eq 86, giving

$$F\{\rho_{\mathbf{q}},\Gamma_{\mathbf{q}}\} = F_0\{\rho_{\mathbf{q}}|d_{\mathbf{q}}^{\mathrm{I}}\} + F_1\{d_{\mathbf{q}}^{\mathrm{I}}\} - \frac{N}{N_e}\sum_{\mathbf{q}} f_{-\mathbf{q}}\Gamma_{\mathbf{q}} + \frac{1}{2}\sum_{\mathbf{q}}(A_{1\mathbf{q}} + A_{2\mathbf{q}})\Gamma_{\mathbf{q}}\Gamma_{-\mathbf{q}} \tag{87}$$

where

$$F_0\{\rho_{\mathbf{q}}|d_{\mathbf{q}}^{\mathrm{I}}\} = \frac{1}{2}\sum_{\mathbf{q}}[T_{\mathbf{q}}^{\mathrm{BB}}|\rho_{\mathbf{q}} - d_{\mathbf{q}}^{\mathrm{A}}|^2 + T_{\mathbf{q}}^{\mathrm{AA}}|\rho_{\mathbf{q}} + d_{\mathbf{q}}^{\mathrm{B}}|^2 + 2T_{\mathbf{q}}^{\mathrm{AB}}(\rho_{\mathbf{q}} - d_{\mathbf{q}}^{\mathrm{A}})(\rho_{-\mathbf{q}} + d_{-\mathbf{q}}^{\mathrm{B}})]/[T_{\mathbf{q}}^{\mathrm{AA}}T_{\mathbf{q}}^{\mathrm{BB}} - (T_{\mathbf{q}}^{\mathrm{AB}})^2] \tag{88}$$

and $d_{\mathbf{q}}^{\mathrm{I}} = d_{\mathbf{q},\mathrm{ref}}^{\mathrm{I}} + \beta_{\mathbf{q}}^{\mathrm{I}}\Gamma_{\mathbf{q}}$. There are apparently three sets of quenched fields in eq 87, $d_{\mathbf{q},\mathrm{ref}}^{\mathrm{A}}$, $d_{\mathbf{q},\mathrm{ref}}^{\mathrm{B}}$, and $f_{-\mathbf{q}}$. However, only two linear combinations of these are actually important (this is a consequence of the guage invariance of the system discussed in ref 11). To see this, we set

$$\Gamma_{\mathbf{q}} = g_{\mathbf{q}} + \frac{N}{N_e(A_{1\mathbf{q}} + A_{2\mathbf{q}})} f_{\mathbf{q}} \tag{89}$$

which gives (apart from an irrelevant constant)

$$F\{\rho_{\mathbf{q}},g_{\mathbf{q}}\} = F_0\{\rho_{\mathbf{q}}|d_{\mathbf{q}}^{\mathrm{I}}\} + F_1\{d_{\mathbf{q}}^{\mathrm{I}}\} + \frac{1}{2}\sum_{\mathbf{q}}(A_{1\mathbf{q}} + A_{2\mathbf{q}})g_{\mathbf{q}}g_{-\mathbf{q}} \tag{90}$$

where now

$$d_{\mathbf{q}}^{\mathrm{I}} = C_{\mathbf{q}}^{\mathrm{I}} + \beta_{\mathbf{q}}^{\mathrm{I}}g_{\mathbf{q}} \tag{91}$$

and

$$C^{\mathrm{I}}_{\mathbf{q}} = d^{\mathrm{I}}_{\mathbf{q},\mathrm{ref}} + \frac{N}{N_{\mathrm{e}}(A_{1\mathbf{q}} + A_{2\mathbf{q}})}\beta^{\mathrm{I}}_{\mathbf{q}} f_{\mathbf{q}} \tag{92}$$

$C^{\mathrm{A}}_{\mathbf{q}}$ and $C^{\mathrm{B}}_{\mathbf{q}}$ are the important quenched fields, implying that we could make transformations of the reference state that change $d^{\mathrm{A}}_{\mathbf{q},\mathrm{ref}}$, $d^{\mathrm{B}}_{\mathbf{q},\mathrm{ref}}$, and $f_{-\mathbf{q}}$ provided these leave $C^{\mathrm{A}}_{\mathbf{q}}$ and $C^{\mathrm{B}}_{\mathbf{q}}$ unchanged. (This "guage invariance" is valid only for small network deformations.)

To obtain an expression for the scattering for a given set of quenched variables $C^{\mathrm{A}}_{\mathbf{q}}$ and $C^{\mathrm{B}}_{\mathbf{q}}$, we integrate out the $g_{\mathbf{q}}$ variables in the partition function (effectively minimizing eq 90 with respect to $g_{\mathbf{q}}$). The result is a free energy in $\rho_{\mathbf{q}}$ only, which represents fluctuations $\Delta\rho_{\mathbf{q}}$ about a nonzero mean $\langle\rho_{\mathbf{q}}\rangle_{\mathrm{an}}$ (which depends on the quenched variables). It is straightforward (though tedious) to obtain expressions for this mean and the magnitude of the fluctuations. This entire process was implemented using MAPLE,[37] giving a scattering function of form

$$\begin{aligned} S(\mathbf{q}) &= \langle\rho_{\mathbf{q}}\rho_{-\mathbf{q}}\rangle_{\mathrm{an}} \\ &= \langle\Delta\rho_{\mathbf{q}}\Delta\rho_{-\mathbf{q}}\rangle_{\mathrm{an}} + \langle\rho_{\mathbf{q}}\rangle_{\mathrm{an}}\langle\rho_{-\mathbf{q}}\rangle_{\mathrm{an}} \\ &= \langle\Delta\rho_{\mathbf{q}}\Delta\rho_{-\mathbf{q}}\rangle_{\mathrm{an}} + r_{\mathrm{A}}{}^2 C^{\mathrm{A}}_{\mathbf{q}}C^{\mathrm{A}}_{-\mathbf{q}} + r_{\mathrm{B}}{}^2 C^{\mathrm{B}}_{\mathbf{q}}C^{\mathrm{B}}_{-\mathbf{q}} - \\ &\qquad 2r_{\mathrm{A}}r_{\mathrm{B}}C^{\mathrm{A}}_{\mathbf{q}}C^{\mathrm{B}}_{-\mathbf{q}} \end{aligned} \tag{93}$$

For a macroscopic sample it is appropriate to average over the quenched variables, giving

$$S(\mathbf{q}) = \langle\Delta\rho_{\mathbf{q}}\Delta\rho_{-\mathbf{q}}\rangle_{\mathrm{an}} + r_{\mathrm{A}}{}^2\overline{C^{\mathrm{A}}_{\mathbf{q}}C^{\mathrm{A}}_{-\mathbf{q}}} + r_{\mathrm{B}}{}^2\overline{C^{\mathrm{B}}_{\mathbf{q}}C^{\mathrm{B}}_{-\mathbf{q}}} - 2r_{\mathrm{A}}r_{\mathrm{B}}\overline{C^{\mathrm{A}}_{\mathbf{q}}C^{\mathrm{B}}_{-\mathbf{q}}} \tag{94}$$

We obtain expressions for $\langle\Delta\rho_{\mathbf{q}}\Delta\rho_{-\mathbf{q}}\rangle$ and the coefficients r_{A} and r_{B} which can be evaluated from the following set of equations:

$$A_{\mathbf{q}} = A_{1\mathbf{q}} + A_{2\mathbf{q}} \tag{95}$$

$$T^{\mathrm{A}}_{\mathbf{q}} = T^{\mathrm{AA}}_{\mathbf{q}} + T^{\mathrm{AB}}_{\mathbf{q}} \tag{96}$$

$$T^{\mathrm{B}}_{\mathbf{q}} = T^{\mathrm{BB}}_{\mathbf{q}} + T^{\mathrm{AB}}_{\mathbf{q}} \tag{97}$$

$$t_1 = T^{\mathrm{A}}_{\mathbf{q}} + T^{\mathrm{B}}_{\mathbf{q}} \tag{98}$$

$$t_2 = \Delta^{\mathrm{AA}}_{0\mathbf{q}}\Delta^{\mathrm{BB}}_{0\mathbf{q}} - (\Delta^{\mathrm{AB}}_{0\mathbf{q}})^2 \tag{99}$$

$$t_3 = T^{\mathrm{AA}}_{\mathbf{q}}T^{\mathrm{BB}}_{\mathbf{q}} - (T^{\mathrm{AB}}_{\mathbf{q}})^2 \tag{100}$$

$$t_4 = (\beta^{\mathrm{A}}_{\mathbf{q}})^2\Delta^{\mathrm{BB}}_{0\mathbf{q}} + (\beta^{\mathrm{B}}_{\mathbf{q}})^2\Delta^{\mathrm{AA}}_{0\mathbf{q}} - 2\beta^{\mathrm{A}}_{\mathbf{q}}\beta^{\mathrm{B}}_{\mathbf{q}}\Delta^{\mathrm{AB}}_{0\mathbf{q}} \tag{101}$$

$$t_5 = [A_{\mathbf{q}}t_1 + (\beta^{\mathrm{A}}_{\mathbf{q}} + \beta^{\mathrm{B}}_{\mathbf{q}})^2]t_2 + t_1t_4 \tag{102}$$

$$t_6 = T^{\mathrm{A}}_{\mathbf{q}}\Delta^{\mathrm{BB}}_{0\mathbf{q}} - T^{\mathrm{B}}_{\mathbf{q}}\Delta^{\mathrm{AA}}_{0\mathbf{q}} \tag{103}$$

$$t_7 = T^{\mathrm{B}}_{\mathbf{q}}\Delta^{\mathrm{AA}}_{0\mathbf{q}} - T^{\mathrm{A}}_{\mathbf{q}}\Delta^{\mathrm{AB}}_{0\mathbf{q}} \tag{104}$$

and

$$\langle\Delta\rho_{\mathbf{q}}\Delta\rho_{-\mathbf{q}}\rangle_{\mathrm{an}} = \frac{(A_{\mathbf{q}}t_2 + t_4)t_3 + [(\beta^{\mathrm{A}}_{\mathbf{q}})^2T^{\mathrm{BB}}_{\mathbf{q}} + (\beta^{\mathrm{B}}_{\mathbf{q}})^2T^{\mathrm{AA}}_{\mathbf{q}} - 2\beta^{\mathrm{A}}_{\mathbf{q}}\beta^{\mathrm{B}}_{\mathbf{q}}T^{\mathrm{AB}}_{\mathbf{q}}]t_2}{t_5} \tag{105}$$

$$r_{\mathrm{A}} = \frac{[A_{\mathbf{q}}T^{\mathrm{B}}_{\mathbf{q}} + \beta^{\mathrm{B}}_{\mathbf{q}}(\beta^{\mathrm{A}}_{\mathbf{q}} + \beta^{\mathrm{B}}_{\mathbf{q}})]t_2 + (\beta^{\mathrm{B}}_{\mathbf{q}})^2t_7 + \beta^{\mathrm{A}}_{\mathbf{q}}\beta^{\mathrm{B}}_{\mathbf{q}}t_6}{t_5} \tag{106}$$

$$r_{\mathrm{B}} = \frac{[A_{\mathbf{q}}T^{\mathrm{A}}_{\mathbf{q}} + \beta^{\mathrm{A}}_{\mathbf{q}}(\beta^{\mathrm{A}}_{\mathbf{q}} + \beta^{\mathrm{B}}_{\mathbf{q}})]t_2 + (\beta^{\mathrm{A}}_{\mathbf{q}})^2t_6 + \beta^{\mathrm{A}}_{\mathbf{q}}\beta^{\mathrm{B}}_{\mathbf{q}}t_7}{t_5} \tag{107}$$

D.1. Evaluation of Quenched Field Averages. In evaluating the scattering function (eq 94), it is required to calculate the averages of form $\overline{C^{\mathrm{A}}_{\mathbf{q}}C^{\mathrm{A}}_{-\mathbf{q}}}$ in the reference state. Using eq 92, we can write these averages as

$$\overline{C^{\mathrm{A}}_{\mathbf{q}}C^{\mathrm{A}}_{-\mathbf{q}}} = \Delta^{\mathrm{AA}}_{\mathbf{q}} + 2\frac{N}{N_{\mathrm{e}}A_{\mathbf{q}}}\beta^{\mathrm{A}}_{\mathbf{q}}\Delta^{\mathrm{Af}}_{\mathbf{q}} + \left(\frac{N}{N_{\mathrm{e}}A_{\mathbf{q}}}\beta^{\mathrm{A}}_{\mathbf{q}}\right)^2\Delta^{\mathrm{ff}}_{\mathbf{q}} \tag{108}$$

$$\overline{C^{\mathrm{B}}_{\mathbf{q}}C^{\mathrm{B}}_{-\mathbf{q}}} = \Delta^{\mathrm{BB}}_{\mathbf{q}} + 2\frac{N}{N_{\mathrm{e}}A_{\mathbf{q}}}\beta^{\mathrm{B}}_{\mathbf{q}}\Delta^{\mathrm{Bf}}_{\mathbf{q}} + \left(\frac{N}{N_{\mathrm{e}}A_{\mathbf{q}}}\beta^{\mathrm{B}}_{\mathbf{q}}\right)^2\Delta^{\mathrm{ff}}_{\mathbf{q}} \tag{109}$$

$$\overline{C^{\mathrm{A}}_{\mathbf{q}}C^{\mathrm{B}}_{-\mathbf{q}}} = \Delta^{\mathrm{AB}}_{\mathbf{q}} + \frac{N}{N_{\mathrm{e}}A_{\mathbf{q}}}(\beta^{\mathrm{A}}_{\mathbf{q}}\Delta^{\mathrm{Bf}}_{\mathbf{q}} + \beta^{\mathrm{B}}_{\mathbf{q}}\Delta^{\mathrm{Af}}_{\mathbf{q}}) + \left(\frac{N}{N_{\mathrm{e}}A_{\mathbf{q}}}\right)^2\beta^{\mathrm{A}}_{\mathbf{q}}\beta^{\mathrm{B}}_{\mathbf{q}}\Delta^{\mathrm{ff}}_{\mathbf{q}} \tag{110}$$

where

$$\Delta^{\mathrm{IJ}}_{\mathbf{q}} = \overline{\langle P^{\mathrm{I}}_{\mathbf{q}}\rangle_0\langle P^{\mathrm{J}}_{-\mathbf{q}}\rangle_0} \tag{111}$$

$$\Delta^{\mathrm{If}}_{\mathbf{q}} = \overline{\langle P^{\mathrm{I}}_{\mathbf{q}}\rangle_0 f_{-\mathbf{q}}} \tag{112}$$

$$\Delta^{\mathrm{ff}}_{\mathbf{q}} = \overline{f_{\mathbf{q}}f_{-\mathbf{q}}} \tag{113}$$

In contrast to the definition of $\Delta^{\mathrm{IJ}}_{0\mathbf{q}}$ in eq 54, these are *not* evaluated subject to a "free" distribution of the quenched variables, which would ignore correlations between tubes from different chains. Instead, the quenched average must be over the particular distribution over the quenched variables *in the reference state*, and this must include correlations between tubes from different chains. Such correlations exist because of excluded-volume interactions between chains in the melt before the stretch. The tube configurations are determined in a state where interchain correlations exist, and as a result there are "intertube" correlations. A method for evaluating the effect of these correlations on quenched fields was developed in ref 21. This is done by defining a field, $\varphi_{\mathbf{q}}$, representing the density of monomers after a wholly affine deformation from the initial unstretched melt. If the initial position of monomer s on chain α is $\mathbf{x}_{\alpha,s}$, then this field is defined as

$$\varphi_{\mathbf{q}}\{\mathbf{x}_{\alpha,s}\} = \frac{1}{(\Omega\rho N)^{1/2}}\sum_{\alpha,s}\exp(i\mathbf{q}\cdot\mathbf{E}\cdot\mathbf{x}_{\alpha,s}) \tag{114}$$

An "RPA" calulation is then done on the fields $\varphi_{\mathbf{q}}$, $d^{\mathrm{I}}_{\mathbf{q},\mathrm{ref}} = \langle P^{\mathrm{I}}_{\mathbf{q}}\rangle_0$ and (in the present calculation) $f_{\mathbf{q}}$, imposing incompressibilty on the field $\varphi_{\mathbf{q}}$. The results are of form

$$\Delta^{\mathrm{IJ}}_{\mathbf{q}} = \Delta^{\mathrm{IJ}}_{0\mathbf{q}} - \frac{D^{\mathrm{I}}_{\mathbf{q}}D^{\mathrm{J}}_{\mathbf{q}}}{S^{\mathrm{tot}}_{\mathbf{q}}} \tag{115}$$

$$\Delta^{\mathrm{If}}_{\mathbf{q}} = \Delta^{\mathrm{If}}_{0\mathbf{q}} - \frac{D^{\mathrm{I}}_{\mathbf{q}}D^{\mathrm{f}}_{\mathbf{q}}}{S^{\mathrm{tot}}_{\mathbf{q}}} \tag{116}$$

$$\Delta^{\mathrm{ff}}_{\mathbf{q}} = \Delta^{\mathrm{ff}}_{0\mathbf{q}} - \frac{(D^{\mathrm{f}}_{\mathbf{q}})^2}{S^{\mathrm{tot}}_{\mathbf{q}}} \tag{117}$$

where we have defined the correlation functions

$$\Delta^{\mathrm{If}}_{0\mathbf{q}} = \overline{\langle P^{\mathrm{I}}_{\mathbf{q}}\rangle_0 f_{-\mathbf{q}}}^{0} \tag{118}$$

$$\Delta^{\mathrm{ff}}_{0\mathbf{q}} = \overline{f_{\mathbf{q}} f_{-\mathbf{q}}}^{0} \tag{119}$$

$$D^{\mathrm{I}}_{\mathbf{q}} = \overline{\langle P^{\mathrm{I}}_{\mathbf{q}}\rangle_0 \langle \varphi_{-\mathbf{q}}\rangle_0}^{0} \tag{120}$$

$$D^{\mathrm{f}}_{\mathbf{q}} = \overline{f_{\mathbf{q}} \langle \varphi_{-\mathbf{q}}\rangle_0}^{0} \tag{121}$$

$$S^{\mathrm{tot}}_{\mathbf{q}} = \overline{\langle \varphi_{\mathbf{q}} \varphi_{-\mathbf{q}}\rangle_0}^{0} \tag{122}$$

As with eq 54, these *are* evaluated subject to a "free" distribution of the quenched variables, ignoring correlations between tubes from different chains, as denoted by the "0" superscript.

The full expression for the scattering function is thus given by eqs 94−110 and 115−117. At this level, we have said very little about the specific model used to describe the polymer chains and tubes (apart from the specific approximations to the elastic behavior of the tube, described above in the definitions of $f_{\mathbf{q}}$ and $A_{\mathbf{q}}$). Neverthless, there are a number of correlation functions to calculate: $T^{\mathrm{IJ}}_{\mathbf{q}}$, $\Delta^{\mathrm{IJ}}_{0\mathbf{q}}$, $\Delta^{\mathrm{If}}_{0\mathbf{q}}$, $\Delta^{\mathrm{ff}}_{0\mathbf{q}}$, $D^{\mathrm{I}}_{\mathbf{q}}$, $D^{\mathrm{f}}_{\mathbf{q}}$, $S^{\mathrm{tot}}_{\mathbf{q}}$, $\beta^{\mathrm{I}}_{\mathbf{q}}$, $A_{1\mathbf{q}}$, and $A_{2\mathbf{q}}$. For a two-component system (I, J = A or B) this represents 17 functions, and each of these is dependent on the polymer chain architecture and the specific model used to describe the chains and tubes. The next section describes their evaluation for a specific model.

Appendix E. Evaluation of Correlation Functions

In this Appendix, we outline the calculation of the numerous correlation functions required in the expression of the scattering. The correlation functions are based upon a generalization of the Warner−Edwards model[24] for the polymer tube, in which polymers are localized by (possibly anisotropic) quadratic potentials acting on each monomer, giving a free energy functional as

$$F_{\mathbf{R}}\{\mathbf{r}_s\} = \frac{1}{2}\sum_{s,\mu}\left\{\frac{3}{b^2}\left(\frac{\partial r_{s,\mu}}{\partial s}\right)^2 + \frac{2b^2}{{d_\mu}^4}(r_{s,\mu} - R_{s,\mu})^2\right\} \tag{123}$$

where the sum is over monomers, s, and Cartesian direction, μ, and the vectors $\mathbf{R}_s$ are the centers of the localizing potentials. A detailed account for the calculation of correlation functions from such a model has been given elsewhere.[21,29,38] Here we note that within the model it is possible to define a "mean path" $\hat{\mathbf{r}}_s$ for the polymer chain within the model.[21,38] In terms of the Fourier modes $\mathbf{r}_p$ along the tube ($\mathbf{r}_s = \sum_p \mathbf{r}_p \exp(isp)$) this mean path is given by

$$\hat{r}_{p,\mu} = \frac{R_{p,\mu}}{\left(1 + \dfrac{3p^2 {d_\mu}^4}{2b^4}\right)} \tag{124}$$

In calculating monomer−monomer correlations, it is convenient to separate out the contributions from this mean path and the fluctuations about it. The root-mean-square amplitude of the fluctuations are proportional to the quantity d_μ in direction μ, so that this quantity has, in previous publications,[21,38,39] been dubbed the "Warner−Edwards tube diameter". We note that this definition of d_μ from the Warner−Edwards model is somewhat arbitrary; it would be incorrect to identify it exactly with the melt tube diameter as obtained from rheology, though it should be of the same order of magnitude and scale in the same way.

In general, expressions obtained for correlation functions within this model depend both on the isotropic tube diameter d_0 in the unstretched state and on the anisotropic d_μ in the stretched state. In the expressions that follow, we represent these via parameters ς and ς_μ respectively, so that

$$\varsigma^2 = \frac{{d_0}^2}{2\sqrt{6}{R_{\mathrm{g}}}^2} \tag{125}$$

$$\varsigma_\mu{}^2 = \frac{{d_\mu}^2}{2\sqrt{6}{R_{\mathrm{g}}}^2} \tag{126}$$

where $R_{\mathrm{g}} = \sqrt{Nb^2/6}$ is the radius of gyration of a *linear* polymer with degree of polymerization N (the reference degree of polymerization). We assume

$$\varsigma_\mu = \varsigma \lambda_\mu^{\nu} \tag{127}$$

where λ_μ is the macroscopic stretch ratio in this Cartesian direction.[26−28]

In this work, we seek a close analogue, within the Warner−Edwards model, of the smooth, coarse-grained "tube", conceptually familiar from melt rheology. (Such smoothness is important particularly in the context of chain retraction along the tube.) A candidate for this is the "mean path" $\hat{\mathbf{r}}_s$. (On the other hand, the configuration defined by the centers of the quadratic potentials $\mathbf{R}_s$ is *less* smooth than a Gaussian chain.) For most of the results presented in this paper, we have made the assumption that the configuration of the mean path $\hat{\mathbf{r}}_s$ is affinely deformed from the initial melt and that any chain retraction in the tube occurs along the mean path. This is by no means the only possible assumption; an alternative assumption made elsewhere[12,29] is that the centers of the quadratic potentials $\mathbf{R}_s$ are affinely deformed. These two assumptions are equivalent only if $d_\mu = d_0$, and differences emerge as soon as one considers the configuration of the mean path produced by each assumption, as follows.

An important quantity for the expressions which follow is the Fourier transformed correlation function for two points on the mean path

$$G_{1\mathbf{q}}(s,s') = \overline{\exp(i\mathbf{q}\cdot(\hat{\mathbf{r}}_s - \hat{\mathbf{r}}_{s'}))} \tag{128}$$

Under the assumption that the mean path is affinely deformed from the melt state, one obtains

$$G_{1\mathbf{q}}(\eta) = \exp\left(-\sum_\mu {Q_\mu}^2 {\lambda_\mu}^2\left[\eta - \varsigma^2\left(1 - \exp\left(-\frac{\eta}{\varsigma^2}\right)\right)\right]\right) \tag{129}$$

where we have defined a normalized wavevector, $\mathbf{Q}$, with components

$$Q_\mu = R_g q_\mu \tag{130}$$

where, as above, $R_g = \sqrt{Nb^2/6}$. The quantity η measures the normalized degree of polymerization of that portion of chain which previously occupied the tube between s and s' *in the unstretched state*. In the absence of any retraction, $\eta = |s - s'|/N$.

On the other hand, under the assumption that the centers of the quadratic potentials are affinely deformed, one obtains the alternative expression

$$G_{1\mathbf{q}}(\eta) = \exp\left\{-\sum_\mu Q_\mu{}^2\lambda_\mu{}^2\left[\eta + \frac{1}{2}\left(1 - \frac{\varsigma^4}{\varsigma_\mu{}^4}\right)\eta \times \exp\left(-\frac{\eta}{\varsigma_\mu{}^2}\right) - \frac{1}{2}\left(3 - \frac{\varsigma^4}{\varsigma_\mu{}^4}\right)\varsigma_\mu{}^2\left(1 - \exp\left(-\frac{\eta}{\varsigma_\mu{}^2}\right)\right)\right]\right\} \tag{131}$$

When used in the expression for the single-chain structure factor (see section E.2), this expression represents a generalization of the result for the particular case $\nu = 1/2$ given by Mergell and Everaers.[29]

A second important quantity is the Fourier transformed correlation function for a point $\hat{\mathbf{r}}_s$ on the mean path with the affine deformation of a point on the mean path of the same tube in the unstretched state, $\hat{\mathbf{x}}_{s'}$.

$$G_{2\mathbf{q}}(s,s') = \overline{\exp(i\mathbf{q}\cdot(\hat{\mathbf{r}}_s - \mathbf{E}\cdot\hat{\mathbf{x}}_{s'}))} \tag{132}$$

Under the assumption that the mean path is affinely deformed, we obtain, trivially,

$$G_{2\mathbf{q}}(\eta) = G_{1\mathbf{q}}(\eta) \tag{133}$$

Under the assumption that the centers of the quadratic potentials are affinely deformed, one obtains

$$G_{2\mathbf{q}}(\eta) = \exp\left\{-\sum_\mu Q_\mu{}^2\lambda_\mu{}^2\left[\eta - \varsigma_\mu{}^2\left(1 - \exp\left(-\frac{\eta}{\varsigma_\mu{}^2}\right)\right) + \frac{\varsigma_\mu{}^2}{4}\left(1 + \frac{\varsigma^4}{\varsigma_\mu{}^4}\right) - \frac{\varsigma^2}{2}\right]\right\} \tag{134}$$

The fact that this is different from eq 131 shows that this assumption produces systematic differences between the mean path of the tube in the deformed and undeformed state. (This is important for a further comparison between models made in Appendix F.)

It is not clear which of these two assumptions is the more appropriate. The differences between them are on length scales smaller than the tube diameter, where the deformation is nonaffine. The assumption of an affinely deformed mean path represents a slightly stronger deformation of the chain at these length scales than is obtained from affinely deforming the centers of the quadratic potentials. However, when comparing to data, the assumption of an affinely deformed mean path appears to give a better repesentation (within the approximations of this theory as a whole). As an example of this, Figure 9 shows a fit to the polybutadiene data using each of these two assumptions (cf. Figure 6 in the accomanying paper[18]). We treat this result with the same caution as the conclusion that $\nu = 1/2$ givs *a* better fit than $\nu = 0$ in ref 18. Neverthless, in all the results reported here and in ref 18, we have used $G_{1\mathbf{q}}(\eta) = G_{2\mathbf{q}}(\eta)$ as given by eq 129.

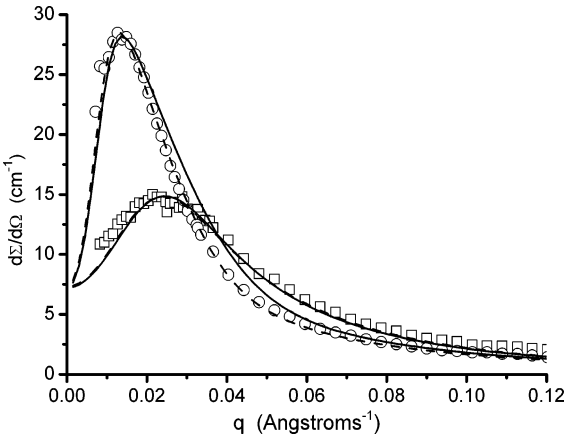

Figure 9. Comparison between fits with the assumption of affinely deformed potential positions (solid line) or affinely deformed tube mean path (dashed line), both with $\nu = 1/2$, for the polybutadiene data from ref 18 at an annealing time of 37.2 s. The fit for affinely deformed tube mean path is the one given in ref 18. The fit for affinely deformed potential positions uses $x = 0.75$ and $x_L = 0.36$, but otherwise uses the same parameters as given for the fit in Table 1 of ref 18.

The expressions given below for the correlation functions are mostly written as integrals over variables X and Y which are normalized chain contour variables such that

$$X = \frac{s_X}{N}$$

$$Y = \frac{s_Y}{N}$$

s_X and s_Y are the usual chain contour variables, which count numbers of monomers along a chain, and N is the reference degree of polymerization. Hence, in calculating the contribution to a particular correlation function of given a section of chain, the limits of the integral should reflect the ratio of the degree of polymerization of that chain section to the reference degree of polymerization.

E.1. Calculation of Δ_{0q}^{IJ}. All correlation functions are obtained by summing up the contributions from *pairs* of chain sections (or "blocks"), including same-block terms, in a manner analogous to the calculation for unstretched chains in ref 40. For two blocks (a and b) that are both trapped in the tube, the contribution is

$$\Delta_{0\mathbf{q}}^{ab} = \int^{f_a} dX \int^{f_b} dY \exp(-\sum_\mu Q_\mu{}^2\varsigma_\mu{}^2)G_{1\mathbf{q}}(\eta_T(X,Y)) \tag{135}$$

where the $f_a = N_a/N$ and $f_b = N_b/N$ are the fractions of the chain in blocks a and b, and these denote the ranges of the X and Y integrals. $\eta_T(X,Y)$ is the (normalized) degree of polymerization of that portion of chain which previously occupied the tube between X and Y *in the unstretched state*. We define the "retraction factor" $\gamma(X')$ of the chain in the tube to be the ratio of lengths of tube occupied by a given section of chain in the affinely deformed and current (retracted) states. In this case

$$\eta_T(X,Y) = \left|\int_X^Y \frac{1}{\gamma(X')}\, dX'\right| \tag{136}$$

For an unretracted chain $\gamma = 1$, and we would have $\eta_T(X,Y) = |X - Y|$. If the chain between X and Y is uniformly retracted by a factor γ, we have $\eta_T(X,Y) = |X - Y|/\gamma$. Note that, in eq 135, the factor $G_{1\mathbf{q}}(\eta_T(X,Y))$ represents the contribution from the mean path of the tube, and the $\exp(-\sum_\mu Q_\mu^2 \varsigma_\mu^2)$ arises from fluctuations about this mean path.

In the case where one block (a) is inside the tube, but the second (b) is contained within a free chain end, we find

$$\Delta_{0\mathbf{q}}^{ab} = \int^{f_a} dX \int^{f_b} dY \exp(-\sum_\mu Q_\mu{}^2 \varsigma_\mu{}^2) \times \exp(-Q^2 Y) G_{1\mathbf{q}}(\eta_T(X,X_E)) \quad (137)$$

In this case, X_E marks the "end" of the tube, and we take $Y = 0$ at the point where the free end meets the tube. The Y integral can be done analytically in this case.

In the case where both blocks (a and b) are in the same free end, we find

$$\Delta_{0\mathbf{q}}^{ab} = \int^{f_a} dX \int^{f_b} dY \exp(-Q^2(X + Y)) \times \exp(-\sum_\mu Q_\mu{}^2 \varsigma_\mu{}^2) \quad (138)$$

in which case we take $X = Y = 0$ at the point where the free ends meet the tube. Both the X and Y integrals are analytic.

Finally, if blocks a and b are within *different* free ends (i.e., separated by a section of tube), we find

$$\Delta_{0\mathbf{q}}^{ab} = \int^{f_a} dX \int^{f_b} dY \exp(-Q^2(X + Y)) \times \exp(-\sum_\mu Q_\mu{}^2 \varsigma_\mu{}^2) G_{1\mathbf{q}}(\eta_T(X_E,X_E')) \quad (139)$$

where X_E and X_E' mark the two ends of the tube and we take $X = 0$ and $Y = 0$ at the two points where the free ends meet the tube. Again, the integrals are analytic.

E.2. Calculation of $T_{\mathbf{q}}^{IJ}$. For the calculation of $T_{\mathbf{q}}^{IJ}$, we make use of the fact that $T_{\mathbf{q}}^{IJ} = S_{0\mathbf{q}}^{IJ} - \Delta_{0\mathbf{q}}^{IJ}$ and calculate contributions to $S_{0\mathbf{q}}^{IJ}$. For two blocks (a and b) that are both trapped in the tube, the contribution is

$$S_{0\mathbf{q}}^{ab} = \int^{f_a} dX \int^{f_b} dY \times \exp\left(-\sum_\mu Q_\mu{}^2 \varsigma_\mu{}^2 \left(1 - \exp\left(-\frac{|X - Y|}{\varsigma_\mu{}^2}\right)\right)\right) G_{1\mathbf{q}}(\eta_T(X,Y)) \quad (140)$$

where the f_a and f_b are the fractions of the chain in blocks a and b and denote the ranges of the X and Y integrals. $|X - Y|$ is the normalized degree of polymerization of the chain linking monomers at X and Y, and the factor $\exp(-\sum_\mu Q_\mu^2 \varsigma_\mu^2(1 - \exp(-|X - Y|/\varsigma_\mu^2)))$ represents the correlated fluctuations of the two linked monomers. For isotropic potentials ($\varsigma = \varsigma_\mu$) and no retraction ($\gamma = 1$), eq 140 is the expression originally derived by Warner and Edwards from this tube model.[24] On the other hand, for $\varsigma_\mu = \varsigma\lambda_\mu^{1/2}$ and $G_{1\mathbf{q}}$ as given by eq 131, this gives the result obtained by Mergell and Everaers[29] for deformed potentials.

In the case where one block (a) is inside the tube, but the second (b) is contained within a free chain end, we find (cf. eq 137)

$$S_{0\mathbf{q}}^{ab} = \int^{f_a} dX \int^{f_b} dY \times \exp\left(-\sum_\mu Q_\mu{}^2 \varsigma_\mu{}^2 \left(1 - \exp\left(-\frac{|X - X_E|}{\varsigma_\mu{}^2}\right)\right)\right) \times \exp(-Q^2 Y) G_{1\mathbf{q}}(\eta_T(X,X_E)) \quad (141)$$

In the case where both blocks (a and b) are in the same free end, we find the standard correlation function for Gaussian chains

$$S_{0\mathbf{q}}^{ab} = \int^{f_a} dX \int^{f_b} dY \exp(-Q^2|X - Y|) \quad (142)$$

Finally, if blocks a and b are within *different* free ends (i.e., separated by a section of tube), we find

$$S_{0\mathbf{q}}^{ab} = \int^{f_a} dX \int^{f_b} dY \times \exp(-Q^2(X + Y)) G_{1\mathbf{q}}(\eta_T(X_E,X_E')) \times \exp\left(-\sum_\mu Q_\mu{}^2 \varsigma_\mu{}^2 \left(1 - \exp\left(-\frac{|X_E' - X_E|}{\varsigma_\mu{}^2}\right)\right)\right) \quad (143)$$

E.3. Calculation of $D_{\mathbf{q}}^{I}$. For calculation of $D_{\mathbf{q}}^{I} = \overline{\langle P_{\mathbf{q}}{}^{I}\rangle_0 \langle \varphi_{-\mathbf{q}}\rangle_0{}^0}$ we are aiming to calculate the correlation function between all monomers on the chain of type I in the stretched state and all monomers on the same chain after a purely affine transformation from the unstretched state, given that they share the same quenched tube variables. We shall use the notation that the "X" monomer is on the "stretched" chain and that the "Y" monomer is on the affinely transformed chain. In particular, it should be noted that no chain retraction or branchpoint withdrawal occurs in the unstretched state, so it may not be the case that the same monomer occupies the same section of tube before and after the stretch. Nevertheless, this correlation function can still be obtained by summing up the contributions from *pairs* of blocks, as before. For two blocks (a and b) that are both trapped in the tube, the contribution is

$$D_{\mathbf{q}}^{ab} = \int^{f_a} dX \int^{f_b} dY \times \exp\left(-\frac{1}{2}\sum_\mu Q_\mu{}^2(\varsigma_\mu{}^2 + \lambda_\mu{}^2\varsigma^2)\right) G_{2\mathbf{q}}(\eta_T(X,Y)) \quad (144)$$

We retain the notation that $\eta_T(X,Y)$ is the (normalized) degree of polymerization of the chain which occupied the tube between X and Y *in the unstretched state*. The factor $\exp(-{}^1/_2\sum_\mu Q_\mu^2(\varsigma_\mu^2 + \lambda_\mu^2\varsigma^2))$ arises from a combination of anisotropic fluctuations (ς_μ^2) about the mean path in the stretched state plus isotropic fluctuations (ς^2) in the unstretched state. (However, $\varphi_{\mathbf{q}}$ includes an affine deformation of these isotropic fluctuations: hence the factor λ_μ^2.)

In the case where the "X" block (a) is inside the tube but the "Y" block (b) is contained within a free chain end, we find

$$D_{\mathbf{q}}^{ab} = \int^{f_a} dX \int^{f_b} dY \exp\left(-\frac{1}{2}\sum_\mu Q_\mu{}^2(\varsigma_\mu{}^2 + \lambda_\mu{}^2\varsigma^2)\right) \times \exp(-Q_s{}^2 Y) G_{2\mathbf{q}}(\eta_T(X,X_E)) \quad (145)$$

where

$$Q_s^2 = \sum_\mu Q_\mu^2 \lambda_\mu^2 \tag{146}$$

In the case where the "*Y*" block (b) is inside the tube but the "*X*" block (a) is contained within a free chain end, we find

$$D_{\mathbf{q}}^{ab} = \int^{f_a} dX \int^{f_b} dY \exp\left(-\frac{1}{2}\sum_\mu Q_\mu^2(\varsigma_\mu^2 + \lambda_\mu^2\varsigma^2)\right) \times \exp(-Q^2X) G_{2\mathbf{q}}(\eta_T(Y,Y_E)) \tag{147}$$

In this case, we take $X = 0$ at the point where the free end meets the tube.

In the case where both blocks (a and b) are in the same free end, we find

$$D_{\mathbf{q}}^{ab} = \int^{f_a} dX \int^{f_b} dY \exp(-Q^2X - Q_s^2 Y) \times \exp\left(-\frac{1}{2}\sum_\mu Q_\mu^2(\varsigma_\mu^2 + \lambda_\mu^2\varsigma^2)\right) \tag{148}$$

Finally, if blocks a and b are within *different* free ends (i.e., separated by a section of tube), we find

$$D_{\mathbf{q}}^{ab} = \int^{f_a} dX \int^{f_b} dY \exp(-Q^2X - Q_s^2 Y) \times \exp\left(-\frac{1}{2}\sum_\mu Q_\mu^2(\varsigma_\mu^2 + \lambda_\mu^2\varsigma^2)\right) G_{2\mathbf{q}}(\eta_T(X_E, X_E')) \tag{149}$$

E.4. Calculation of $\beta_{\mathbf{q}}^{\mathbf{I}}$. As given in eq 68, $\beta_{\mathbf{q}}^{I}$ is related to the fluctuations $\delta\mathbf{r}_{\alpha,s}$ of a monomer about its mean position. It involves a simple sum over all the monomers of type I. Hence, for blocks in the tube, the contribution according to the Warner−Edwards model is simply

$$\beta_{\mathbf{q}}^{a} = \int^{f_a} dX \exp\left(-\frac{1}{2}\sum_\mu Q_\mu^2 \varsigma_\mu^2\right) \tag{150}$$

For a block in a free chain end, the contribution is

$$\beta_{\mathbf{q}}^{a} = \int^{f_a} dX \exp\left(-\frac{1}{2}\sum_\mu Q_\mu^2 \varsigma_\mu^2 - Q^2X\right) \tag{151}$$

where we take $X = 0$ at the point where the free end meets the tube.

E.5. Calculation of $S_{\mathbf{q}}^{\mathbf{tot}}$. $S_{\mathbf{q}}^{tot} = \overline{\langle\varphi_{\mathbf{q}}\varphi_{-\mathbf{q}}\rangle_0}^0$ is simply the total scattering function for a chain affinely deformed from the unstretched melt. Hence, for any two blocks a and b we find the usual (analytically integrable) form of scattering function for a Gaussian chain:

$$S_{\mathbf{q}}^{tot,a,b} = \int^{f_a} dX \int^{f_b} dY \exp(-Q_s^2|X - Y|) \tag{152}$$

E.6.Calculation of $\Delta_{0\mathbf{q}}^{\mathbf{ff}}$. We need to calculate $\Delta_{0\mathbf{q}}^{ff} = \overline{f_{\mathbf{q}} f_{-\mathbf{q}}}^0$, where $f_{\mathbf{q}}$ is as given in eq 83. Hence, $\Delta_{0\mathbf{q}}^{ff}$ involves a double sum over all tube segments in the system, which we can write as

$$\Delta_{0\mathbf{q}}^{ff} = \frac{N_e^2}{\Omega\rho N}\sum_{\alpha,m}\sum_{\alpha',m'} \overline{(\phi^{\alpha,m} - 1)(\phi^{\alpha',m'} - 1) d_{\mathbf{q}}^{\alpha,m} d_{-\mathbf{q}}^{\alpha',m'}}^0 \tag{153}$$

The quantity $\phi^{\alpha,m}$ depends on the orientation of tube segment α, m, expressed through the vector $\mathbf{H}^{\alpha,m}$, whereas the quantity $d_{\mathbf{q}}^{\alpha,m}$ depends on the position of the tube segment $\hat{\mathbf{r}}_{ref,\alpha,m}$. For the present calculation, we shall assume that $\mathbf{H}^{\alpha,m}$ and $\hat{\mathbf{r}}_{ref,\alpha,m}$ are uncorrelated. In fact, there is a correlation because the separation vector between two tube segments on the same chain will depend, to a small extent, on the orientation of those tube segments. However, this correlation will be small if the number of tube segments on a chain is large and, moreover, will have the greatest effect on the calculation for wavevectors near the inverse tube diameter. The effects of elastic fluctuations on the overall scattering calculation are, in practice, important for smaller wavevectors than this.

Making this approximation, then, we write

$$\overline{(\phi^{\alpha,m} - 1)(\phi^{\alpha',m'} - 1) d_{\mathbf{q}}^{\alpha,m} d_{-\mathbf{q}}^{\alpha',m'}}^0 \approx \overline{(\phi^{\alpha,m} - 1)(\phi^{\alpha',m'} - 1)}^0 \overline{d_{\mathbf{q}}^{\alpha,m} d_{-\mathbf{q}}^{\alpha',m'}}$$

We note that

$$\overline{d_{\mathbf{q}}^{\alpha,m} d_{-\mathbf{q}}^{\alpha',m'}}^0 = 0 \quad \text{for } \alpha \neq \alpha'$$

so that we can ignore different-chain terms in the double sum. (In fact, this statement is independent of the above approximation.) We also use the identity

$$\overline{(\phi^{\alpha,m} - 1)(\phi^{\alpha,m'} - 1)}^0 = [\overline{\phi^{\alpha,m}\phi^{\alpha,m'}}^0 - \overline{\phi^{\alpha,m}}^0\,\overline{\phi^{\alpha,m'}}^0] + (\overline{\phi^{\alpha,m}}^0 - 1)(\overline{\phi^{\alpha,m'}}^0 - 1)$$

and note that the term in square brackets is zero for $m \neq m'$ because there is no correlation in the model between the orientation of one tube segment and another. Hence, we can write

$$\Delta_{0\mathbf{q}}^{ff} = \frac{N_e^2}{\Omega\rho N}[\sum_{\alpha,m} W_2^{\alpha,m}\,\overline{d_{\mathbf{q}}^{\alpha,m} d_{-\mathbf{q}}^{\alpha,m}}^0 + \sum_{\alpha,m,m'} W_1^{\alpha,m} W_1^{\alpha,m'} \overline{d_{\mathbf{q}}^{\alpha,m} d_{-\mathbf{q}}^{\alpha,m'}}^0] = \Delta_{\mathbf{q},inc}^{ff} + \Delta_{\mathbf{q},coh}^{ff} \tag{154}$$

where

$$W_1^{\alpha,m} = \overline{\phi^{\alpha,m}}^0 - 1 \tag{155}$$

$$W_2^{\alpha,m} = \overline{\phi^{\alpha,m}\phi^{\alpha,m}}^0 - \overline{\phi^{\alpha,m}}^0\,\overline{\phi^{\alpha,m}}^0 \tag{156}$$

There are two terms in eq 154. The first is of form

$$\Delta_{\mathbf{q},inc}^{ff} = \frac{N_e^2}{\Omega\rho N}\sum_{\alpha,m} W_2^{\alpha,m}\,\overline{d_{\mathbf{q}}^{\alpha,m} d_{-\mathbf{q}}^{\alpha,m}}^0 \tag{157}$$

and this is independent of the spatial arrangement of the tube segments, depending only on the fluctuations in the orientation of individual tube segments. In this sense, it is equivalent to the "incoherent" neutron scattering contribution (arising from fluctuations in the spin state of individual nuclei). The function $\overline{d_{\mathbf{q}}^{\alpha,m} d_{-\mathbf{q}}^{\alpha,m}}^0$ provides a cutoff to the stress contributions at wavevectors larger than the inverse tube diameter. In practice, the final scattering function is broadly insensitive to the precise form of this function provided the cutoff wavevec-

tor is of the right order, so we write approximately

$$\overline{d_{\mathbf{q}}^{\alpha,m} d_{-\mathbf{q}}^{\alpha,m0}} = \exp(-\sum_{\mu} Q_{\mu}{}^2 \varsigma_{\mu}{}^2) \tag{158}$$

It is possible to replace the sum over tube segments in eq 157 with a sum over monomers within the tube and also to replace the sum over chains α with a sum over *species j* in a multicomponent system, giving

$$\Delta_{\mathbf{q},\mathrm{inc}}^{\mathrm{ff}} = \frac{N_{\mathrm{e}}}{N}\sum_{j}\frac{\phi_j}{f_j}\int\frac{\mathrm{d}X}{\gamma(X)} W_2^{\alpha,\mathrm{X}} \exp(-\sum_{\mu} Q_{\mu}{}^2 \varsigma_{\mu}{}^2) \tag{159}$$

where ϕ_j is the volume fraction of species j and $f_j = N_j/N$ is the ratio of the degree of polymerization of species j to the reference degree of polymerization, N. The integral is over all monomers in the tube.

The second term in eq 154 is of form

$$\Delta_{\mathbf{q},\mathrm{coh}}^{\mathrm{ff}} = \frac{N_{\mathrm{e}}{}^2}{\Omega\rho N}\sum_{\alpha,m,m'} W_1^{\alpha,m} W_1^{\alpha,m'} \overline{d_{\mathbf{q}}^{\alpha,m} d_{-\mathbf{q}}^{\alpha,m'0}} \tag{160}$$

In this case, the factor $\overline{d_{\mathbf{q}}^{\alpha,m} d_{-\mathbf{q}}^{\alpha,m'}}0$ contains information about the spatial arrangement of segments m and m'. Hence, $\Delta_{\mathbf{q},\mathrm{coh}}^{\mathrm{ff}}$ is related to spatial fluctuations in tube segment density, weighted by the factor $W_1^{\alpha,m}$. In this sense it is equivalent to the "coherent" neutron scattering contribution (which is related to fluctuations in the density of nuclei, weighted by the scattering length).

As defined in eq 74, $d_{\mathbf{q}}^{\alpha,m}$ contains an explicit sum over monomers, which we can use to turn the double sum over tube segments into a double sum over monomers in $\Delta_{\mathbf{q},\mathrm{coh}}^{\mathrm{ff}}$. We then use the Warner−Edwards model to determine the required correlation between monomer positions. Again, we can replace the sum over chains α with a sum over *species j* in a multicomponent system, giving (after a little rearrangement)

$$\Delta_{\mathbf{q},\mathrm{coh}}^{\mathrm{ff}} = \sum_{j}\frac{\phi_j}{f_j}\sum_{\mathrm{a,b}}\Delta_{\mathbf{q},\mathrm{coh}}^{\mathrm{ff,ab}} \tag{161}$$

There is an explicit double sum over blocks a and b within a molecule of species *j*; the contribution from blocks a and b is of form

$$\Delta_{\mathbf{q},\mathrm{coh}}^{\mathrm{ff,ab}} = \int^{f_{\mathrm{a}}}\frac{\mathrm{d}X}{\gamma(X)}\int^{f_{\mathrm{b}}}\frac{\mathrm{d}Y}{\gamma(Y)} W_1^{\alpha,\mathrm{X}} W_1^{\alpha,\mathrm{Y}} \times \exp(-\sum_{\mu} Q_{\mu}{}^2 \varsigma_{\mu}{}^2) G_{1\mathbf{q}}(\eta_{\mathrm{T}}(X,Y)) \tag{162}$$

Note that this is very similar in form to eq 135, but with extra local weightings $1/\gamma(X)$ to convert from counting over monomers to counting over tube segments, and $W_1^{\alpha,\mathrm{X}}$ to represent the stress contribution from a given tube segment.

There remains the determination of algebraic expressions for the factors $W_1^{\alpha,\mathrm{X}}$ and $W_2^{\alpha,\mathrm{X}}$. These are evaluated using the Gaussian distribution of tube segments given in eq 69, giving

$$W_1^{\alpha,m} = B_1(\mathbf{E},\hat{\mathbf{q}})\frac{n_{\mathrm{C}}^{\alpha,m}\alpha(\mathbf{E})}{\gamma^{\alpha,m}} - 1 \tag{163}$$

$$W_2^{\alpha,m} = B_2(\mathbf{E},\hat{\mathbf{q}})\left(\frac{n_{\mathrm{C}}^{\alpha,m}\alpha(\mathbf{E})}{\gamma^{\alpha,m}}\right)^2 \tag{164}$$

where $\alpha(\mathbf{E})$ is the Doi−Edwards tube elongation factor. $B_1(\mathbf{E},\hat{\mathbf{q}})$ and $B_2(\mathbf{E},\hat{\mathbf{q}})$ are numbers which depend on the orientation of the wavevector relative to the deformation and upon the size of the deformation. It is these factors that give rise to the mathematical prediction of the "butterfly" pattern. For a volume-conserving uniaxial extension by a factor λ in the z-direction, we find

$$B_1(\mathbf{E},\hat{\mathbf{q}}) = \frac{(q_x{}^2 + q_y{}^2)l_x + q_z{}^2 l_z}{q^2} \tag{165}$$

$$B_2(\mathbf{E},\hat{\mathbf{q}}) = [(L_{xx} - l_x{}^2)(q_x{}^2 + q_y{}^2)^2 + (L_{zz} - l_z{}^2)q_z{}^4 + 2(L_{xz} - l_x l_z)(q_x{}^2 + q_y{}^2)q_z{}^2]/q^4 \tag{166}$$

where

$$l_x = \frac{3}{4}\frac{(2\lambda^3 - 1)\ln(\lambda^{3/2} + (\lambda^3 - 1)^{1/2}) - \lambda^{3/2}(\lambda^3 - 1)^{1/2}}{\lambda^{1/2}(\lambda^3 - 1)^{3/2}} \tag{167}$$

$$l_z = \frac{3}{2}\lambda^{5/2}\frac{\lambda^{3/2}(\lambda^3 - 1)^{1/2} - \ln(\lambda^{3/2} + (\lambda^3 - 1)^{1/2})}{(\lambda^3 - 1)^{3/2}} \tag{168}$$

$$L_{xx} = \frac{15}{8}\frac{3\lambda^6 \tan^{-1}((\lambda^3 - 1)^{1/2}) + (2 - 5\lambda^3)(\lambda^3 - 1)^{1/2}}{\lambda(\lambda^3 - 1)^{5/2}} \tag{169}$$

$$L_{zz} = 5\lambda^5\frac{3\tan^{-1}((\lambda^3 - 1)^{1/2}) + (\lambda^3 - 4)(\lambda^3 - 1)^{1/2}}{(\lambda^3 - 1)^{5/2}} \tag{170}$$

$$L_{xz} = \frac{15}{2}\lambda^2\frac{(2\lambda^3 + 1)(\lambda^3 - 1)^{1/2} - 3\tan^{-1}((\lambda^3 - 1)^{1/2})}{(\lambda^3 - 1)^{5/2}} \tag{171}$$

It should be noted that the precise form of these is dependent upon the particular assumptions made about the tube model in Appendix C.

In the limit of no stretching ($\lambda = 1$) these expressions reduce to $B_1 = 1$ and $B_2 = 2$. It is also true that $n_{\mathrm{C}}^{\alpha,m}\alpha(\mathbf{E})/\gamma^{\alpha,m} = 1$ in this limit, and hence $W_1^{\alpha,m} = 0$. This means that there is no "coherent" component to the fluctuations in $f_{\mathbf{q}}$ (i.e., $\Delta_{\mathbf{q},\mathrm{coh}}^{\mathrm{ff,ab}} = 0$) in the limit of no stretching, as discussed in section 3.5; there are only "incoherent" fluctuations.

E.7. Calculation of $\Delta_{\mathbf{0q}}^{\mathbf{If}}$. The calculation of this correlation between monomer density and quenched stress proceeds in a manner similar to the above, resulting in a sum over pairs of blocks. For a pair of blocks "a" (contributing to stress) and "b" (contributing to monomer density), both in the tube, the contribution is

$$\Delta_{0\mathbf{q}}^{\mathrm{If,ab}} = \int^{f_{\mathrm{a}}}\frac{\mathrm{d}X}{\gamma(X)} W_1^{\alpha,\mathrm{X}}\int^{f_{\mathrm{b}}}\mathrm{d}Y \times \exp(-\sum_{\mu} Q_{\mu}{}^2 \varsigma_{\mu}{}^2) G_{1\mathbf{q}}(\eta_{\mathrm{T}}(X,Y)) \tag{172}$$

We also need to include the case where the block contributing to "monomer density" (b) is contained

within a free chain end; this gives

$$\Delta_{0\mathbf{q}}^{\mathrm{If,ab}} = \int^{f_a} \frac{\mathrm{d}X}{\gamma(X)} W_1^{\alpha,\mathrm{X}} \int^{f_b} \mathrm{d}Y \exp(-\sum_\mu Q_\mu{}^2 \zeta_\mu{}^2) \times \exp(-Q^2 Y) G_{1\mathbf{q}}(\eta_{\mathrm{T}}(X,X_{\mathrm{E}})) \quad (173)$$

Note that, in the unstretched limit ($\lambda = 1$), we find $W_1^{\alpha,\mathrm{X}} = 0$ and hence $\Delta_{0\mathbf{q}}^{\mathrm{If}} = 0$, as discussed in section 3.5.

E.8. Calculation of $D_{\mathbf{q}}^{\mathrm{f}}$. The calculation of this correlation between monomer density (on the unstretched chain) and quenched stress proceeds in a manner similar to the above, resulting in a sum over pairs of blocks. For a pair of blocks "a" (contributing to stress) and "b" (contributing to monomer density), both in the tube, the contribution is

$$D_{\mathbf{q}}^{\mathrm{f,ab}} = \int^{f_a} \frac{\mathrm{d}X}{\gamma(X)} W_1^{\alpha,\mathrm{X}} \int^{f_b} \mathrm{d}Y \times \exp\left(-\frac{1}{2}\sum_\mu Q_\mu{}^2(\zeta_\mu{}^2 + \lambda_\mu{}^2 \varsigma^2)\right) G_{2\mathbf{q}}(\eta_{\mathrm{T}}(X,Y)) \quad (174)$$

We also need to include the case where the block contributing to "monomer density" (b) is contained within a free chain end; this gives

$$D_{\mathbf{q}}{}^{\mathrm{f,ab}} = \int^{f_a} \frac{\mathrm{d}X}{\gamma(X)} W_1{}^{\alpha,\mathrm{X}} \int^{f_b} \mathrm{d}Y \times \exp\left(-\frac{1}{2}\sum_\mu Q_\mu{}^2(\zeta_\mu{}^2 + \lambda_\mu{}^2 \varsigma^2)\right) \exp(-Q_{\mathrm{s}}{}^2 Y) G_{2\mathbf{q}}(\eta_{\mathrm{T}}(X,X_{\mathrm{E}})) \quad (175)$$

E.9. Calculation of $A_{1\mathbf{q}}$ and $A_{2\mathbf{q}}$. As given in eqs 80 and 82, both $A_{1\mathbf{q}}$ and $A_{2\mathbf{q}}$ involve the factor $d_{\mathbf{q}}^{\alpha,m}\, d_{-\mathbf{q}}^{\alpha,m}$, for which we use the same approximation as given in eq 158. They also both involve a sum over chains and tube segments. As with the calculation of $\Delta_{\mathbf{q},\mathrm{inc}}^{\mathrm{ff}}$ above, these can be replaced by a sum over species j and monomers respectively, giving

$$A_{1\mathbf{q}} = \frac{N}{N_{\mathrm{e}}} \sum_j \frac{\phi_j}{f_j} \int \frac{\mathrm{d}X}{\gamma(X)} \exp(-\sum_\mu Q_\mu{}^2 \zeta_\mu{}^2) \quad (176)$$

$$A_{2\mathbf{q}} = \frac{N}{N_{\mathrm{e}}} \sum_j \frac{\phi_j}{f_j} \int \frac{\mathrm{d}X}{\gamma(X)} (W_1^{\alpha,\mathrm{X}} + 1) \exp(-\sum_\mu Q_\mu{}^2 \zeta_\mu{}^2) \quad (177)$$

where the integral is over all monomers in the tube. Given that $W_1^{\alpha,\mathrm{X}} = 0$ and $W_2^{\alpha,\mathrm{X}} = 2$ in the unstretched limit ($\lambda = 1$), it is straightforward to show that

$$\Delta_{0\mathbf{q}}^{\mathrm{ff}} = \left(\frac{N_{\mathrm{e}}}{N}\right)^2 (A_{1\mathbf{q}} + A_{2\mathbf{q}}) \quad (178)$$

in this limit, as discussed in section 3.5.

E.10. Correlation Functions in Multicomponent Mixtures. The above contributions to the various correlation functions are presented as contributions from pairs of "blocks" on the same molecule. To obtain the contribution from a given molecule, one sums over pairs of blocks within that molecule. In a polydisperse mixture, or in a mixture with impurities, however, it is necessary to sum up the contributions from the different chemical species, j, in the system. The form of the result is given explicitly above in the calculation of $\Delta_{0\mathbf{q}}^{\mathrm{ff}}$, but the same form holds for all the correlation functions:

$$CF = \sum_j \frac{\phi_j}{f_j} \sum_{\mathrm{a,b}} CF^{ab} \quad (179)$$

where CF is the total correlation function from all the species, CF^{ab} is the correlation function from blocks a and b within an individual species, ϕ_j is the volume fraction of species j, and $f_j = N_j/N$ is the ratio of the degree of polymerization of species j to the reference degree of polymerization, N.

The functions $\beta_{\mathbf{q}}^{\mathrm{I}}$ are given by a single sum over blocks, and in a multicomponent system this gives

$$\beta_{\mathbf{q}}^{\mathrm{I}} = \sum_j \frac{\phi_j}{f_j} \sum_{\mathrm{a}} \beta_{\mathbf{q}}^{\mathrm{a}} \quad (180)$$

Appendix F. Comparison with the Panyukov−Potemkin Model

Panyukov and Potemkin[12] (PP) presented a model for the density−density correlation function of an entangled network after a step strain deformation. Their model made use of a "Warner−Edwards" model for entangled network chains, with anisotropic localizing potentials (with exponent $\nu = {}^1/_2$). Since they were interested mainly in the crossover between liquidlike and solidlike behavior at the tube diameter, they took the limit of infinite chains ($N \to \infty$). They considered the network to be prepared in the melt state (so that the total density fluctuations in this state were close to zero because of incompressibility) but examined fluctuations in the total network density in a swollen state. (In this sense, their system was somewhat simpler than the one considered here—they did not, for example, consider partially labeled polymers.) In this Appendix we compare their results against the model developed here.

To make a comparison between their results and ours, note that they use a different measure (a) of monomer step length, such that $a^2 = 2/3\ b^2$. They also define an "entanglement molecular weight" $N_{\mathrm{e}}^{\mathrm{PP}}$ related to the Warner−Edwards tube diameter used here via

$$N_{\mathrm{e}}^{\mathrm{PP}} = \frac{\sqrt{6} d_0{}^2}{2b^2} \quad (181)$$

Because they considered the limit $N \to \infty$, some of the normalizations of (for example) density variables used in this paper, made for convenience in dealing with finite chains, are inappropriate. To make the comparison as clean as possible, we redefine the Fourier transformed density variable as

$$\tilde{\rho}_{\mathbf{q}} = \sum_{\alpha,s} \exp(i\mathbf{q}\cdot\mathbf{r}_{\alpha,s}) \quad (182)$$

and our field variable for network fluctuations as

$$\tilde{\Gamma}_{\mathbf{q}} = i\mathbf{q}\cdot\mathbf{w}_{\mathbf{q}} \quad (183)$$

With these definitions, the free energy functional obtained for such a network system using the theory presented in this current paper is of form

$$F\{\tilde{\rho}_{\mathbf{q}},\tilde{\Gamma}_{\mathbf{q}}\} = \frac{1}{\Omega}\sum_{\mathbf{q}}\frac{|\tilde{\rho}_{\mathbf{q}} - \tilde{d}_{\mathbf{q},\mathrm{ref}} - \rho\tilde{\Gamma}_{\mathbf{q}}\beta_{\mathbf{q}}|^2}{2\tilde{T}_{\mathbf{q}}} + \frac{|\tilde{d}_{\mathbf{q},\mathrm{ref}} + \rho\tilde{\Gamma}_{\mathbf{q}}\beta_{\mathbf{q}}|^2}{2\tilde{\Delta}_{0\mathbf{q}}} + B|\tilde{\rho}_{\mathbf{q}}|^2 - \tilde{f}_{-\mathbf{q}}\tilde{\Gamma}_{\mathbf{q}} + \frac{\tilde{A}_{\mathbf{q}}}{2}\tilde{\Gamma}_{\mathbf{q}}\tilde{\Gamma}_{-\mathbf{q}} \quad (184)$$

where B is an excluded-volume parameter. If we take $\nu = {}^1/_2$, then

$$\tilde{T}_{\mathbf{q}} = 2N_{\mathrm{e}}^{\mathrm{PP}}\rho\int_0^\infty \mathrm{d}y\ \tilde{G}_{1\mathbf{q}}(y)\exp(-\sum_\mu \tilde{Q}_\mu^2\lambda_\mu)\times \left[\exp\left(\sum_\mu \tilde{Q}_\mu^2\lambda_\mu \exp\left(-\frac{y}{\lambda_\mu}\right)\right) - 1\right] \quad (185)$$

and

$$\tilde{\Delta}_{0\mathbf{q}} = 2N_{\mathrm{e}}^{\mathrm{PP}}\rho\int_0^\infty \mathrm{d}y\ \tilde{G}_{1\mathbf{q}}(y)\exp(-\sum_\mu \tilde{Q}_\mu^2\lambda_\mu) \quad (186)$$

where we have defined a normalized wavevector so that $\tilde{Q}^2 = N_{\mathrm{e}}^{\mathrm{PP}}b^2q^2/6$ (Panyukov and Potemkin use a different normalized wavevector, $Q_{\mathrm{PP}}{}^2 = N_{\mathrm{e}}^{\mathrm{PP}}a^2q^2 = 4\tilde{Q}^2$).

If we assume the mean path is affinely deformed, then the function $\tilde{G}_{1\mathbf{q}}(y)$ takes the form

$$\tilde{G}_{1\mathbf{q}}(y) = \exp(-\sum_\mu \tilde{Q}_\mu{}^2\lambda_\mu{}^2(y - 1 + \exp(-y))) \quad (187)$$

On the other hand, if we assume the centers of the quadratic potentials are affinely deformed, we obtain

$$\tilde{G}_{1\mathbf{q}}(y) = \exp\left(-\sum_\mu \tilde{Q}_\mu{}^2\left(\lambda_\mu{}^2 y + \frac{1}{2}(\lambda_\mu{}^2 - 1)y\times \exp\left(-\frac{y}{\lambda_\mu}\right) - \frac{1}{2}(3\lambda_\mu{}^3 - \lambda_\mu)\left(1 - \exp\left(-\frac{y}{\lambda_\mu}\right)\right)\right)\right) \quad (188)$$

The cutoff function $\beta_{\mathbf{q}}$ is given by

$$\beta_{\mathbf{q}} = \exp\left(-\frac{1}{2}\sum_\mu \tilde{Q}_\mu{}^2\lambda_\mu\right) \quad (189)$$

and

$$\tilde{A}_{\mathbf{q}} = \frac{\rho}{N_{\mathrm{e}}}\left(1 + \frac{\mathbf{q}\cdot\mathbf{E}\cdot\mathbf{E}^{\mathrm{T}}\cdot\mathbf{q}}{q^2}\right)\exp(-\sum_\mu \tilde{Q}_\mu{}^2\lambda_\mu) \quad (190)$$

Since the network is prepared in the incompressible melt state, we anticipate the frozen-in density variation $\tilde{d}_{\mathbf{q},\mathrm{ref}}$ to be small (though not nonzero—we still expect a relation of form eq 115 for $\overline{\tilde{d}_{\mathbf{q},\mathrm{ref}}\tilde{d}_{-\mathbf{q},\mathrm{ref}}}$ and note that such a careful treatment of quenched fields is necessary for reproduction of the standard RPA results in the limit of no stretch). Similarly, we expect the random stress variations $\tilde{\Delta}_{\mathbf{q}}^{\mathrm{ff}} = \overline{\tilde{f}_{\mathbf{q}}\tilde{f}_{-\mathbf{q}}}$ to be dominated by the "incoherent" component of the fluctuations, the coherent part being largely suppressed by incompressibility in the state of preparation and (in any case) zero in the limit of no stretching:

$$\tilde{\Delta}_{\mathbf{q}}^{\mathrm{ff}} \approx \tilde{\Delta}_{\mathbf{q},\,\mathrm{inc}}^{\mathrm{ff}} = 2\frac{\Omega\rho(\mathbf{q}\cdot\mathbf{E}\cdot\mathbf{E}^{\mathrm{T}}\cdot\mathbf{q})^2}{N_{\mathrm{e}}\quad q^4}\exp(-\sum_\mu \tilde{Q}_\mu{}^2\lambda_\mu) \quad (191)$$

Note that in the limit of no stretching

$$\tilde{\Delta}_{\mathbf{q}}^{\mathrm{ff}} = \Omega\tilde{A}_{\mathbf{q}} \quad (192)$$

which is equivalent to the condition given in section 3.5 for reproduction of standard RPA results in this limit.

The free energy functional given by Panyukov and Potemkin (their eq 17) is similar in form to eq 184 and (using their notation as closely as possible) is

$$F\{\tilde{\rho}_{\mathrm{q}},\mathbf{w}_{\mathbf{q}}\} = \frac{1}{\Omega}\sum_{\mathbf{q}}\frac{|\tilde{\rho}_{\mathrm{q}} + \rho\sum_\mu iq_\mu A_{\mu\mathbf{q}}^{\mathrm{PP}}w_{\mu\mathbf{q}}|^2}{\Delta_{\mathbf{q}}^{\mathrm{PP}}} + B|\tilde{\rho}_{\mathrm{q}}|^2 + \sum_\mu F_{\mu\mathbf{q}}w_{\mu-\mathbf{q}} + \sum_\mu E_{\mu\mathbf{q}}w_{\mu\mathbf{q}}w_{\mu-\mathbf{q}} \quad (193)$$

Certain identifications between this and eq 184 are immediately possible. For example, we would anticipate $\Delta_{\mathbf{q}}^{\mathrm{PP}} = 2\tilde{T}_{\mathbf{q}}$. Since Panyukov and Potemkin assume affine deformation of the centers of the localizing potentials, their $\Delta_{\mathbf{q}}^{\mathrm{PP}}$ is given (setting aside a troublesome factor of 4) by eqs 185 and 188. Similarly, one would identify their $A_{\mu\mathbf{q}}^{\mathrm{PP}}$ with our $\beta_{\mathbf{q}}$. The expression they give appears somewhat different to eq 189, however:

$$A_{\mu\mathbf{q}}^{\mathrm{PP}} = \frac{1}{\lambda_\mu}\int_0^\infty \mathrm{d}y\ \exp\left[-\frac{y}{\lambda_\mu} + \sum_\nu \tilde{Q}_\nu{}^2\left\{\frac{3}{4}(\lambda_\nu{}^3 - \lambda_\nu) - \lambda_\nu{}^2\left(y + \lambda_\nu\exp\left(-\frac{y}{\lambda_\nu}\right)\right)\right\}\right] \quad (194)$$

The differences between these expressions can be understood by examining the underlying assumptions of the models. In deriving our expression for $\beta_{\mathbf{q}}$ (see Appendix B and eqs 36 and 45), we assumed that the deformation field $\mathbf{w}_s$ for monomer s acted upon the mean path of the tube, with a magnitude $\mathbf{w}_s = \mathbf{w}(\hat{\mathbf{r}}_s)$ depending on the position of the mean path. Panyukov and Potemkin, however, allow $\mathbf{w}_s$ to act upon the centers of the confining potentials, $\mathbf{R}_s$. In their model, the magnitude of the deformation depends on the position of the monomer *before the deformation* (i.e., they use $\mathbf{w}_s = \mathbf{w}(\mathbf{E}\cdot\boldsymbol{x}_s)$—in their notation $u_\mu(\lambda^*\mathbf{x}_s)$—in their eq 6). The more obvious choice of $\mathbf{w}(\mathbf{R}_s)$ was not used, perhaps because it leads to a meaningless expression for $A_{\mu\mathbf{q}}^{\mathrm{PP}}$ due to the fact that $\mathbf{R}_s$ is not a smooth function of s.

Equation 194 can be derived using the methodology of Appendix B, but making the alternative assumptions of Panyokov and Potemkin outlined above. It can be reasonably well approximated by

$$A_{\mu\mathbf{q}}^{\mathrm{PP}} \approx \exp\left(-\sum_\nu \frac{\tilde{Q}_\nu^2}{4}(\lambda_\nu{}^3 + 3\lambda_\nu)\right) \quad (195)$$

The presence of the strong factor $\exp(-\Sigma_\mu \tilde{Q}_\nu^2/4\lambda_\mu^3)$, which dominates parallel to the stretch, occurs in the derivation because of the specific use of $\mathbf{w}(\mathbf{E}\cdot\boldsymbol{x}_s)$ and the assumption of affine deformation of the centers of the localizing potentials. It arises under these assumptions because of the differences between the tube mean paths in the stretched and unstretched states (the same factor is present in eq 134). Since there is no physical reason why tube fluctuations in the stretched state should

depend on monomer positions in the unstretched state, it would appear that the use of $\mathbf{w}(\mathbf{E}\cdot\mathbf{x}_s)$ is inappropriate.

The model used by Panyukov and Potemkin is, in one respect, more self-consistent than the one used here in that they use the same tube model to calculate the polymer density and elastic components of their free energy functional. (In contrast, we used the model outlined in Appendix C for the elastic comonents because (i) it is more consistent with current models of melt rheology, (ii) it allows for an obvious way to include chain retraction, and (iii) it is more tractable within the approximations of the current theory.) As a result, their equations for elastic contributions to the free energy are somewhat different to ours, and (for example) they give

$$E_{\mu\mathbf{q}} = \frac{\rho}{N_e^{PP}} \frac{(\mathbf{q}\cdot\mathbf{E}\cdot\mathbf{E}^T\cdot\mathbf{q})}{\lambda_\mu} \frac{1}{4 + \lambda_\mu N_e^{PP} a^2 (\mathbf{q}\cdot\mathbf{E}\cdot\mathbf{E}^T\cdot\mathbf{q})} \quad (196)$$

The particular form of this *does not* allow the splitting of $\mathbf{w}_\mathbf{q}$ into parallel and perpendicular components, which suggests that the use of the field variable $\Gamma_\mathbf{q}$ in this present paper represents a special case. In general, one must use all components of $\mathbf{w}_\mathbf{q}$ as is done by Panyukov and Potemkin. (Of course, for the more complicated system considered in this paper the resulting expressions will be somewhat longer!)

Only in the special case of zero stretch can the Panyukov−Potemkin model be rewritten in terms of $\tilde{\Gamma}_\mathbf{q} = i\mathbf{q}\cdot\mathbf{w}_\mathbf{q}$, and this gives

$$F\{\tilde{\rho}_q, \mathbf{w}_\mathbf{q}\} = \frac{1}{\Omega}\sum_\mathbf{q} \frac{|\tilde{\rho}_\mathbf{q} + \rho A_\mathbf{q}^{PP}\tilde{\Gamma}_\mathbf{q}|^2}{\Delta_\mathbf{q}^{PP}} + B|\tilde{\rho}_\mathbf{q}|^2 - \tilde{f}_{-\mathbf{q}}\tilde{\Gamma}_\mathbf{q} + \frac{\tilde{E}_\mathbf{q}}{2}\tilde{\Gamma}_\mathbf{q}\tilde{\Gamma}_{-\mathbf{q}} \quad (197)$$

with

$$\tilde{E}_\mathbf{q} = \frac{\rho}{2N_e^{PP}} \frac{1}{1 + \frac{N_e^{PP} a^2 q^2}{4}} \quad (198)$$

$$\overline{\tilde{f}_\mathbf{q}\tilde{f}_{-\mathbf{q}}} = \frac{\Omega\rho}{8N_e^{PP}}\left(1 + \frac{1}{1 + \frac{N_e^{PP} a^2 q^2}{2}} + \frac{1}{1 + \frac{N_e^{PP} a^2 q^2}{8}}\right) \quad (199)$$

Note that these do not satisfy the requirement $\overline{\tilde{f}_\mathbf{q}\tilde{f}_{-\mathbf{q}}} = \Omega\tilde{E}_\mathbf{q}$ for reproduction of the standard RPA results from our model (not even in the zero wavevector limit). Comparing eq 193 with eq 184, we also note the absence of the term

$$\frac{|\tilde{d}_{\mathbf{q},\mathrm{ref}} + \rho\tilde{\Gamma}_\mathbf{q}\beta_\mathbf{q}|^2}{2\tilde{\Delta}_{0\mathbf{q}}}$$

in their model or any reference to a frozen in composition $\tilde{d}_{\mathbf{q},\mathrm{ref}}$. Since each of these elements are essential in the present theory for the (vital) reproduction of the standard RPA results in the limit of no stretch, it seems highly unlikely that this could be achieved through an extension of their results to the systems considered in this paper. (The reproduction of the correct density fluctuations for their network model in the melt state of preparation ($\tilde{\rho}_q = 0$) is trivially achieved by letting $B \rightarrow \infty$.)

References and Notes

(1) Doi, M.; Edwards, S. F. *The Theory of Polymer Dynamics*; Clarendon: Oxford, 1986.
(2) Boué, F.; Nierlich, M.; Jannink, G.; Ball, R. C. *J. Phys. (Paris)* **1982**, *43*, 137. Boué, F.; Nierlich, M.; Jannink, G.; Ball, R. C. *J. Phys., Lett.* **1982**, *43*, L585. Boué, F.; Nierlich, M.; Jannink, G.; Ball, R. C. *J. Phys., Lett.* **1982**, *43*, L593.
(3) Boué, F. *Adv. Polym. Sci.* **1987**, *82*, 47.
(4) Boué, F.; Bastide, J.; Buzier, M.; Lapp, A.; Herz, J.; Vilgis, T. A. *Colloid Polym. Sci.* **1991**, *269*, 195.
(5) Mendes, E.; Oeser, R.; Hayes, C.; Boué, F.; Bastide, J. *Macromolecules* **1996**, *29*, 5574.
(6) Hayes, C.; Bokobza, L.; Boué, F.; Mendes, E.; Monnerie, L. *Macromolecules* **1996**, *29*, 5036.
(7) Rouf, C.; Bastide, J.; Pujol, J.; Schosseler, F.; Munch, J. P. *Phys. Rev. Lett.* **1994**, *73*, 830.
(8) Bastide, J.; Leibler, L.; Prost, J. *Macromolecules* **1990**, *23*, 1821.
(9) Onuki, A. *J. Phys. II* **1992**, *2*, 45.
(10) Panyukov, S. *JETP* **1992**, *75*, 347.
(11) Panyukov, S.; Rabin, Y. *Macromolecules* **1996**, *29*, 7960.
(12) Panyukov, S. V.; Potemkin, I. I. *J. Phys. I* **1997**, *7*, 273.
(13) Onuki, A. In *Phase Transition Dynamics*; Cambridge University Press: Cambridge, 2002; Chapter 7.
(14) McLeish, T. C. B. *Macromolecules* **1988**, *21*, 1062.
(15) McLeish, T. C. B. *Polym. Commun.* **1989**, *30*, 4.
(16) McLeish, T. C. B.; Allgaier, J.; Bick, D. K.; Bishko, G.; Biswas, P.; Blackwell, R.; Blottière, B.; Clarke, N.; Gibbs, B.; Groves, D. J.; Hakiki, A.; Heenan, R.; Johnson, J. M.; Kant, R.; Read, D. J.; Young, R. N. *Macromolecules* **1999**, *32*, 6734.
(17) Heinrich, M.; Pyckhout-Hintzen, W.; Allgaier, J.; Richter, D.; Straube, E.; Read, D. J.; McLeish, T. C. B.; Groves, D. J.; Blackwell, R. J.; Wiedenmann, A. *Macromolecules* **2002**, *35*, 6650.
(18) Heinrich, M.; Pyckhout-Hintzen, W.; Allgaier, J.; Richter, D.; Straube, E.; McLeish, T. C. B.; Wiedenmann, A.; Blackwell, R. J.; Read, D. J. *Macromolecules* **2004**, *37*, 5054.
(19) de Gennes, P. G. *J. Phys. (Paris)* **1970**, *31*, 235.
(20) Leibler, L. *Macromolecules* **1980**, *13*, 1602.
(21) Read, D. J. *Eur. Phys. J. B* **1999**, *12*, 431.
(22) Blackwell, R. J.; McLeish, T. C. B.; Harlen, O. G. *J. Rheol.* **2000**, *44*, 121.
(23) Read, D. J.; Brereton, M. G.; McLeish, T. C. B. *J. Phys. II* **1995**, *5*, 1679.
(24) Warner, M.; Edwards, S. F. *J. Phys. A* **1978**, *11*, 1649.
(25) Milner, S. T.; McLeish, T. C. B. *Macromolecules* **1997**, *30*, 2159.
(26) Heinrich, G.; Straube, E. *Polym. Bull. (Berlin)* **1987**, *17*, 255.
(27) Rubinstein, M.; Panyukov, S. *Macromolecules* **1997**, *30*, 8036.
(28) Rubinstein, M.; Panyukov, S. *Macromolecules* **2002**, *35*, 6670.
(29) Mergell, B.; Everaers, R. *Macromolecules* **2001**, *34*, 5675.
(30) Fetters, L. J.; Lohse, D. J.; Richter, D.; Witten, T. A.; Zirkel, A. *Macromolecules* **1994**, *27*, 4639.
(31) Marrucci, G. *J. Non-Newtonian Fluid Mech.* **2000**, *95*, 369.
(32) Mead, D. W.; Larson, R. G.; Doi, M. *Macromolecules* **1998**, *31*, 7895.
(33) Milner, S. T.; McLeish, T. C. B.; Likhtman, A. E. *J. Rheol* **2001**, *45*, 539.
(34) Graham, R. S.; Likhtman, A. E.; McLeish, T. C. B.; Milner, S. T. *J. Rheol.* **2003**, *47*, 1171.
(35) Marrucci, G.; Greco, F.; Ianniruberto, G. *Rheol. Acta* **2001**, *40*, 98.
(36) Fredrickson, G. H.; Milner, S. T.; Leibler, L. *Macromolecules* **1992**, *25*, 6341.
(37) MAPLE, Waterloo Maple Inc., Ontario, Canada.
(38) Read, D. J.; McLeish, T. C. B. *Macromolecules* **1997**, *30*, 6376.
(39) Straube, E.; Urban, V.; Pyckhout-Hintzen, W.; Richter, D. *Macromolecules* **1994**, *27*, 7681.
(40) Read, D. J. *Macromolecules* **1998**, *31*, 899.

MA030438U